

ESCOLA POLITÉCNICA
PROGRAMA DE PÓS-GRADUAÇÃO EM ENGENHARIA E TECNOLOGIA DE MATERIAIS
DOUTORADO EM ENGENHARIA E TECNOLOGIA DE MATERIAIS

MICHELE OLIVEIRA VIEIRA

DESIGN DE LÍQUIDOS IÔNICOS PARA CONVERSÃO DE CO₂

Porto Alegre

2018

PÓS-GRADUAÇÃO - *STRICTO SENSU*



Pontifícia Universidade Católica
do Rio Grande do Sul



**DESIGN DE LÍQUIDOS IÔNICOS PARA
CONVERSÃO DE CO₂**

MICHELE OLIVEIRA VIEIRA

QUÍMICA INDUSTRIAL E LICENCIADA

MESTRE EM ENGENHARIA E TECNOLOGIA DE MATERIAIS

**TESE PARA A OBTENÇÃO DO TÍTULO DE DOUTOR EM ENGENHARIA E
TECNOLOGIA DE MATERIAIS**

Porto Alegre

Dezembro, 2018



DESIGN DE LÍQUIDOS IÔNICOS PARA CONVERSÃO DE CO₂

MICHELE OLIVEIRA VIEIRA

QUÍMICA INDUSTRIAL E LICENCIADA

MESTRE EM ENGENHARIA E TECNOLOGIA DE MATERIAIS

ORIENTADOR: PROF(a). DR(a). SANDRA EINLOFT

Tese realizada no Programa de Pós-Graduação em Engenharia e Tecnologia de Materiais (PGETEMA) da Pontifícia Universidade Católica do Rio Grande do Sul, como parte dos requisitos para a obtenção do título de Doutor em Engenharia e Tecnologia de Materiais.

Trabalho vinculado ao Projeto: Avaliação de líquidos iônicos miscíveis em água para captura de CO₂ em gás natural.

**Porto Alegre
Dezembro, 2018**

Ficha Catalográfica

V658d Vieira, Michele Oliveira

Design de líquidos iônicos para conversão de CO₂ / Michele Oliveira Vieira . – 2018.

120 f.

Tese (Doutorado) – Programa de Pós-Graduação em Engenharia e Tecnologia de Materiais, PUCRS.

Orientadora: Profa. Dra. Sandra Einloft.

1. Líquido Iônico. 2. Conversão de CO₂. 3. Carbonatos Cíclicos. I. Einloft, Sandra. II. Título.

Elaborada pelo Sistema de Geração Automática de Ficha Catalográfica da PUCRS
com os dados fornecidos pelo(a) autor(a).

Bibliotecária responsável: Salete Maria Sartori CRB-10/1363



Pontifícia Universidade Católica do Rio Grande do Sul
ESCOLA POLITÉCNICA
PROGRAMA DE PÓS-GRADUAÇÃO EM ENGENHARIA E TECNOLOGIA DE MATERIAIS

DESIGN DE LÍQUIDOS IÔNICOS PARA CONVERSÃO DE CO₂

CANDIDATA: MICHELE OLIVEIRA VIEIRA

Esta Tese de Doutorado foi julgada para obtenção do título de DOUTOR EM ENGENHARIA E TECNOLOGIA DE MATERIAIS e aprovada em sua forma final pelo Programa de Pós-Graduação em Engenharia e Tecnologia de Materiais da Pontifícia Universidade Católica do Rio Grande do Sul.

DRA. SANDRA MARA OLIVEIRA EINLOFT - ORIENTADORA

BANCA EXAMINADORA

DR. JACKSON DAMIANI SCHOLTEN - DO INSTITUTO DE QUÍMICA - UFRGS

DRA. KATIA BERNARDO GUSMÃO - DO INSTITUTO DE QUÍMICA - UFRGS

DR. EDUARDO CASSEL - PGETEMA - PUCRS

PUCRS

Campus Central

Av. Ipiranga, 6681 - Prédio 32 - Sala 505 - CEP: 90619-900

Telefone: (51) 3353.4059 - Fax: (51) 3320.3625

E-mail: engenharia.pg.materiais@pucrs.br

www.pucrs.br/politecnica

HAPPINESS ONLY REAL WHEN SHARED
(Christopher McCandless – “Alexander Supertramp”)

DEDICATÓRIA

Para todos que já tiveram um momento de fraqueza. Não vai doer para sempre, então não deixe isso afetar o que há de melhor em nós.

AGRADECIMENTOS

É difícil lembrar de todas as pessoas que de alguma forma, nas horas serenas ou apreensivas, fizeram parte da minha vida e me ajudaram, direta ou indiretamente, na construção deste trabalho e mais esta etapa de minha formação. Por isso, o meu muito obrigada à todos, de coração.

SUMÁRIO

DEDICATÓRIA	7
AGRADECIMENTOS	8
SUMÁRIO	9
LISTA DE FIGURAS	11
LISTA DE TABELAS	12
LISTA DE QUADROS.....	13
LISTA DE SÍMBOLOS.....	14
RESUMO	16
ABSTRACT.....	17
1. INTRODUÇÃO	18
2. OBJETIVOS	20
2.1. Objetivos específicos	20
3. REVISÃO BIBLIOGRÁFICA.....	21
3.1. Utilização do CO₂	27
3.2. Conversão de CO₂.....	30
3.3. Líquidos Iônicos.....	33
3.4. Líquidos iônicos para conversão de CO₂	37
3.5. Influência da temperatura na formação de carbonatos cíclicos.....	40
3.6. Influência da pressão de CO₂ na formação de carbonatos cíclicos.....	41
3.7. Influência do tempo na formação de carbonatos cíclicos	45
4. PROCEDIMENTOS EXPERIMENTAIS E RESULTADOS	46
4.1. Capítulo I.....	46
4.1.1. Características dos líquidos iônicos.....	47
4.2. Capítulo II	48
4.3. Capítulo III.....	60
4.4. Capítulo IV.....	72
5. CONCLUSÕES	102

6. PROPOSTA PARA TRABALHOS FUTUROS	105
7. OUTROS TRABALHOS REALIZADOS / APRESENTADOS	106
8. REFERÊNCIAS BIBLIOGRÁFICAS	110

LISTA DE FIGURAS

Figura 3.1. Emissões globais de GEE.....	21
Figura 3.2. Fontes de energia primária global.....	22
Figura 3.3. Concentração de CO ₂ atmosférico.....	23
Figura 3.4. Aumento das emissões de CO ₂ atmosférico.....	24
Figura 3.5. Variação da temperatura média global nas últimas décadas.....	25
Figura 3.6. Os 12 princípios da Química do CO ₂ (e tradução).....	26
Figura 3.7. Possibilidades de utilização de CO ₂	28
Figura 3.8. Possibilidades de reações de conversão de CO ₂	31
Figura 3.9. Alguns exemplos de carbonatos orgânicos alifáticos.....	32
Figura 3.10. Alguns exemplos de carbonatos orgânicos cíclicos.....	32
Figura 3.11. Esquema de formação: (a) cátion imidazólio e (b) troca de ânion.	35
Figura 3.12. Influência da temperatura na reação do PC utilizando o líquido iônico [TMTC ₃ H ₆ OH]Br sintetizado por Dai <i>et al.</i> 2017.....	40
Figura 3.13. Reação de formação de carbonatos cíclicos em 3 horas e 40 bar utilizando [TBA][Br] como catalisador.	41
Figura 3.14. Líquido iônico [TMTC ₃ H ₆ OH]Br sintetizado por Dai <i>et al.</i> 2017.	42
Figura 3.15. Fotografia da influência da pressão na formação do SC onde (a) 4 MPa, (b) 8 MPa, (c) 15 MPa e (d) 18 MPa; (e) esquema da reação e (f) rendimento com variação de pressão.	43
Figura 3.16. Gráfico da conversão de epóxido em função da pressão.	44
Figura 3.17. Influência do tempo na conversão do óxido de propileno utilizando o líquido iônico [TMTC ₃ H ₆ OH]Br sintetizado por Dai <i>et al.</i> 2017.....	45

LISTA DE TABELAS

Tabela 3.1. Registros de emissões de CO ₂ por setores econômicos.	23
Tabela 3.2. Utilização anual de CO ₂ no segmento industrial.	29
Tabela 3.3. Propriedades dos líquidos iônicos.....	33
Tabela 3.4. Resultados de rendimento obtidos por Zhang <i>et al.</i> (2016) para cicloadição de CO ₂ em epóxidos.	38
Tabela 3.5. Resultados (conversão e seletividade) de Dai <i>et al.</i> (2017) para cicloadição de CO ₂ em epóxidos.	39
Tabela 4.1. Dados reacionais da síntese e características físicas dos líquidos iônicos.....	47

LISTA DE QUADROS

Quadro 3.1. Cátions e ânions mais comumentes reportados na literatura.	35
---	----

LISTA DE SÍMBOLOS

[bmim][Cl]	Cloreto de 1-butil-3-metilimidazólio
[bmim][C ₁₂ SO ₄]	Lauril sulfato de 1-butil-3-metilimidazólio
[bmim][C ₁₂ ESO ₄]	Lauril éter sulfato de 1-butil-3-metilimidazólio
[bmim][C ₁₂ BSO ₃]	Lauril benzeno sulfonato de 1-butil-3-metilimidazólio
[bmim][C ₁₂ SAR]	Lauroil sarcosinato de 1-butil-3-metilimidazólio
[TBA][Br]	Brometo de tetra-n-butilamônio
[TBA][C ₁₂ SO ₄]	Lauril sulfato de tetra-n-butilamônio
[TBA][C ₁₂ ESO ₄]	Lauril éter sulfato de tetra-n-butilamônio
[TBA][C ₁₂ BSO ₃]	Lauril benzeno sulfonato de tetra-n-butilamônio
[TBA][C ₁₂ SAR]	Lauroil sarcosinato de tetra-n-butilamônio
¹ H-RMN	Ressonância magnética nuclear de hidrogênio (do inglês, <i>nuclear magnetic resonance</i>)
AAS	Espectroscopia por absorção atômica (do inglês, <i>atomic absorption spectroscopy</i>)
CG	Cromatografia gasosa
CO ₂	Dióxido de carbono
DEC	Carbonato de dietila (do inglês, <i>diethyl carbonate</i>)
DMC	Carbonato de dimetila (do inglês, <i>dimethyl carbonate</i>)
DME	Éter dimetila (do inglês, <i>dimethyl ether</i>)
DPC	Carbonato de difenila (do inglês, <i>diphenyl carbonate</i>)
DSC	Calorimetria diferencial de varredura (do inglês, <i>differential scanning calorimetry</i>)
EC	Carbonato de epícloridrina (do inglês, <i>epichlorohydrin carbonate</i>)
EGR	Recuperação avançada de gás (do inglês, <i>enhanced gas recovery</i>)
EGS	Sistema geotérmico avançado (do inglês, <i>enhanced geothermal systems</i>)
EOR	Recuperação avançada de petróleo (do inglês, <i>enhanced oil recovery</i>)
FID	Detector de ionização de chama (do inglês, <i>flame ionization detector</i>)

FTIR	Espectroscopia no infravermelho com transformada de Fourier (do inglês, <i>Fourier transform infrared spectroscopy</i>)
GC	Carbonato de glicidil isopropil éter (do inglês, <i>glycidyl isopropyl ether carbonate</i>)
GEE	Gases de efeito estufa
IPCC	Painel intergovernamental sobre mudança do clima (do inglês, <i>intergovernmental panel on climate change</i>)
LD	Limite de detecção
LIs	Líquidos iônicos
MM	Massa molar
ND	Não detectado
NOx	Óxidos de nitrogênio
PC	Carbonato de propileno (do inglês, <i>propylene carbonate</i>)
SC	Carbonato de estireno (do inglês, <i>styrene carbonate</i>)
SOV	Solvente orgânico volátil
T	Transmitância (%)
TBME	Éter metil terc-butilico (do inglês, <i>methyl tertbutyl ether</i>)
TGA	Análise termogravimétrica (do inglês, <i>thermogravimetric analysis</i>)
TOF	Frequência de rotação (do inglês, <i>turnover frequency</i>)
TON	Número de rotação (do inglês, <i>turnover number</i>)

RESUMO

VIEIRA, Michele Oliveira. **Design de líquidos iônicos para conversão de CO₂**. Porto Alegre. 2018. Tese. Programa de Pós-Graduação em Engenharia e Tecnologia de Materiais, PONTIFÍCIA UNIVERSIDADE CATÓLICA DO RIO GRANDE DO SUL.

A crescente aceitação mundial de que as mudanças climáticas estão diretamente ligadas ao aumento da emissão de gases de efeito estufa, dióxido de carbono (CO₂) em particular, e a necessidade de aperfeiçoamento de sínteses com o emprego de insumos reutilizáveis são algumas das preocupações da atualidade. Sendo assim, esta tese visa contribuir para o desenvolvimento de novos materiais ativos como catalisadores de processos que exploram as possibilidades de produção de carbonatos orgânicos a partir de CO₂. Os carbonatos cíclicos possuem diversas aplicações. Além disso, a sua produção partindo de CO₂ representaria um enorme passo para a mitigação dos impactos ambientais. Para isso, novos líquidos iônicos (LIs) de cátions imidazólios ([bmim⁺]) e tetra-n-alquilamônio ([TBA⁺]) com ânions derivados de sais surfactantes ([C₁₂SO₄⁻], [C₁₂ESO₄⁻], [C₁₂BSO₃⁻], [C₁₂SAR⁻]) foram sintetizados e testados como catalisadores de diferentes cicloadições de CO₂ em epóxidos. Os LIs foram caracterizados por FTIR, ¹H-RMN, TGA e DSC. A pureza do material foi determinada pelos residuais de [Cl⁻], [Na⁺] e umidade. Os LIs mostraram boa atividade na síntese do carbonato de propileno (PC), atingindo 79,2% de conversão e 87,7% de seletividade quando utilizado o [TBA][C₁₂SO₄]. Para esta reação o catalisador manteve sua atividade por pelo menos 5 ciclos. Na síntese do carbonato de estireno (SC) o [TBA][C₁₂BSO₃] se mostrou o LI mais eficiente atingindo 81,4% de conversão e 87,0% de seletividade. Este LI também mostrou significativa atividade na síntese do carbonato de glicidil isopropil éter (GC) e no carbonato de epícloridrina (EC).

Palavras-Chaves: líquido iônico; conversão de CO₂; carbonatos cíclicos.

ABSTRACT

VIEIRA, Michele Oliveira. **Design of ionic liquids for CO₂ conversion.** Porto Alegre. 2018. PhD Thesis. Graduation Program in Materials Engineering and Technology, PONTIFICAL CATHOLIC UNIVERSITY OF RIO GRANDE DO SUL.

The acceptance that climate change is directly related to increasing greenhouse gas emissions, carbon dioxide (CO₂) in particular, and the need to improve synthesis with reusable inputs are some of the current concerns. Thus, this thesis aims to contribute to the development of new catalytic materials for the processes that explore the possibilities of production of organic carbonates from CO₂. Cyclic carbonates have several applications. Furthermore, their production from CO₂ would represent a huge step towards mitigating environmental impacts. For this, new ionic liquids (ILs) of imidazolium ([bmim⁺]) and tetra-n-alkylammonium ([TBA⁺]) cations with anions derived from surfactant salts ([C₁₂SO₄⁻], [C₁₂ESO₄⁻], [C₁₂BSO₃⁻], [C₁₂SAR⁻]) were synthesized and tested as catalysts of different cycloaddition of CO₂ in epoxides. ILs were characterized by FTIR, ¹H-NMR, TGA and DSC. The [Cl⁻], [Na⁺] and moisture residues determined the purity of the material. The ILs showed good activity in propylene carbonate (PC) synthesis, 79.2% of conversion and 87.7% of selectivity when [TBA][C₁₂SO₄] was used. For this reaction, catalyst kept its activity for at least 5 cycles. In the synthesis of styrene carbonate (SC), [TBA][C₁₂BSO₃] was the most efficient IL reaching 81.4% of conversion and 87.0% of selectivity. This IL also showed significant activity in the synthesis of glycidyl isopropyl ether carbonate (GC) and epichlorohydrin carbonate (EC).

Key-words: ionic liquids; CO₂ conversion; cyclic carbonates.

1. INTRODUÇÃO

A crescente aceitação mundial de que as mudanças climáticas e aquecimento global estão diretamente ligadas ao aumento da emissão de gases de efeito estufa, em particular de CO₂, aliados a estudos que apontam a contribuição deste fenômeno para acidificação do oceano, aumento do nível do mar e do número de espécies em extinção, cria a necessidade de ações que visam à redução ou mitigação dessas emissões. Estima-se que a concentração atmosférica global de dióxido de carbono tenha aumentado de um valor pré-industrial de cerca de 280 ppm para 410 ppm em setembro de 2018 (NOAA, 2018), ultrapassando em muito a faixa natural dos últimos 650.000 anos (180 a 300 ppm), como determinado a partir de testemunhos de gelo (IPCC, 2011).

Nos últimos anos tem havido um aumento significativo na implementação de energias renováveis, como a eólica e a solar. Além disso, após alguns anos de crescimento modesto, a eficiência energética de vários países voltou a crescer significativamente, devido ao aumento de investimentos públicos na área de pesquisa e desenvolvimento energético. Estas iniciativas representam apenas os primeiros passos de uma longa caminhada para transformar a maneira de fornecer e utilizar a energia. É provável que por várias décadas ainda, os combustíveis fósseis sejam responsáveis por grande parte da produção de energia. Desta forma, a captura e utilização do CO₂ surgem como uma opção viável para mitigar as emissões de gases do efeito estufa (Mofarahi, 2008; IEA, 2015).

Já a algumas décadas, a utilização de líquidos iônicos (LIs), materiais que pertencem a uma classe de compostos orgânicos iônicos, vem despertando grande interesse da comunidade científica, por serem versáteis e menos danosos ao meio-ambiente do que os solventes orgânicos convencionais. Estes compostos

apresentam grandes expectativas de potencial de aplicação em diversos segmentos, como catalisadores de diversas reações químicas. Possuem características peculiares, ou seja, pressão de vapor extremamente baixa, alta estabilidade térmica (geralmente superior a 200°C) e a possibilidade de variar suas propriedades físicas e químicas, por meio da combinação de cátions e ânions distintos (Koel, 2009; Bara *et al.*, 2009; Bermúdez, 2009; Plechkova e Seddon, 2008; Freudenmann *et al.*, 2011).

A variabilidade estrutural dos líquidos iônicos é enorme e neste sentido é possível a criação de compostos com características e propriedades específicas, para uma determinada aplicação (Koel, 2009; Freudenmann *et al.*, 2011).

A transformação química do CO₂ visa agregar valor comercial a um gás inerte. A aplicação do dióxido de carbono como matéria prima nas indústrias químicas tem grande valia quando se visa os benefícios ambientais envolvidos, porém, são poucos os processos industriais que utilizam CO₂ como material de partida (Arakawa *et al.*, 2001; Sakakura, Choi e Yasuda, 2007; Vieira, 2015).

Vários produtos químicos valiosos podem ser obtidos na síntese utilizando CO₂ como reagente, por exemplo: carbonatos orgânicos, carbamatos, uretanos, lactonas, policarbonatos, ureia, ácido acético, ácido fórmico, ácido salicílico, entre muitos outros (Arakawa *et al.*, 2001; Sakakura, Choi e Yasuda, 2007; Maeda, Miyazaki e Ema, 2014).

Neste contexto, pretende-se neste trabalho sintetizar/modificar líquidos iônicos de cátions alquilimidazólio e alquilamônio, com diferentes ânions que possam ser empregados como catalisadores na transformação química do CO₂, visando um sistema eficiente, seletivo e viável economicamente.

2. OBJETIVOS

Sintetizar e caracterizar diferentes líquidos iônicos para serem empregados como catalisadores na síntese de diversos carbonatos cíclicos.

2.1. Objetivos específicos

- Sintetizar líquidos iônicos de cátion imidazólios e tetra-n-butilamônio com diferentes ânions derivados de surfactantes;
- Caracterizar os LIs sintetizados por FTIR, ¹H-RMN, TGA e DSC;
- Determinar a pureza dos LIs sintetizados pelo residual de [Cl⁻], [Na⁺] e umidade;
- Estudar a interação água / LI;
- Testar os LIs como potenciais catalisadores na síntese do carbonato de propileno (PC), carbonato de estireno (SC), carbonato de glicidil isopropil éter (GC) e carbonato de epicloridrina (EC).

3. REVISÃO BIBLIOGRÁFICA

A fina camada de gases que circunda a Terra, a qual chamamos atmosfera, é cerca de 99% constituída de nitrogênio e oxigênio. Alguns outros gases se fazem presentes em pequenas quantidades, dentre estes, o dióxido de carbono (CO_2), o metano (CH_4) e os óxidos de nitrogênio (NO_x), conhecidos como “gases de efeito estufa” (GEE). Este efeito é fundamental para a manutenção do clima e do ecossistema (Hansen *et al.*, 2008; IPCC, 2011).

A partir da revolução industrial, a industrialização e o desenvolvimento tecnológico ganharam grande impulso aumentando significativamente a concentração de dióxido de carbono na atmosfera terrestre. O CO_2 é o GEE de maior impacto em termos de quantidades emitidas, como podemos observar na Figura 3.1 (IPCC, 2014).

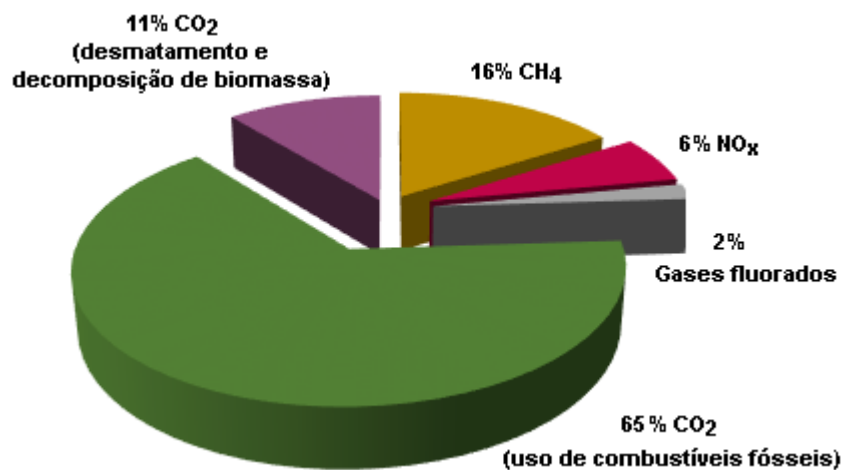


Figura 3.1. Emissões globais de GEE.

Fonte: Adaptação de IPCC, 2014.

A origem de boa parte dessas emissões decorre de fontes antropogênicas (IPCC, 2014). O CO₂ é emitido através de queima de combustíveis fósseis, desmatamento, decomposição de biomassa, além de desflorestamento de grandes áreas para uso agrícola. As emissões de CH₄ derivam basicamente da atividade pecuária e da decomposição de biomassa. Já o NO_x vem do uso desenfreado de fertilizantes e da queima de combustíveis fósseis. E finalmente, a origem dos gases fluorados são os processos industriais e de refrigeração em grande escala (IPCC, 2014).

Além disso, como mostrado na Figura 3.2, as queimas de combustíveis fósseis ainda representam a maior fonte de energia primária global, embora a porcentagem de energia renovável implantada nos últimos anos tenha aumentado para 13,3% (IPCC, 2014).

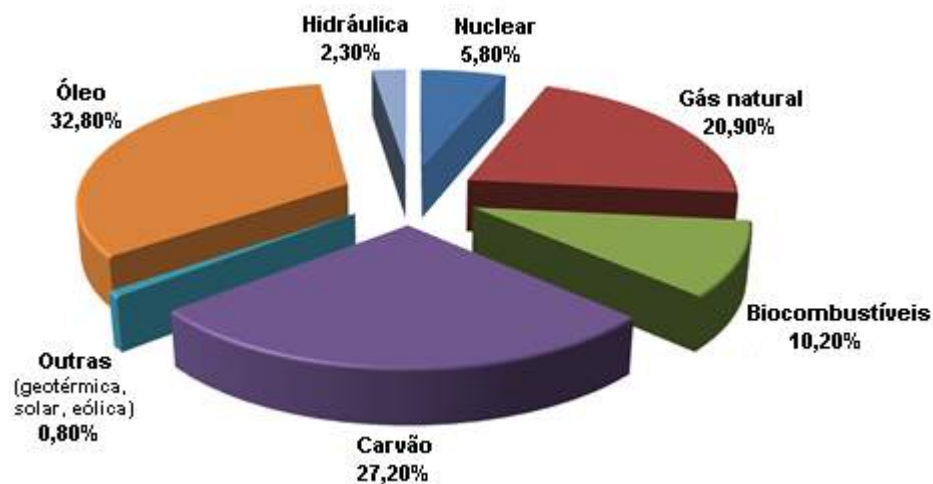


Figura 3.2. Fontes de energia primária global.

Fonte: Adaptação de IPCC, 2014.

O mapeamento das fontes emissoras é o primeiro passo para se pensar em como mitigar esses gases de efeito estufa. Com relação ao CO₂, é mostrado na Tabela 3.1 o registro das emissões por setores econômicos e vemos que energia e transporte são os principais emissores (IEA, 2015). Existe também a dificuldade em encontrar dados atualizados dessas informações, normalmente os disponibilizados já apresentam alguma defasagem de tempo.

Tabela 3.1. Registros de emissões de CO₂ por setores econômicos.

Setor Industrial	Emissão (MtCO ₂ / ano)	%
Eletricidade e produção de calor	13665,6	42,4
Transporte	7384,9	23,0
Indústrias de manufaturamento e construção	6114,8	19,0
Residencial	1868,9	5,8
Serviços	861,9	2,7
Outros (agricultura, pesca, aviação)	2303,8	7,1
TOTAL	32189,7	100

Fonte: IEA, 2015.

Como consequência, a geração de gases poluentes, provenientes da atividade humana, atinge patamares nunca antes vistos (Rogelj, Meinshausen e Knutti, 2012; IEA, 2015). A concentração de CO₂ apresentou um aumento de 280 ppm na era pré-industrial para uma média global de 410 ppm registrada esse ano (2018) como mostra o gráfico de tendência da Figura 3.3, onde a linha vermelha representa os valores médios mensais da concentração de CO₂ e a linha preta representa estes valores após correção para a média do ciclo sazonal (NOAA, 2018). Na Figura 3.4 é observado o aumento da quantidade de emissões de CO₂ desde a época pré-industrial. Nos últimos 30 anos foi emitido 20% a mais de CO₂ e esta tendência ainda é uma crescente.

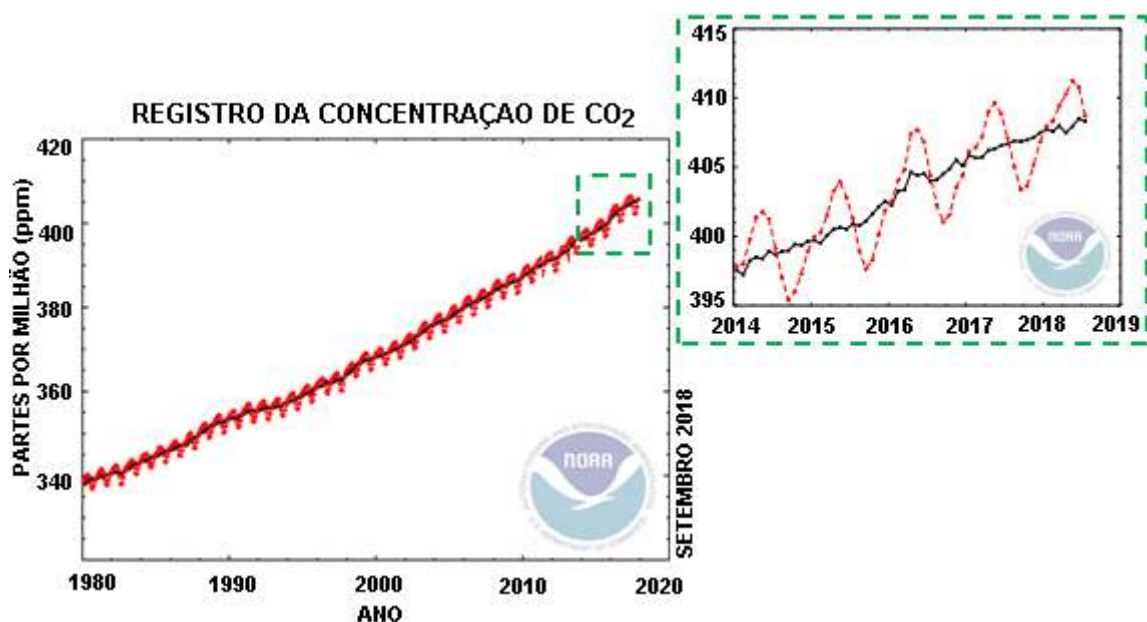


Figura 3.3. Concentração de CO₂ atmosférico.

Fonte: Adaptação de NOAA, 2018.

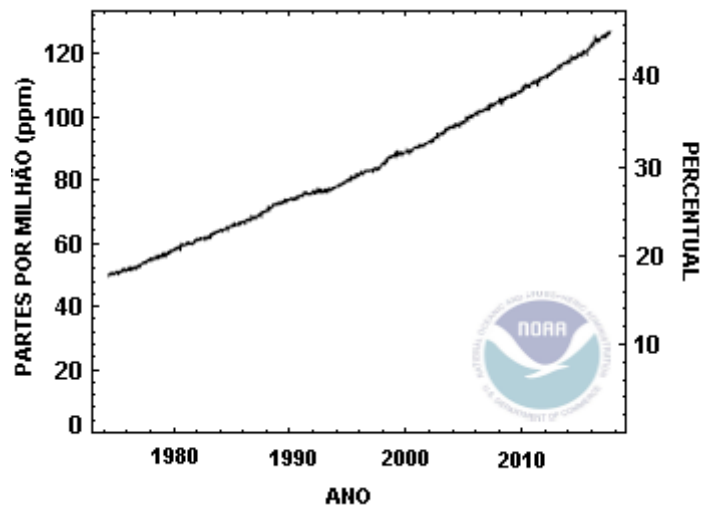


Figura 3.4. Aumento das emissões de CO₂ atmosférico.

Fonte: Adaptação de NOAA, 2018.

A crescente demanda de energia, o aumento populacional e o uso desenfreado de combustíveis fósseis têm um impacto negativo na atmosfera, pois as emissões antropogênicas de CO₂ são consideradas uma das principais contribuintes ao aquecimento global, visto que o CO₂ é tido como o principal gás de efeito estufa (Herzog *et al.*, 2012).

Como consequência da crescente concentração de CO₂ na atmosfera, observa-se um aumento de 0,8 °C na temperatura média na superfície da Terra no período de 1900 até o presente (Hansen *et al.*, 2008; IPCC, 2011; NOAA, 2018). A Figura 3.5 apresenta um gráfico que mostra a variação da temperatura nas últimas décadas.

O aumento da temperatura global tem sido acompanhado por várias mudanças meteorológicas e climáticas. Muitos lugares têm sofrido alterações nas precipitações, resultando em mais inundações e secas. Ondas de calor e frio também estão se tornando mais frequentes. Além disso, os oceanos estão aquecendo e se acidificando, enquanto que as calotas de gelo estão derretendo e elevando o nível do mar (EPA, 2017).

Em 2015, na Convenção Internacional sobre Mudanças Climáticas, em Paris, foi mostrado que apesar dos esforços e dos planejamentos quanto às emissões de

CO₂, a temperatura média do planeta ainda permanecerá 2 °C acima do ideal, podendo aumentar para 3 °C até 2050.

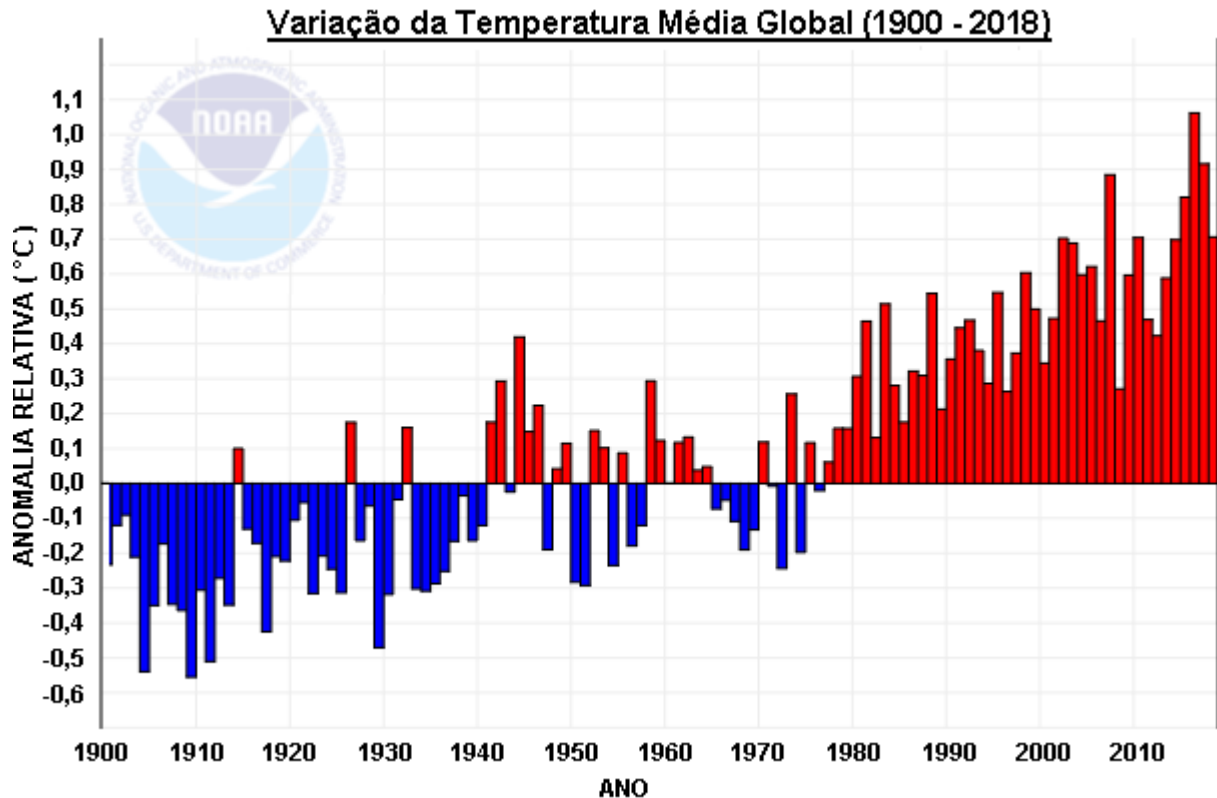


Figura 3.5. Variação da temperatura média global nas últimas décadas.

Fonte: Adaptação de NOAA, 2018.

Existem algumas alternativas que podem contribuir para a mitigação destas mudanças climáticas, como por exemplo, a redução das emissões dos GEE produzidos durante a geração de energia. Outras formas também relevantes são a eficiência energética, fontes renováveis de energia, mudança para combustíveis que emitam menor quantidade de CO₂, aprimoramento dos biocombustíveis, redução das emissões dos outros GEE além do CO₂ e a captura, transformação e armazenamento de CO₂ (IPCC, 2011, Rafiee *et al.*, 2018).

Acredita-se que apenas com a captura do CO₂ emitidos por grandes fontes pontuais, tais como centrais de energia que utilizam combustíveis fósseis, plantas de processamento de combustíveis, cimenteiras e outras grandes plantas industriais, seja suficiente para um início eficaz da mitigação dos impactos ambientais (Arshad, 2009).

A química verde pode ser definida como a criação, o desenvolvimento e a aplicação de produtos químicos e processos para reduzir ou eliminar a utilização ou a geração de substâncias prejudiciais à saúde humana e/ou ao meio ambiente (Poliakoff *et al.*, 2002). Promover e implementar uma química verde em processos industriais, principalmente de grande porte, nem sempre é fácil, por isso, todo este conceito pode ser dividido em três grandes categorias: o uso de fontes renováveis ou recicladas de matéria-prima; o aumento da eficiência de energia, ou a utilização de menos energia para produzir a mesma ou maior quantidade de produto; e finalmente, evitar o uso de substâncias persistentes, bioacumulativas e tóxicas (Poliakoff *et al.*, 2002).

Poliakoff *et al.* (2002) criaram o que ficou famoso como os Princípios da Química Verde. Eles elaboraram uma lista de doze passos que devem ser pensados e refletidos antes de qualquer criação de processo químico ou manipulação de produtos químicos. Em 2015 Poliakoff, Leitner e Streng atualizaram estes princípios e elaboraram os Princípios da Química do CO₂, como mostra a tradução na Figura 3.6.

C	Catalysis is crucial	→	A catálise é crucial
O	Origin of the CO ₂ ?	→	Origem do CO ₂ ?
2	Tomorrow's world may be different	→	O mundo de amanhã pode ser diferente
C	Cleaner than existing process?	→	Mais limpo do que o processo existente?
H	High volume or high value products?	→	Alto volume ou produtos de alto valor?
E	E-factor must be low	→	O fator E deve ser baixo
M	Maximize integration	→	Maximizar a integração
I	Innovative process technology	→	Tecnologia de processo inovadora
S	Sustainability is essential	→	Sustentabilidade é essencial
T	Thermodynamics cannot be beaten	→	Termodinâmica não pode ser derrotada
R	Renewable (& reasonable) energy input	→	Energia renovável
Y	Your enthusiasm is not enough	→	Seu entusiasmo não é suficiente

Figura 3.6. Os 12 princípios da Química do CO₂ (e tradução).

Fonte: Adaptação de Poliakoff, Leitner e Streng, 2015.

Estes novos doze princípios condensam pensamentos que ajudam a destacar as questões mais pertinentes e a estruturar futuras discussões pertinentes ao assunto (Poliakoff, Leitner e Streng, 2015).

3.1. Utilização do CO₂

A utilização do dióxido de carbono capturado de fontes estacionárias poderia contribuir para fechar o ciclo global do CO₂. A necessidade de uma química mais verde e de processos mais limpos em conjunto com perspectivas de um desenvolvimento mais sustentável, fazem com que o dióxido de carbono se transforme em uma matéria prima reutilizável (Aresta e Dibenedetto, 2004; Tkatchenko *et al.*, 2006).

A finalidade da captura de CO₂ é produzir um fluxo concentrado de CO₂ com alta pressão que possa ser facilmente transportado ao lugar de armazenamento ou utilizado em processos industriais e comerciais (Wappel *et al.*, 2010). O CO₂ pode ser considerado um importante bloco de construção em diversos segmentos, agregando considerável valor a um produto que normalmente é considerado resíduo.

Vários estudos têm apresentado diferentes maneiras de armazenamento do CO₂. Algumas das alternativas são: armazenamento em rochas porosas, campos de petróleo em estágio final de exploração ou já extintos e o armazenamento em aquíferos ou camadas de carvão. Essas tecnologias vêm sendo estudadas, apesar de se conhecer alguns dos problemas associados, como o aumento do pH em águas profundas decorrente do CO₂ dissolvido e a alteração da fauna e flora aquáticas. Além disso, o CO₂ capturado também é muito utilizado na recuperação avançada de petróleo (EOR) (IPCC, 2011).

A Figura 3.7 ilustra várias possibilidades de utilização do CO₂ capturado de fontes estacionárias. Dentro destas possibilidades, podem aparecer os processos químicos, onde o CO₂ é convertido em algum produto de maior valor agregado, como solventes industriais, polímeros ou qualquer segmento que necessite de uma fonte de carbono (Rafiee *et al.*, 2018). Também pode ser utilizado em um processo físico, onde ele permanece em sua forma química inalterada, como na gaseificação de bebidas, extintores de incêndio, agentes de expansões em espumas e até mesmo na recuperação avançada do petróleo (EOR) (Rafiee *et al.*, 2018).

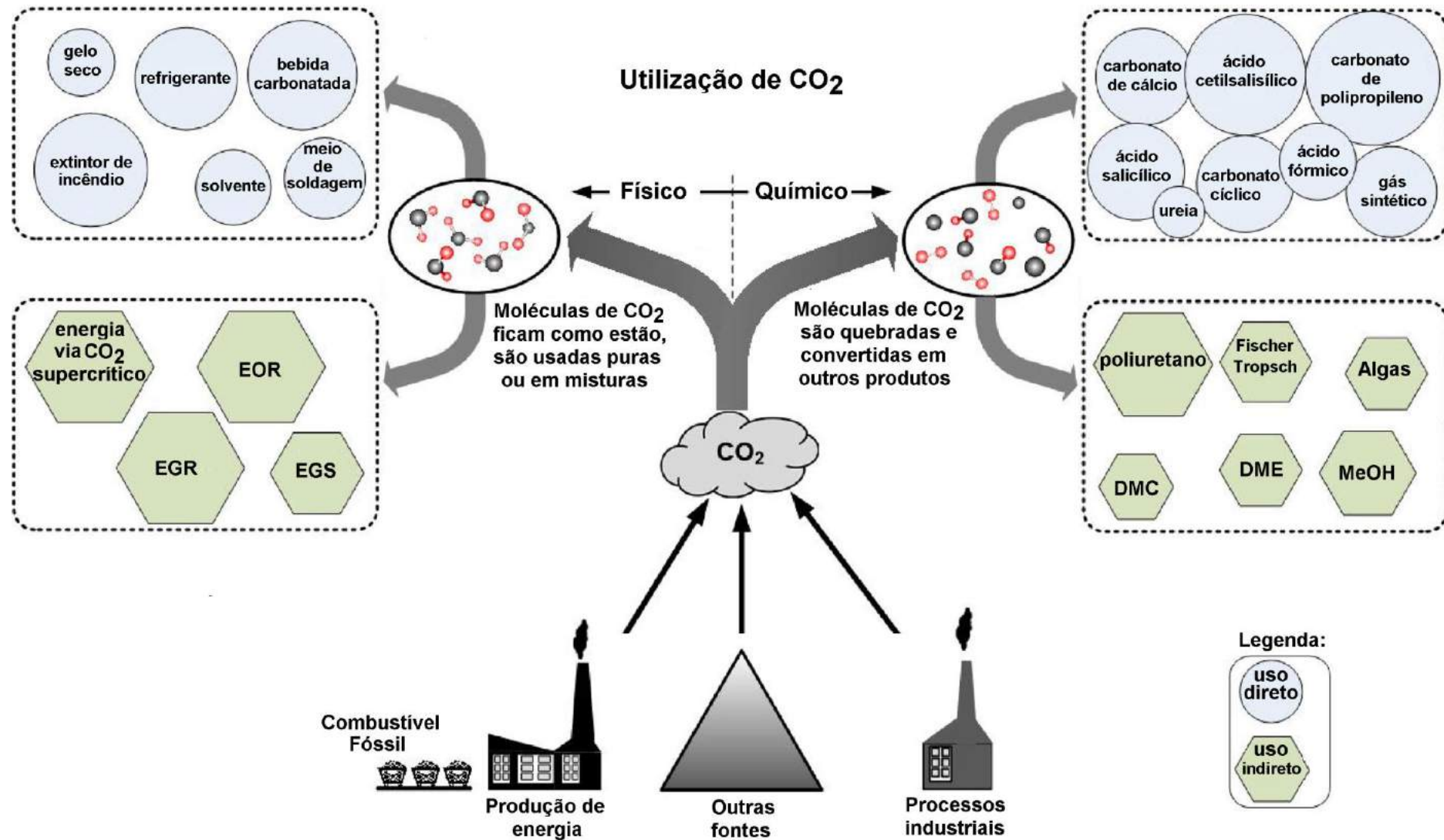


Figura 3.7. Possibilidades de utilização de CO₂.

Fonte: Adaptação de Rafiee *et al.*, 2018.

Tanto nos processos de utilização do CO₂ por meios químicos quanto físicos, pode-se segmentar por duas vias a aplicação, o uso direto ou indireto. Nos casos de utilização direta, o processo não pode ser formado sem o CO₂ como molécula inteira. Enquanto que para a utilização indireta, as moléculas de CO₂ ajudam melhorar o processo, adicionar valor ou facilitar a retirada de outros materiais.

Anualmente é utilizado cerca de 200 milhões de toneladas de CO₂ para produção de produtos com valor agregado, sendo 57% destes, somente para a produção de ureia (Otto *et al.*, 2015; Rafiee *et al.*, 2018). A Tabela 3.2 detalha os segmentos industriais que utilizam CO₂ como matéria prima e as respectivas quantidades anuais (Aresta, Dibenedetto e Angelini, 2013; Rafiee *et al.*, 2018).

Tabela 3.2. Utilização anual de CO₂ no segmento industrial.

Industria (produção)	Uso (MtCO₂ / ano)
Ureia	114
Metanol	8
Éter dimetílico (DME)	3
Éter metil terc-butílico (TBME)	1,5
Formaldeído	3,5
Carbonatos	0,005
Policarbonatos	0,01
Carbonatos inorgânicos	50
Tecnologias	28
Alimentação de algas para produção de biodiesel	0,01
TOTAL	208

Fonte: Aresta, Dibenedetto e Angelini, 2013.

Toda esta utilização de CO₂ ainda é insignificante (~0,6%) quando se pensa em mitigação de impactos ambientais (Cokoja *et al.*, 2011; Rafiee *et al.*, 2018). A necessidade de ampliar essas aplicações e aumentar a utilização do CO₂ vindo de fontes de captura é uma linha de estudo eminente.

3.2. Conversão de CO₂

A aplicação do dióxido de carbono como matéria prima nas indústrias químicas tem grande valia quando se visa os benefícios ambientais envolvidos, porém, são poucos os processos industriais que utilizam CO₂ como material de partida devido à grande quantidade de energia necessária para sua transformação direta.

Assim, algumas das metodologias para transpor a transformação em produtos químicos úteis consistem em utilizar materiais de partida com alta energia, como hidrogênio, compostos insaturados, anéis com poucos carbonos e organometálicos; escolher alvos sintéticos oxidados de baixa energia, tais como carbonatos orgânicos ou fornecer alguma fonte de energia. Além disso, na maioria das reações é necessário utilizar um sistema catalítico, que pode ser homogêneo, heterogêneo ou enzimático (Sakakura, Choi e Yasuda, 2007). O potencial da catálise homogênea para a transformação do CO₂ vem sendo discutido há bastante tempo. Um dos motivos seria o fato dos sistemas catalíticos homogêneos normalmente apresentarem melhores resultados frente aos heterogêneos (Sakakura, Choi e Yasuda, 2007).

Vários produtos químicos valiosos podem ser obtidos na síntese utilizando CO₂ como reagente de partida, como por exemplo, carbonatos orgânicos, carbamatos, uretanos, lactonas, policarbonatos, ureia, ácido acético, ácido fórmico, ácido salicílico, entre muitos outros, conforme ilustrado na Figura 3.9 (Arakawa *et al.*, 2001; Sakakura, Choi e Yasuda, 2007; Maeda, Miyazaki e Ema, 2014).

Nos últimos anos são descritos na literatura o uso de CO₂ supercrítico para síntese, na chamada química verde, sem o uso de solventes voláteis, bem como reações de hidrogenação, redução eletroquímica e fotoquímica do CO₂ (Arakawa *et al.*, 2001; Sakakura, Choi e Yasuda, 2007).

Unindo as possibilidades de utilização do CO₂ em rotas de síntese, como mostradas na Figura 3.8, com os inúmeros benefícios da utilização dos líquidos iônicos como solventes e/ou catalisadores em reações de síntese orgânica, na

substituição dos solventes tóxicos normalmente empregados nas reações de Friedel-Crafts e de Diels-Alder, hidrogenações, polimerizações, entre outras, é uma promissora alternativa tecnológica para mitigar os impactos ambientais e também seguir vários dos princípios da química verde (Bourbigou, Magna e Morvan, 2010).

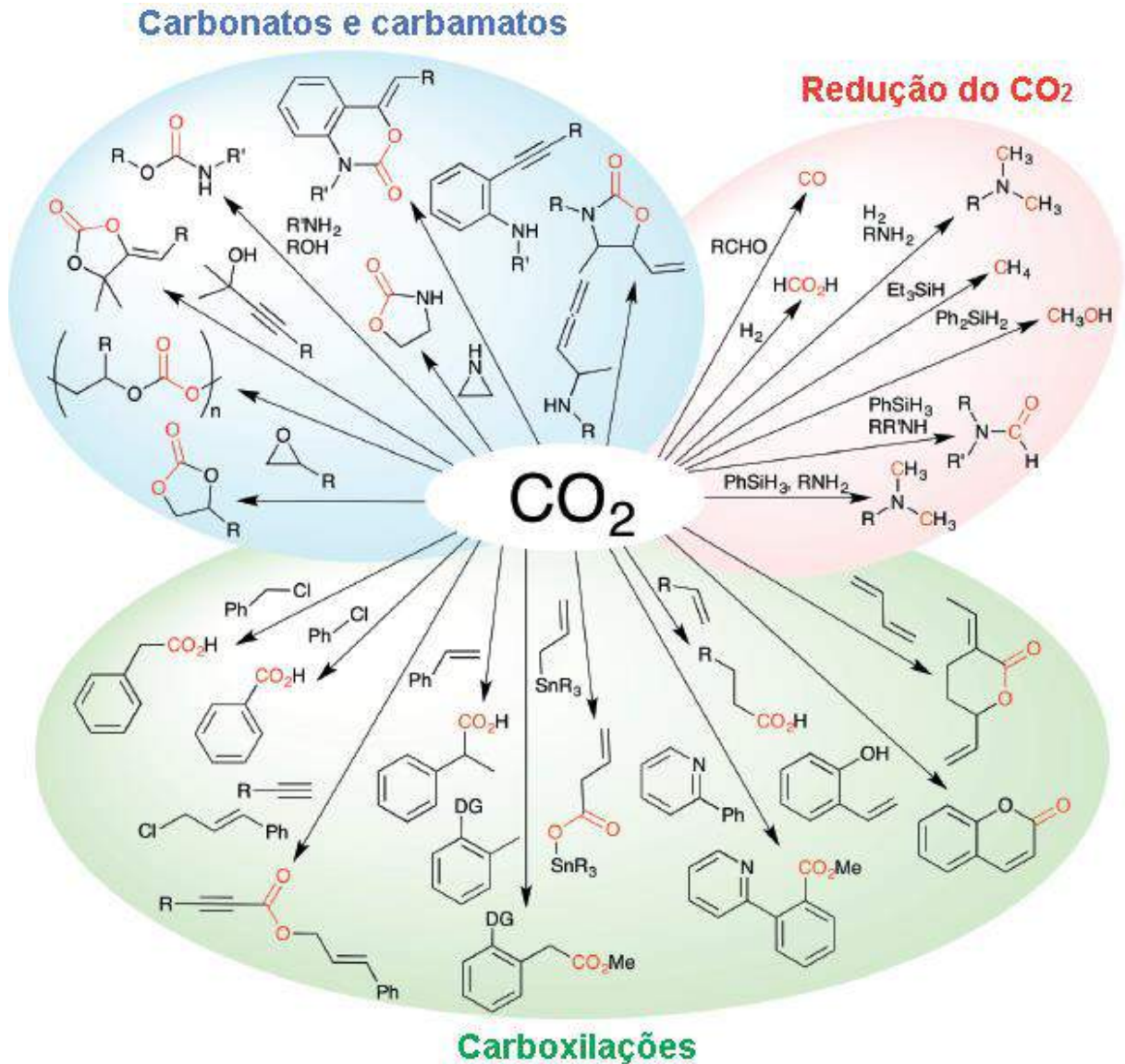


Figura 3.8. Possibilidades de reações de conversão de CO₂.

Fonte: Adaptação de Maeda, Miyazaki e Ema, 2014.

Uma rota bastante importante das várias possibilidades de transformações químicas do CO₂ é a carbonatação. Carbonatos orgânicos, também chamados de ésteres de ácido carbônico, formam um grupo de substâncias que contém uma carbonila rodeada por dois grupos alcóxi. Numa molécula, esses grupos podem ser

iguais, diferentes ou formar estruturas cíclicas (Sakakura, Choi e Yasuda, 2007; North, Pasquale e Young, 2010).

Os principais carbonatos orgânicos acíclicos (Figura 3.9) relatados na literatura são: carbonato de dimetila (DMC), carbonato de dietila (DEC) e o carbonato de difenila (DPC) (North, Pasquale e Young, 2010).

Já os carbonatos orgânicos cíclicos (Figura 3.10) mais reportados são: carbonato de propileno (PC), carbonato de estireno (SC), carbonato de glicidil isopropil éter (GC) e o carbonato de epicloridrina (EC) (North, Pasquale e Young, 2010).

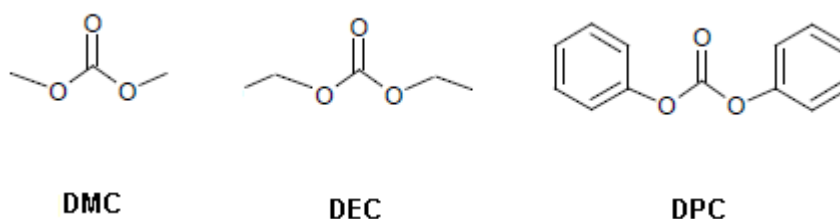


Figura 3.9. Alguns exemplos de carbonatos orgânicos acíclicos.

Fonte: Adaptação de North, Pasquale e Young, 2010.

São todos compostos com propriedades interessantes, pois são apolares, com elevado ponto de ebulição, baixa toxicidade e biodegradáveis (North, Pasquale e Young, 2010).

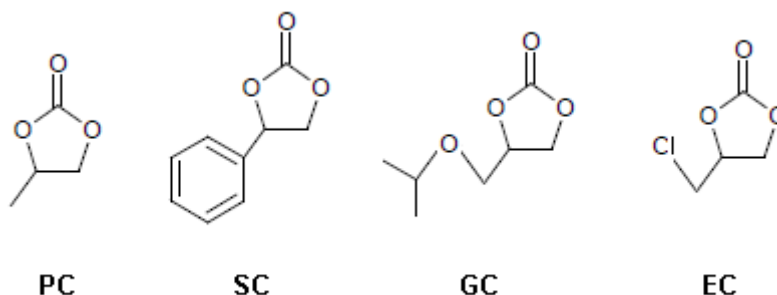


Figura 3.10. Alguns exemplos de carbonatos orgânicos cíclicos.

Fonte: Adaptação de North, Pasquale e Young, 2010.

Carbonatos orgânicos vêm ganhando espaço em diversos segmentos industriais por substituírem, sem grandes alterações, os solventes orgânicos voláteis (SOV). Um exemplo disso são as indústrias farmacêuticas que investem bastante em trabalho com materiais, os mais inertes possíveis, para síntese de fármacos (Leitner, 2009).

3.3. Líquidos Iônicos

Sempre é de interesse tecnológico a busca por novos materiais. Nas últimas décadas uma classe de solventes orgânicos, denominados líquidos iônicos, vem ganhando grande destaque no meio científico por substituírem com vantagens os tradicionais solventes orgânicos, sendo conhecidos assim como solventes verdes, além de possuírem grande potencial catalítico (Plechkova e Seddon, 2008).

Os Líquidos Iônicos (LIs) são sais orgânicos constituídos por um cátion orgânico e um ânion que pode ser orgânico ou inorgânico. São comumente líquidos a temperatura ambiente com baixo ponto de fusão e alto ponto de ebulição (Welton, 2004; Anout *et al.*, 2009; Earle e Seddon, 2000; Tarik *et al.*, 2009). Possuem propriedades como baixa pressão de vapor, baixa volatilidade e inflamabilidade, grande estabilidade química e térmica, boa condutividade iônica e grande potencial para serem regenerados (reciclados) (Huddleston *et al.*, 2001). A Tabela 3.3 apresenta dados (Ionic Liquid Database, 2006) de algumas propriedades dos líquidos iônicos comerciais das marcas Sigma Aldrich e Merck do Brasil de cátion imidazólio.

Tabela 3.3. Propriedades dos líquidos iônicos.

Propriedade	Líquidos Iônicos			
	[bmim][Cl]	[bmim][BF ₄]	[bmim][PF ₆]	[bmim][NTf ₂]
T fusão	67 °C	não informado	10 °C	não informado
T transição vítrea	- 69 °C	- 97 °C	- 80 °C	- 92 °C
Densidade	1080 kg/m ³	1120 kg/m ³	1360 kg/m ³	1414 kg/m ³
Viscosidade	40,890 Pa.s	0,154 Pa.s	0,450 Pa.s	0,599 Pa.s
Massa molar	174,67 g/mol	226,03 g/mol	284,18 g/mol	419,13 g/mol
Volume molar	não informado	1,90 x 10 ⁻⁴ m ³ /mol	2,05 x 10 ⁻⁴ m ³ /mol	não informado

Fonte: Ionic Liquid Database, 2006.

Estes materiais são promissores para diversas aplicações, pois com o estudo de sua estrutura e conhecimento das suas propriedades, é possível desenvolver combinações diferentes de cátions e ânions para conferir-lhes uma gama de características que se ajustem às condições de trabalho e a eventuais necessidades específicas de cada processo. Em função disso, os líquidos iônicos são popularmente chamados de “*solventes projetados*” (Blanchard, Gu e Brennecke, 2001; Welton, 2004; Antony *et al.*, 2005).

Originalmente a maioria das aplicações dos LIs tanto na pesquisa quanto na indústria eram voltadas à química verde como substitutos de solventes orgânicos, porém, estes vem encontrando um número crescente de aplicações em outras áreas, como: catálise, química orgânica e de polímeros, eletroquímica, química analítica, energia, nanotecnologia, biotecnologia, captura de CO₂, entre outros (Migliorini, 2009; Vieira, 2015).

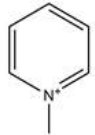
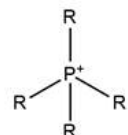
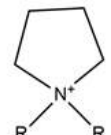
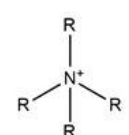
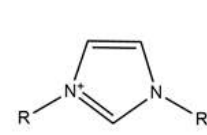
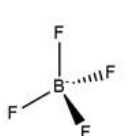
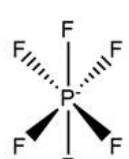
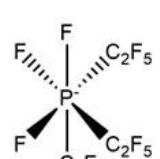
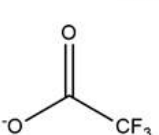
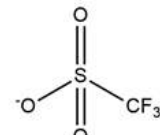
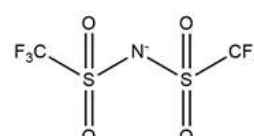
Historicamente, o primeiro líquido iônico foi sintetizado em 1914, o nitrato de etilamônio (ponto de fusão de 12 °C), formado pela adição de ácido nítrico concentrado a etilamina, porém este produto era muito instável em presença de ar ou água e isso foi uma limitação à sua utilização. Em 1982, foram preparados líquidos iônicos com base em cátions 1,3-dialquilimidazólio que eram estáveis na presença de água e ar em uma ampla faixa de temperatura, comumente referenciados como a “*segunda geração*” de líquidos iônicos (Wilkes *et al.*, 1982).

Seddon, em 1997, descreveu a utilização dos líquidos iônicos para síntese e processos catalíticos. Com este estudo se destacaram algumas propriedades, como a possibilidade combinações de cátions/ânions, que lhes permitem grandes vantagens, principalmente nos processos de extração (Blanchard *et al.*, 1999; Huddleston *et al.*, 2001).

Os líquidos iônicos mais comumente estudados são os sais baseados nos cátions imidazólio, piridínico, pirrolidínio, sais de amônio quaternário e os alquilfosfônios. Já os ânions amplamente utilizados na síntese de LIs são constituídos pela família dos halogênios, como cloretos ([Cl⁻]), brometos ([Br⁻]), iodetos ([I⁻]); os ânions fluorados como tetrafluoroborato ([BF₄⁻]), hexafluorofosfato

([PF₆⁻]) e, ainda os, trifluoroacetato ([CF₃CO₂⁻]), trifluorometilsulfonato ([CF₃SO₃⁻]) e bis(trifluorometilsulfonyl)imidato ([NTf₂⁻]) como se pode observar no Quadro 3.1 (Welton, 2004; Muldoon *et al.*, 2007; Rahman, Siaj e Larachi, 2010).

Quadro 3.1. Cátions e ânions mais comumente reportados na literatura.

Cátions						
	1-alkilpiridíneo	alquilfosfônio	1,1-dialquilpirrolidíneo	alquilamônio	1,3-dialquilimidazólio	
Ânions	Cl ⁻ cloreto	Br ⁻ brometo	I ⁻ iodeto			
				tetrafluoroborato	hexafluorofosfato	tris(perfluoroetil)trifluorofosfato
	trifluoroacetato	trifluorometilsulfonato	bis(trifluorometanosulfonyl)imidato			

Fonte: Adaptação de Rahman, Siaj e Larachi, 2010.

A síntese dos LIs pode ser de forma genérica simplificada em duas etapas. Na primeira há formação do cátion de interesse (Figura 3.11 a) e na segunda, a troca do ânion necessário para formação do produto final (Figura 3.11 b).

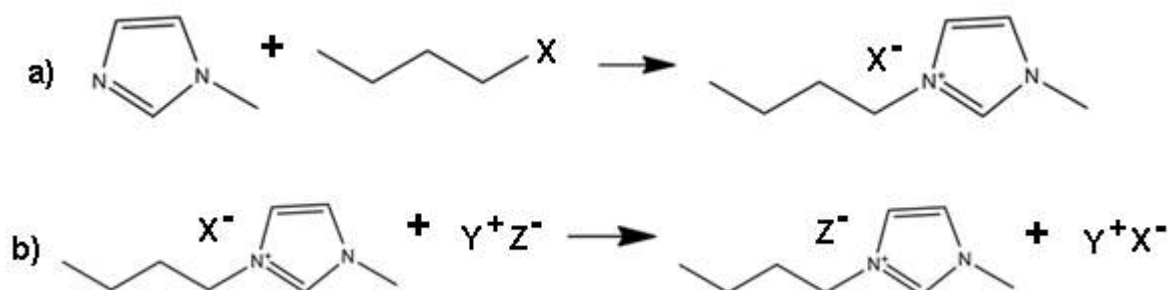


Figura 3.11. Esquema de formação: (a) cátion imidazólio e (b) troca de ânion.

Em determinados casos, somente a primeira etapa é necessária, como na síntese do nitrato do etilamônio, mas na maioria das vezes, é mais comum realizar a síntese em duas etapas: primeiro a formação do cátion desejado via protonação

com um ácido livre ou pela reação de quaternização de uma amina, muito comumente empregando um haloalcano; e depois proceder-se uma troca de ânion, que pode ser efetuada, tanto pela adição de um sal metálico contendo o ânion de interesse, ou pela adição de um ácido de Brønsted que contenha o ânion pretendido (Wasserscheid e Welton, 2008).

A quaternização de aminas com haloalcanos é conhecida há muitos anos, mas no que se refere ao desenvolvimento dos líquidos iônicos, tem despertado interesse em estudos para melhoria de técnicas reacionais. Em geral, as reações mais conhecidas utilizam cloroalcanos, bromoalcanos ou iodoalcanos, sendo elas, reações de substituição nucleofílica (Wang *et al.*, 2007).

A princípio, as reações de quaternização são bastante simples: a amina é adicionada ao agente de alquilação (em excesso) desejado e a mistura permanece sob agitação, aquecimento, refluxo e sob atmosfera inerte. A temperatura e o tempo de reação dependem do agente de alquilação utilizado. Normalmente nestas reações é imprescindível aquecimento durante um dia para reação completa (Wilkes *et al.*, 1982; Wang *et al.*, 2007).

Ao término da reação, faz-se necessária a remoção do excesso de haloalcano. Como normalmente estes são compostos bastante voláteis, sua retirada é feita facilmente sob pressão reduzida (Wasserscheid e Welton, 2008).

Os procedimentos descritos até então, compreendem somente a primeira etapa para síntese do líquido iônico, ou seja, a formação do cátion. A reação de troca do ânion pode ser realizada de duas formas: reação direta do sal halogenado com um ácido de Lewis, e/ou, através da formação do líquido iônico via “metátese aniônica”, mais conhecida como reação de dupla-troca, pois ocorre entre dois sais halogenados (Wasserscheid e Welton, 2008).

A reação de um sal halogenado quaternário com um ácido de Lewis resulta na formação de mais de uma espécie de ânion, dependendo da relação de proporção dos reagentes. Um exemplo deste tipo de reação é a obtenção de

líquidos iônicos com o ânion cloroaluminato a partir do cloreto de alumínio, que se procede em uma série de etapas em equilíbrio (Welton, 2004).

A obtenção do líquido iônico via metátese aniônica pode ser exemplificada pela preparação do [bmim][BF₄], a qual ocorre pela mistura do [bmim][Cl] com NaBF₄. O produto é extraído em diclorometano, depois é filtrado em coluna com alumina e seco sob atmosfera reduzida. Este tipo de reação pode ser executado desde o princípio em presença de solvente (diclorometano ou acetona), na forma de suspensão, pois os reagentes de partida não são solúveis no solvente e o rendimento aproximado é de 70%. O subproduto, NaCl neste caso, é insolúvel no solvente orgânico, sendo retirado por meio de uma filtração simples ao final da reação (Docherty, Dixon e Kulpa, 2007; Aquino, 2010).

Neste tipo de reação é comum permanecer algum resquício de haleto (cloreto) no líquido iônico, devendo este então, ser lavado diversas vezes com água para purificação até que as águas de lavagens deem teste negativo para cloreto utilizando nitrato de prata. Mesmo com estes processos de purificação, ainda pode permanecer resquícios na ordem de ppm ou ppb que podem ser prejudiciais ou benéficos dependendo do foco de utilização do líquido iônico (Wasserscheid e Welton, 2008).

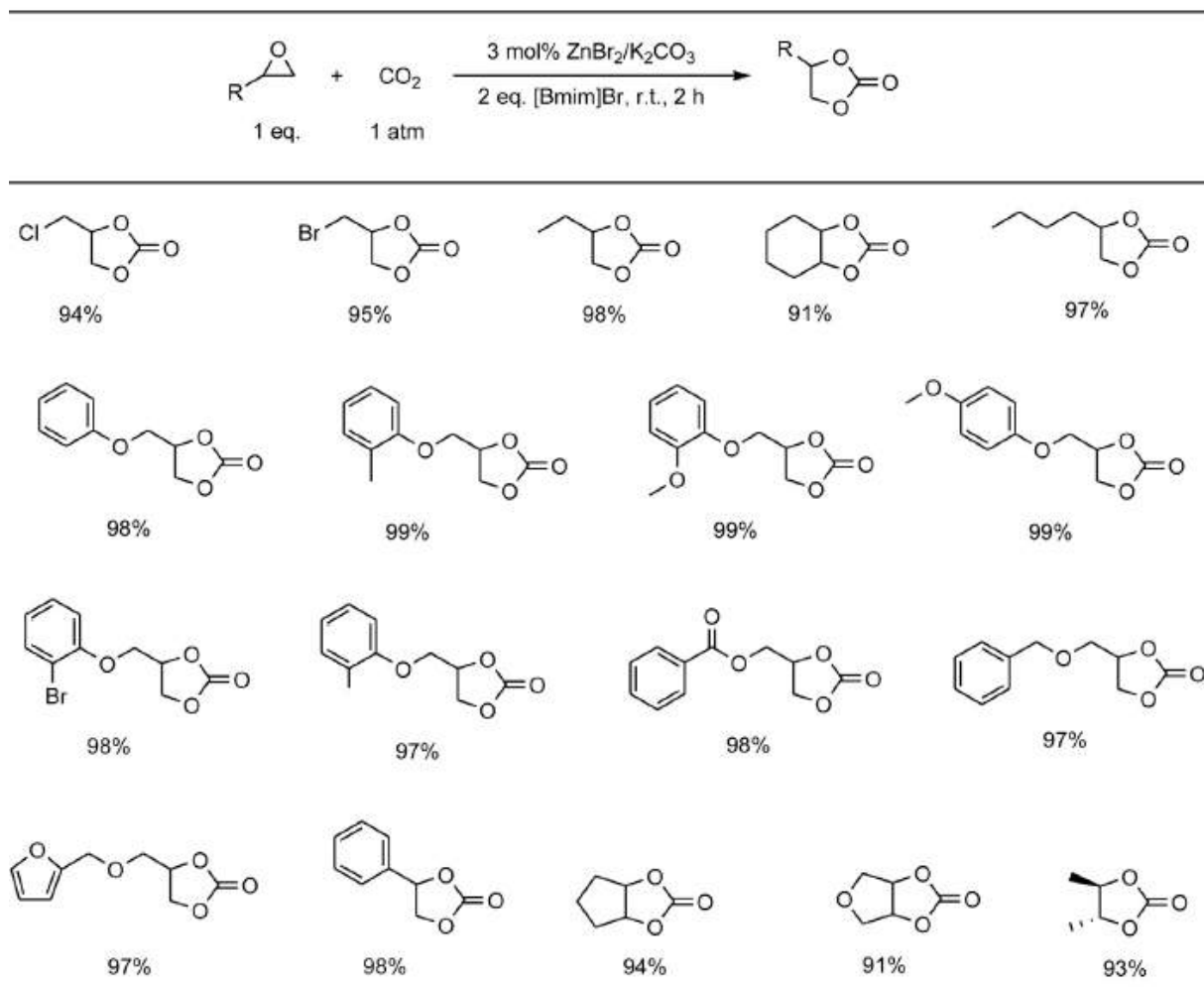
3.4. Líquidos iônicos para conversão de CO₂

Estudos anteriores já relatam o uso de líquidos iônicos na síntese de carbonatos acíclicos e cíclicos, na qual os LIs atuam como catalisadores (Sakakura e Kohno, 2009; Yang *et al.*, 2010; Aquino *et al.*, 2014; Vieira *et al.*, 2017). Eta *et al.*, 2011, sintetizaram carbonato de dimetila e constataram que a utilização dos LIs aumenta cerca de 12% na conversão e atinge 90% de seletividade para o carbonato desejado.

Um estudo conduzido por Zhang *et al.* (2016) apresenta o líquido iônico [bmim][Br] como catalisador em um sistema ternário associado a ZnBr₂ e K₂CO₃ para conversão química de CO₂ em carbonatos cíclicos. A Tabela 3.4 apresenta os resultados de rendimento obtidos. Foi relatado também, que as seletividades para

os produtos desejados foram todas > 99% (Zhang *et al.*, 2016), sendo assim, os valores de rendimento são os mesmos de conversão.

Tabela 3.4. Resultados de rendimento obtidos por Zhang *et al.* (2016) para cicloadição de CO₂ em epóxidos.

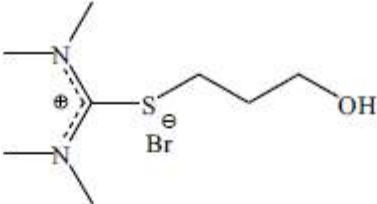
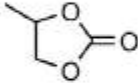
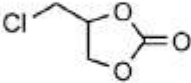
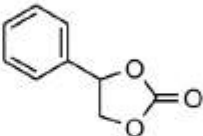
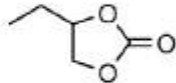
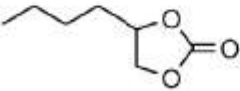
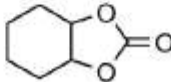


Fonte: Adaptação de Zhang *et al.* 2016.

Um diferencial deste estudo são as condições de trabalho escolhidas, como baixa pressão e temperatura. Podemos ver que os valores de rendimento nas sínteses destes diversos carbonatos cíclicos são excelentes, sendo todas superiores a 90%. A presença de grupos funcionais no epóxido de partida, como cloretos, brometos e fenilas não alteraram de forma significativa os rendimentos reacionais, indicando que o volume molecular ou a eletronegatividade da cadeia lateral do epóxido não causa influência expressiva.

Dai *et al.* (2017) também estudaram a cicloadição de CO₂ em epóxidos utilizando o líquido iônico [TMTc₃H₆OH][Br] como catalisador. Os resultados de conversão e seletividade são apresentados na Tabela 3.5.

Tabela 3.5. Resultados (conversão e seletividade) de Dai *et al.* (2017) para cicloadição de CO₂ em epóxidos.

Catalisador [TMTc ₃ H ₆ OH] ⁺ Br ⁻					
					
98,0% / 99,9%	98,1% / 99,7%	96,6% / 99,8%	99,2% / 100%		
					
	95,5% / 100%	72,7% / 99,7%			

Fonte: Adaptação de Dai *et al.*, 2017.

Estes ensaios foram conduzidos a 140 °C e 20 bar de pressão. Os resultados para maioria dos carbonatos foram completamente satisfatórios, tanto em conversão quanto em seletividade, com exceção do carbonato oriundo do óxido-ciclohexeno que apresentou 72,7% de conversão. Esse fato é explicado pelo impedimento do ataque nucleofílico do ânion brometo do LI devido a presença dos dois anéis (Dai *et al.*, 2017).

É importante destacar que variáveis como temperatura e pressão são fatores determinantes para o sucesso das reações (Ju *et al.* (A)(B), 2007; Dong *et al.*, 2008).

3.5. Influência da temperatura na formação de carbonatos cíclicos

Dai *et al.* (2017) fizeram o estudo da influência da temperatura na síntese do carbonato de propileno, partindo do CO₂ + óxido de propileno, e concluíram que com o aumento da temperatura, o rendimento é bastante favorecido com manutenção dos altos valores de seletividade. Os resultados do grupo são apresentados na Figura 3.12 e as condições reacionais foram: 35,7 mmol de PO, 20 bar de pressão de CO₂, 1 mmol% de catalisador ([TMTC₃H₆OH]Br) por 2 horas.

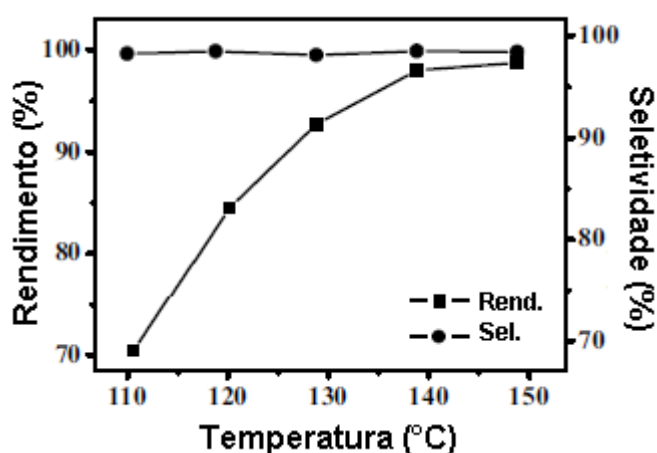


Figura 3.12. Influência da temperatura na reação do PC utilizando o líquido iônico [TMTC₃H₆OH]Br sintetizado por Dai *et al.* 2017.

Fonte: Adaptação de Dai *et al.*, 2017.

Esta dependência da temperatura se deve ao fator cinético, ou seja, com a maior agitação das moléculas de CO₂ e óxido de propileno, maior a chance de formação de produtos (Dai *et al.* 2017).

Um estudo recente (2018) mostrou a influência da temperatura na formação de carbonatos distintos e os resultados podem ser observados na Figura 3.13.

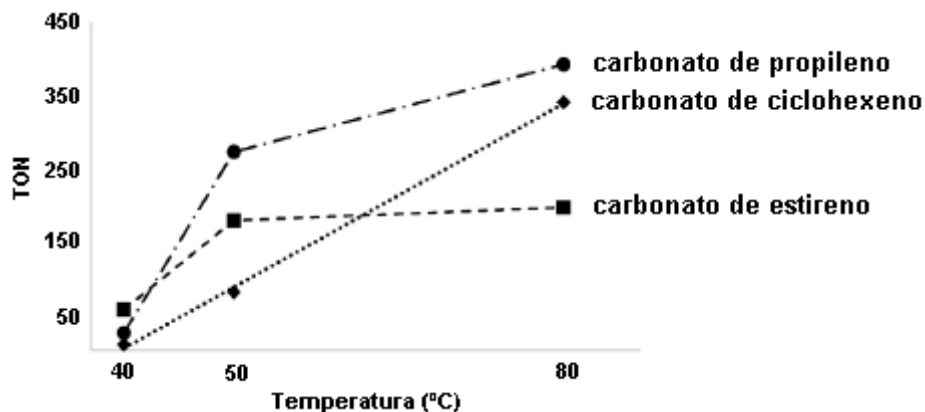


Figura 3.13. Reação de formação de carbonatos cíclicos em 3 horas e 40 bar utilizando [TBA][Br] como catalisador.

Fonte: Adaptação de Paninho *et al.*, 2018.

Os autores do estudo relatam que em todos os casos, a seletividade ao produto desejado foi superior a 95%. Podemos observar pelo ângulo da reta que o óxido de propileno foi altamente reativo pois a formação de carbonato de propileno é bem acentuada (Paninho *et al.*, 2018). Já em relação ao carbonato de estireno, visivelmente não há necessidade de um gasto energético muito elevado, pois em baixa temperatura (50 °C) ele já se encontra em equilíbrio (Paninho *et al.*, 2018).

3.6. Influência da pressão de CO₂ na formação de carbonatos cíclicos

A pressão é um dos fatores que mais fortemente afeta a conversão de epóxidos com CO₂ a carbonato (Felix, 2013). Dai *et al.* (2017) fizeram o estudo da influência da pressão na síntese do carbonato de propileno, partindo do CO₂ + óxido de propileno, e concluíram que o acréscimo de pressão resultou em um aumento rápido da produção de PC em menores pressões (até 20 bar), enquanto que uma diminuição moderada do rendimento em alta pressão (20 - 30 bar) é observada. Os resultados do grupo são apresentados na Figura 3.14 e as condições reacionais foram: 35,7 mmol de PO, 140 °C de temperatura, 1 mmol% de catalisador ([TMTC₃H₆OH]Br) por 2 horas.

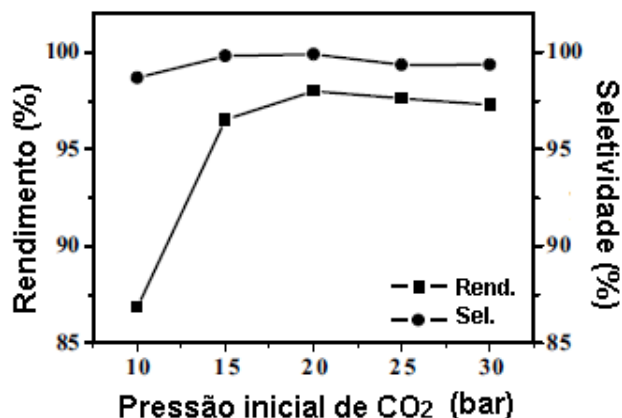


Figura 3.14. Líquido iônico [TMTc₃H₆OH]Br sintetizado por Dai *et al.* 2017.

Fonte: Adaptação de Dai *et al.*, 2017.

Como a difusão de gás pode ter um efeito sobre a cinética da reação e na transferência de massa, houve uma faixa ótima de pressão de CO₂ para o rendimento máximo de PC. A leve diminuição de rendimento em pressões mais elevadas, segundo os autores, está relacionada a maior dissolução do CO₂ na fase líquida, pois o CO₂ começaria a competir com o óxido de propileno a vizinhança do catalisador. Sendo assim, o contato do reagente com o catalisador pode estar desfavorecido (Dai *et al.*, 2017). A sutil diminuição da seletividade também é em função da maior dissolução do CO₂ na fase líquida, pois assim, favorece reações competitivas (Dai *et al.*, 2017).

Ainda há discussão em relação ao comportamento físico dos reagentes sob pressão. Sun *et al.* (2004) estudou a fundo a influência da pressão no rendimento através da síntese do carbonato de estireno (SC). Para isso ele variou a pressão de zero até 18 MPa utilizando 17,3 mmol de óxido de estireno, 2 mmol de catalisador ([TBA][Br]), 80 °C de temperatura durante 6 horas. Os resultados podem ser observados na Figura 3.15 e mostram que o rendimento diminui fortemente entre 1 e 2 MPa e depois demonstra um comportamento complicado. O rendimento máximo de carbonato de estireno acontece em 1 MPa, 8 MPa e 15 MPa como mostra a Figura 3.15 (f). Para melhor compreensão destes resultados, a reação foi observada por janelas de safira, como ilustrado nos itens (a), (b), (c) e (d) da respectiva Figura.

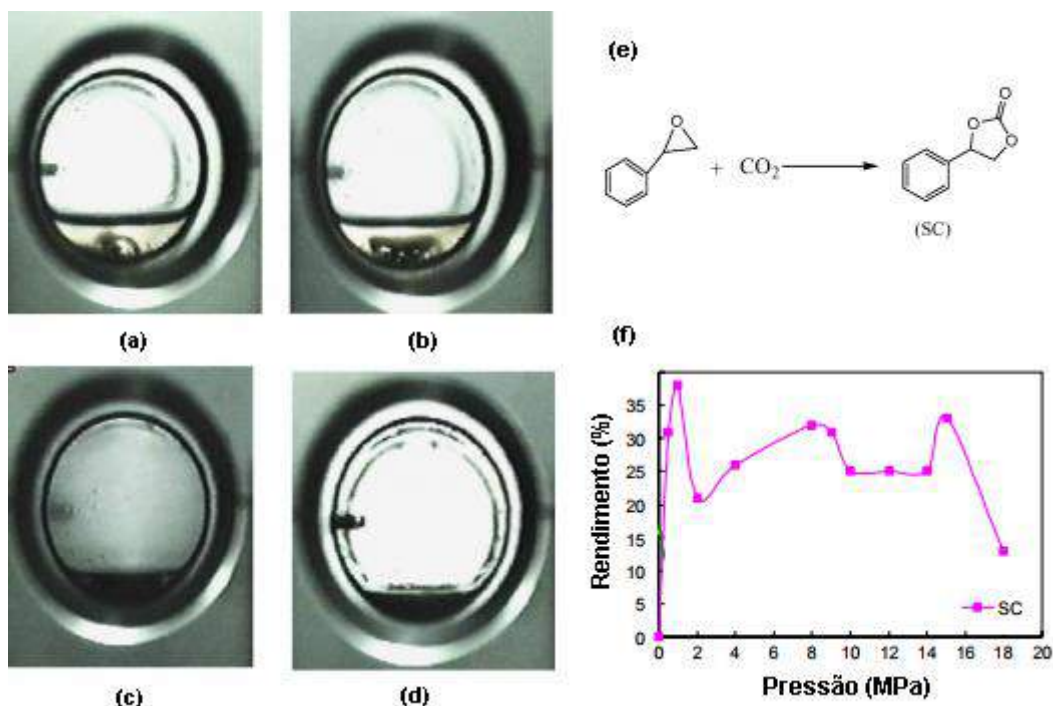


Figura 3.15. Fotografia da influência da pressão na formação do SC onde (a) 4 MPa, (b) 8 MPa, (c) 15 MPa e (d) 18 MPa; (e) esquema da reação e (f) rendimento com variação de pressão.

Fonte: Adaptação de Sun *et al.*, 2004.

A mistura permanece em três fases nas pressões abaixo de 15 MPa (a) e (b), opaco a 15 MPa (c) e transparente a 18 MPa (d). A reação geral depende do volume e propriedades das fases, a concentração de espécies que reagem nessas fases e o estado de contato entre essas fases. Com pressões de CO_2 mais baixas, o volume das fases dificilmente mudou, mas a concentração de CO_2 na fase orgânica aumentou com a pressão. Essa mudança pode ser responsável para o primeiro aumento do rendimento de SC até 1 MPa. A introdução adicional de CO_2 possivelmente causa uma diluição das outras espécies que reagiram na fase orgânica e, provavelmente, isso faz com que diminua o rendimento do SC em 2 MPa (Sun *et al.*, 2004).

Com pressões de CO_2 mais elevadas, o volume e as propriedades das fases mudam e vários outros fatores passam a se tornar significativos. O segundo pico máximo de rendimento aparece ao redor 8 MPa, próximo da pressão crítica do CO_2 . Alguns outros estudos relatam melhora de resultados nesta faixa (Arai, Nishiyama e Ikushima, 1998). Com 18 MPa, o sistema de reação estava em fase homogênea supercrítica e, portanto, o contato entre as espécies melhoraria em comparação com

o sistema multifásico. Porém, em 18 MPa, a baixa concentração de reagentes foi novamente responsável pela diminuição de rendimento de SC, além de que começam formações bem significativas de alguns oligômeros (Sun *et al.*, 2004).

Ainda neste contexto do comportamento das fases durante a reação, Felix (2013) sintetizou carbonato de propileno partindo de 2 mL de óxido de propileno durante seis horas e a uma temperatura de 80 °C. Como se pode observar na Figura 3.16, a conversão máxima é atingida numa pressão de 100 bar. A partir deste ponto, a conversão diminui até atingir um valor mínimo de 30% a 150 bar. Com a continuação do aumento da pressão, a conversão aumenta novamente, e essa tendência se mantém até 180 bar.

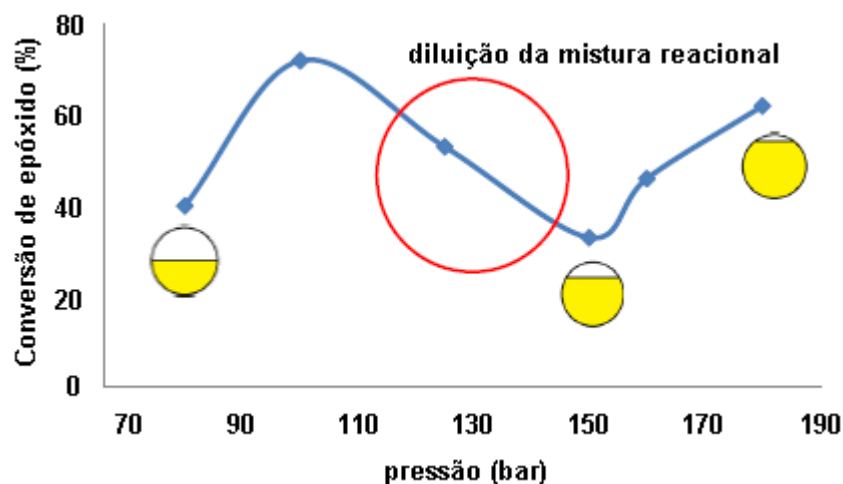


Figura 3.16. Gráfico da conversão de epóxido em função da pressão.

Fonte: Adaptação de Felix, 2013.

Estes resultados podem estar relacionados com o fato de inicialmente estarmos numa zona em que a adição de CO₂ provoca uma diluição da mistura reacional, portanto, diminuição da conversão (fase destacada no gráfico por um círculo). No entanto, à medida que nos aproximamos da região supercrítica da mistura, a conversão volta a subir consideravelmente (Felix, 2013).

Temos, portanto, um sistema reacional bifásico, em que a fase reacional é um líquido que se expande com o aumento da pressão, no qual o catalisador está totalmente dissolvido, sendo assim, uma catálise homogênea (Felix, 2013).

3.7. Influência do tempo na formação de carbonatos cíclicos

Um estudo da influência do tempo na síntese do carbonato de propileno, partindo do CO₂ + óxido de propileno (PO) foi realizado por Dai *et al.* (2017). As condições reacionais foram: 35,7 mmol de PO, 20 bar de pressão de CO₂, 140 °C e 1 mmol% de catalisador ([TMTC₃H₆OH]Br) e os resultados mostrados na Figura 3.17.

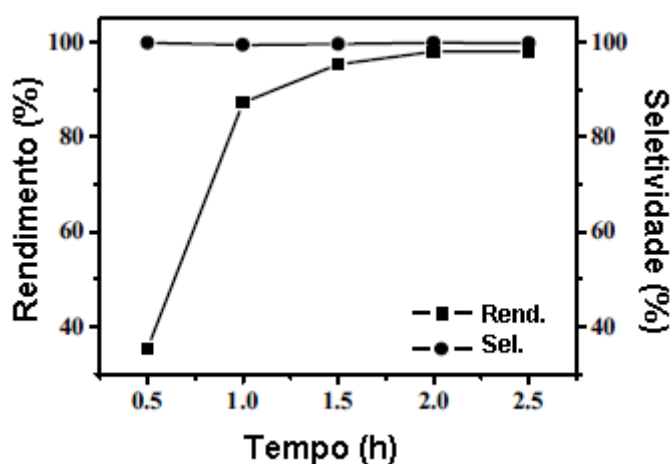


Figura 3.17. Influência do tempo na conversão do óxido de propileno utilizando o líquido iônico [TMTC₃H₆OH]Br sintetizado por Dai *et al.* 2017.

Fonte: Adaptação de Dai *et al.*, 2017.

No gráfico notamos que a reação de cicloadição prossegue rapidamente na primeira hora de reação, atingindo um rendimento de PC de 87,3%. A partir deste ponto, o rendimento do PC torna-se gradualmente lento. O aumento adicional de tempo de reação resulta em quase nenhum aumento de produção de PC. Em todos os tempos, a seletividade fica próxima a 99%.

A influência do tempo na maioria destas cicloadições tradicionais se deve a fatores cinéticos, quanto maior o tempo de reação, maior o rendimento (Dai *et al.*, 2017).

4. PROCEDIMENTOS EXPERIMENTAIS E RESULTADOS

Nesta secção, em forma de artigo, serão apresentados os métodos, resultados e discussões pertinentes a essa tese, divididas da seguinte forma:

- Capítulo I: Motivação e informações relevantes dos líquidos iônicos sintetizados.
- Capítulo II: Interação de quatro líquidos iônicos ([bmim][C₁₂SO₄], [bmim][C₁₂ESO₄], [TBA][C₁₂SO₄] e [TBA][C₁₂ESO₄]) com a água. Estes resultados foram publicados no *Journal of Molecular Liquids*.
- Capítulo III: Utilização dos oito líquidos iônicos sintetizados para aplicação na síntese do carbonato de propileno (PC). Estes resultados foram publicados na revista *Catalysis Letters*.
- Capítulo IV: Utilização dos oito líquidos iônicos sintetizados para aplicação na síntese do carbonato de estireno (SC), carbonato de glicidil isopropil éter (GC) e carbonato de epícloridrina (EC). Estes resultados no momento da Defesa de Tese encontram-se submetidos sob revisão em revista internacional especializada da área.

4.1. Capítulo I

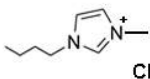
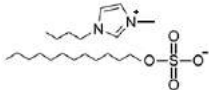
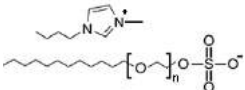
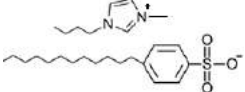
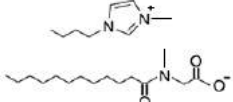
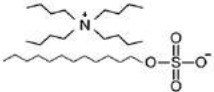
A busca por materiais de baixo custo foi a principal motivação para a escolha dos líquidos iônicos que foram desenvolvidos nesta tese. É de conhecimento geral que líquidos iônicos são materiais versáteis, “verdes” e de alto custo de síntese, por isso a grande dificuldade em torná-los mais populares. Pensando nisso, foi utilizado

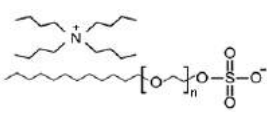
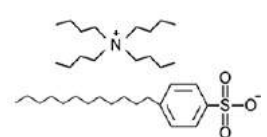
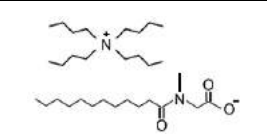
os dois cátions mais comumente reportados na literatura e de menor custo, o [bmim⁺] e [TBA⁺], mas não foi estudado modificações nos cátions. Quanto a escolha dos ânions, geralmente o componente que mais eleva o valor do líquido iônico, foi escolhido surfactantes aniônicos comerciais, abundantes e de baixo valor, como o dodecil sulfato de sódio ([NaC₁₂SO₄]), dodecil éter sulfato de sódio ([NaC₁₂ESO₄]), dodecil benzeno sulfonato de sódio ([NaC₁₂BSO₃]) e a lauroil sarcosina ([NaC₁₂SAR]).

4.1.1. Características dos líquidos iônicos

Na Tabela 4.1 são apresentadas as características físicas dos líquidos iônicos sintetizados, como a aparência e solubilidade em água. Nesta Tabela também contém informações do rendimento reacional da síntese de cada um dos LIs.

Tabela 4.1. Dados reacionais da síntese e características físicas dos líquidos iônicos.

Síntese do LI MM (g.mol ⁻¹)	Estrutura do LI	Rendimento Reacional	Aparência do LI	Solubilidade do LI em água
[bmim][Cl] MM = 174,45		84%	Sólido branco amarelado altamente higroscópico	Solúvel
[bmim][C ₁₂ SO ₄] MM = 404,38		47%	Líquido amarelo translúcido extremamente viscoso	Solúvel
[bmim][C ₁₂ ESO ₄] MM = 535,95		76%	Líquido amarelo translúcido viscoso	Solúvel
[bmim][C ₁₂ BSO ₃] MM = 464,94		81%	Sólido amarelo translúcido gelatinoso	Solúvel
[bmim][C ₁₂ SAR] MM = 409,33		63%	Líquido amarelado translúcido viscoso	Solúvel
[TBA][C ₁₂ SO ₄] MM = 507,85		87%	Líquido transparente viscoso	Insolúvel

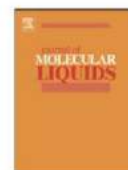
[TBA][C ₁₂ ESO ₄] MM = 639,48		90%	Líquido transparente viscoso	Solúvel
[TBA][C ₁₂ BSO ₃] MM = 568,06		92%	Sólido transparente ceroso	Solúvel
[TBA][C ₁₂ SAR] MM = 512,90		79%	Líquido transparente viscoso	Solúvel

O baixo rendimento reacional do [bmim][C₁₂SO₄] é devido a etapa de lavagem com água. Nesta etapa, o líquido iônico que se encontra dissolvido em diclorometano, tende a formar muita emulsão com a adição da água e esta emulsão é de difícil desestabilização, mesmo permanecendo várias horas em repouso para separação das fases. Parte desta emulsão é descartada com a fase aquosa, sendo eliminado assim, o líquido iônico que está emulsionando os solventes.

4.2. Capítulo II

Tendo em vista que este trabalho está vinculado a um projeto de pesquisa Petrobras intitulado “*Avaliação de líquidos iônicos miscíveis em água para captura de CO₂ em gás natural*”, havia a necessidade de testar os líquidos iônicos sintetizados em água. É sempre de interesse comercial, a fim de baratear despesas de processos, que materiais de mais elevado custo sejam diluídos em água desde que ainda mantenham suas propriedades e seu propósito, como no caso da captura de CO₂, por exemplo. Sendo assim, neste primeiro artigo foi estudado o comportamento físico-químico de quatro líquidos iônicos em água, sendo eles: [bmim][C₁₂SO₄], [bmim][C₁₂ESO₄], [TBA][C₁₂SO₄] e [TBA][C₁₂ESO₄]. Descobriu-se um comportamento bastante peculiar dos LIs de cátion [bmim⁺] quando em contato com água, a interação entre eles foi tão intensa que fez com que a viscosidade da solução aumente até 5000x, como foi observado no [bmim][C₁₂ESO₄] quando na concentração de 80%.

Este artigo intitulado "*Ionic liquids composed of linear amphiphilic anions: synthesis, physicochemical characterization, hydrophilicity and interaction with carbon dioxide*", DOI: 10.1016/j.molliq.2017.06.006, foi publicado em 2017 no *Journal of Molecular Liquids*, ISSN: 0167-7322.



Ionic liquids composed of linear amphiphilic anions: Synthesis, physicochemical characterization, hydrophilicity and interaction with carbon dioxide



Michele O. Vieira^a, Wesley F. Monteiro^a, Rosane Ligabue^a, Marcus Seferin^a, Vitaly V. Chaban^b, Nadezhda A. Andreeva^c, Jailton F. do Nascimento^d, Sandra Einloft^{a,*}

^a Post-Graduation Program in Materials Engineering and Technology, Pontifical Catholic University of Rio Grande do Sul - PUCRS, Brazil

^b Institute of Science and Technology (ICT), Federal University of São Paulo (UNIFESP), São José dos Campos, SP, Brazil

^c PRAMO, St. Petersburg, Leningrad Oblast, Russian Federation

^d Petrobras/CENPES, Ilha do Fundão Qd. 07, Rio de Janeiro, RJ, Brazil

ARTICLE INFO

Article history:

Received 6 January 2017

Received in revised form 4 May 2017

Accepted 1 June 2017

Available online 3 June 2017

Keywords:

Ionic liquids
Surfactant
Surface active ionic liquids
Amphiphilic anions, carbon dioxide

ABSTRACT

Development of new task-specific ionic liquids (ILs) constitutes an important goal in chemistry and chemical technology. We hereby report four surface active ILs (SAILs) composed of the well-known cations (1-butyl-3-methylimidazolium [bmim⁺], tetrabutylammonium [TBA⁺]) and long-alkyl-chain anions (lauryl sulfate [C₁₂SO₄⁻], lauryl ether sulfate [C₁₂ESO₄⁻]). Thermal stabilities, viscosities, interactions with water and polarized optical microscopy (POM) were investigated suggesting that new SAILs are highly viscous and thermally stable until 180 °C. [bmim][C₁₂SO₄], [bmim][C₁₂ESO₄] and [TBA][C₁₂ESO₄] are miscible with water, whereas [TBA][C₁₂SO₄] is immiscible. Ab initio calculations were employed to characterize hydrophilicity/hydrophobicity balance of all four compounds, the results being in concordance with our experimental observations. [bmim][C₁₂SO₄] and [bmim][C₁₂ESO₄] normally exhibit non-Newtonian behaviors and form liquid crystals (LCs) with water, but [TBA][C₁₂SO₄] and [TBA][C₁₂ESO₄] are Newtonian liquids. Using semiempirical molecular dynamics simulations, we show that the sulfate group of the synthesized SAILs exhibits certain potential to capture dissolved CO₂.

© 2017 Elsevier B.V. All rights reserved.

1. Introduction

Ionic liquids (ILs) are composed of organic cations and organic or inorganic anions. These compounds present melting points below 100 °C, practically no vapor pressure, high thermal and chemical stability, ionic conductivity, recyclability and tunable properties depending on the cation/anion components [1–5].

Water addition to ILs has been extensively studied in order to improve their properties, such as viscosity and density [1–2,6–9]. Another relevant benefit of the IL dilution is a significant reduction of total costs, since the prices of ILs still remain high, reaching, for instance, \$700.00 kg⁻¹ for the acetate ILs, \$300.00 kg⁻¹ for the chloride ILs [10–11]. Development of less expensive ILs would lower engineering costs and, therefore, foster more intensive ILs usage in the industrial processes.

Surface active ionic liquids (SAILs) constitutes a class of ILs that in the last years has been quite developed. SAILs contain significantly long hydrophobic (tensoactive) chains in cation, anion, or both [12–26].

Most ILs cations, such as imidazolium, pyrrolidinium, pyridinium, and quaternary ammonium, possess amphiphilic structures, provided that they contain sufficiently long side chains [27–28]. A long chain, C₆–C₁₆, in imidazolium cations act as an emulsifier providing surface activity and improving IL solubility in hydrophobic media. The hydrophobic chain, furthermore, facilitates preparation of microemulsions containing aggregates of peculiar structures, shapes, and physicochemical properties [13–16,18,21–22,25,27]. The long-chained anions behave similarly to the cations [18–19,23–24,29] and modulate surface activity [18,23]. Such ILs are thermodynamically stable and form self-organized structures, such as micelles, microemulsions, vesicles, and liquid crystals (LCs) [18,23,27,30–31]. Gels can also be produced by [C₁₀mim][Br] and [C₁₀mim][NO₃] in their aqueous solutions, e.g. [C₁₆mim][Cl]–H₂O [27,32–35], and in binary mixtures of different ILs. As noted elsewhere [36], a ternary system containing [C₁₆mim][Cl], sodium dodecyl sulfate (SDS), and water forms a gel phase at about 90% of water content.

Common surfactants, such as SDS, sodium dodecyl ether sulfate (SDES), and sodium dodecyl benzene sulfonate (SDBS), as well as

* Corresponding author.

E-mail address: einloft@pucrs.br (S. Einloft).

SAILs based on these compounds can find numerous applications in industrial segments, such as proteins processing, pharmaceuticals, cosmetics, paints, coatings, detergents, and various biochemical segments [37–40].

Many ILs interact strongly with carbon dioxide, CO₂, being thus actively pursued as greenhouse gas scavengers [41–43]. Design of highly selective ILs for CO₂ sorption can be performed by combining specifically tuned cationic and anionic structures [44–47]. It was reported that water addition in ILs foster CO₂ capture by facilitating the gas diffusibility into the medium [48–50]. We hereby report syntheses of four SAILs based on the imidazolium ([bmim]⁺) and tetrabutylammonium ([TBA]⁺) cations coupled with tensoactive anions, SDS ([C₁₂SO₄⁻]) and SDES ([C₁₂ESO₄⁻]). For the first time, we report physicochemical properties of these SAILs in their pure state and in aqueous mixtures. Furthermore, based on the physicochemical properties we evaluated the CO₂ sorption potential of SAILs using semiempirical molecular dynamics simulations as a prospective application.

2. Methodology

2.1. Materials

1-methylimidazole (Sigma Aldrich, 99.0%), acetone (Vetec, 98.0%), dichloromethane (Vetec, 99.0%), methanol HPLC (99.9%), tetra-n-butylammonium bromide (Panreac, 98.0%), 1-chlorobutane (Acros Organics, 99.0%), sodium lauryl sulfate (Synth, 90.0%), sodium lauryl ether sulfate (Synth, 50.0%), were used as purchased.

2.2. Characterization of the new surface active ionic liquids

The obtained compounds were characterized Fourier transform infrared spectroscopy using universal attenuated total reflectance sensor (UATR-FTIR) with Perkin-Elmer spectrophotometer model 100 FT-IR Spectrum. Nuclear magnetic resonance (NMR) measurements were performed in Bruker Spectrophotometer, operating at 600 MHz, using DMSO-*d*₆ as solvent and glass tubes of diameter 5 mm. The differential scanning calorimetry (DSC) analyses were carried out in TA Instruments Q20 by scanning temperatures from -90 °C to 300 °C at heating/cooling/heating rate of 10 °C/min in nitrogen atmosphere. Thermogravimetric analysis (TGA) analyses were carried out in TA Instruments Q600 with a heating rate of 20 °C min⁻¹, from 25 to 1000 °C in the nitrogen atmosphere. The moisture contents of SAILs were determined by Karl Fisher method using a KF-1000 Analyzer (Brazil) and Karl Fischer reagent without pyridine (Merck) as titrating solution and methanol as solvent. The chloride (Cl⁻) content was performed in a portable Vernier LabQuest system with a specific sensor for this ion. The sodium (Na⁺) content was determined by atomic absorption spectroscopy (AAS) by Varian AAS 55 spectrometer with an air/acetylene flame (99.99% Air Products). The viscosity analysis was carried out using Haake RotoVisco 1 at 30 and 60 °C using plate-cone geometry (Ti spindle d = 20 mm, 0.5°), with shear rate from 0 to 30 s⁻¹ during 5 min. Birefringence was detected by Zeiss Axioskop 40 (Carl Zeiss, Oberkochen, Germany) polarizing optical microscope (POM) equipped with CoolSnap Pro videocamera (Media Cybernetics, Bethesda, MD, USA). The device was connected to computer with a plaque Image Pro Capture Kit. Images were captured using the ×20 objective.

2.3. Synthesis of surface active ionic liquids

The ionic liquid 1-butyl-3-methylimidazolium chloride [bmim][Cl] was synthesized following procedures developed elsewhere [51–53].

[bmim][Cl] - FTIR ν (cm⁻¹): 3137–3045 (C–H aromatic), 2957 (C–H of CH₂), 2871 (C–H of CH₃), 1634 (C=N aromatic), 1567–1463 (C=C aromatic), 1231 (C–N aromatic), 1169 (C–N alifatic), 754 (Cl). ¹H NMR (600 MHz, DMSO-*d*₆) δ (ppm): 9.31 [s, 1H]; 7.86 [d, 1H, J = 1.8 Hz]; 7.80 [d, 1H, J = 1.6 Hz]; 4.25 [t, 2H, J = 7.2 Hz]; 3.94 [s, 3H];

1.91–1.76 [m, 2H, J = 14.9; 7.5 Hz]; 1.33 [dt, 2H, J = 14.7; 7.3 Hz]; 0.97 [t, 3H, J = 7.3 Hz].

1-butyl-3-methylimidazolium lauryl sulfate [bmim][C₁₂SO₄] and 1-butyl-3-methylimidazolium lauryl ether sulfate [bmim][C₁₂ESO₄] were obtained using an equimolar mixture of 1-butyl-3-methylimidazolium chloride and sodium lauryl sulfate for [C₁₂SO₄] and sodium lauryl ether sulfate for [C₁₂ESO₄]. The reactants were dissolved in water and kept at 333.15 K during 12 h. Water was removed from the reaction mixture after reaction completion using reduced pressure. The product was extracted with dichloromethane and washed with water for several times to achieve a complete removal of chloride ions (monitored with acidic solution of AgNO₃) and complete desiccation at 363.15 K for 6 h in the drying oven.

[bmim][C₁₂SO₄] - FTIR ν (cm⁻¹): 3178–3126 (C–H aromatic), 2970 (C–H of CH₂), 2897 (C–H of CH₃), 1628 (C=N aromatic), 1579–1471 (C=C aromatic), 1286 (C–N aromatic), 1172 (C–N alifatic), 1042 (S=O). ¹H NMR (600 MHz, DMSO-*d*₆) δ (ppm): 9.10 [s, 1H]; 7.75 [d, 1H]; 7.69–7.67 [d, 1H]; 4.16 [t, 2H, J = 6.9 Hz]; 3.85 [s, 3H]; 3.86 [t, 2H, J = 6.3 Hz]; 1.82–1.68 [m, 2H, J = 14.9; 7.5 Hz]; 1.48 [dt, 2H, J = 14.7; 7.3 Hz]; 1.24 [s, 20H]; 0.95–0.81 [m, 6H]. Moisture content = 1.43%, residual Cl⁻ = 0.08%, residual Na⁺ = 0.2%.

[bmim][C₁₂ESO₄] - FTIR ν (cm⁻¹): 3158–3120 (C–H aromatic), 2966 (C–H of CH₂), 2882 (C–H of CH₃), 1628 (C=N aromatic), 1568–1459 (C=C aromatic), 1282 (C–N aromatic), 1215 (C–O), 1170 (C–N alifatic), 1019 (S=O). ¹H NMR (600 MHz, DMSO-*d*₆) δ (ppm): 9.11 [s, 1H]; 7.77 [d, 1H]; 7.70 [d, 1H]; 4.17 [t, 2H, J = 6.8 Hz]; 3.78 [s, 3H]; 3.86 [t, 2H, J = 15.7 Hz]; 3.54–3.41 [dt, 4H]; 1.82–1.70 [m, 2H, J = 13.4; 7.5 Hz]; 1.47 [dt, 2H, J = 12.8; 6.8 Hz]; 1.24 [s, 24H]; 0.93–0.79 [m, 6H]. Moisture content = 0.42%, residual Cl⁻ = 0.05%, residual Na⁺ = not detected.

Tetra-n-butylammonium lauryl sulfate [TBA][C₁₂SO₄] and tetra-n-butylammonium lauryl ether sulfate [TBA][C₁₂ESO₄] were synthesized following procedures described above.

[TBA][C₁₂SO₄] - FTIR ν (cm⁻¹): 2962 (C–H of CH₂), 2877 (C–H of CH₃), 1280 (N–C alifatic), 1216 (C–O), 1023 (S=O). ¹H NMR (600 MHz, DMSO-*d*₆) δ (ppm): 3.67 [t, 2H, J = 6.1 Hz]; 3.23–3.12 [m, 8H]; 1.54 [m, 8H]; 1.44 [m, 8H, J = 7.2 Hz]; 1.37–1.21 [m, 20H]; 0.94 [m, 12H]; 0.86 [t, 3H]. Moisture content = 0.19%, residual Cl⁻ = not detected, residual Na⁺ = not detected.

[TBA][C₁₂ESO₄] - FTIR ν (cm⁻¹): 2969 (C–H of CH₂), 2872 (C–H of CH₃), 1269 (N–C alifatic), 1216 (C–O), 1020 (S=O). ¹H NMR (600 MHz, DMSO-*d*₆) δ (ppm): 3.79 [t, 2H]; 3.67 [t, 2H, J = 6.0 Hz]; 3.49 [t, 2H, J = 17.2 Hz]; 3.23–3.11 [m, 8H]; 1.58 [m, 8H]; 1.36–1.19 [m, 8H, J = 5.8 Hz]; 0.94 [s, 26H]; 0.85 [t, 12H, J = 6.1 Hz]. Moisture content = 0.46%, residual Cl⁻ = not detected, residual Na⁺ = not detected.

Structural formulas and appearances of the synthesized SAILs are shown in Fig. 1.

2.4. Electronic-structure simulations

Solubility of the ionic compounds in water was described in terms of the n-octanol to water transfer free energy. Implicit solvation was used to represent n-octanol and water in the framework of polarizable continuum model with the integral equation formalism. Truhlar and co-workers recently devised the universal solvation model, which is based on solute electron density. The solvent is provided as its bulk dielectric constant and atomic surface tensions [54].

An electronic structure of ion pairs was obtained at the Becke-3-Lee-Yang-Parr hybrid density functional level of theory [55–56] in conjunction with the atom-centered split-valence double-zeta polarized basis set 6-31G (d). The self-consistent field convergence criterion was set to 10⁻⁸ Hartree. The geometry convergence criteria were set to 0.012 kJ pm⁻¹ for maximum force, 0.00797 kJ pm⁻¹ for root-mean-squared force, 0.18 pm for maximum displacement and 0.12 pm root-mean-squared displacement.

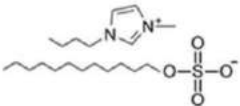

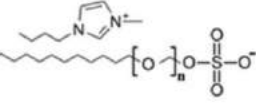

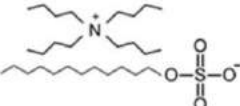

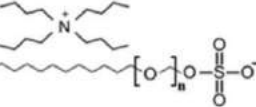

Abbreviation	Name	Structure	Water solubility	Appearance
[bmim][C ₁₂ SO ₄]	1-butyl-3-methylimidazolium lauryl sulfate		miscible in all proportions	
[bmim][C ₁₂ ESO ₄]	1-butyl-3-methylimidazolium lauryl ether sulfate		miscible in all proportions	
[TBA][C ₁₂ SO ₄]	tetra-n-butylammonium lauryl sulfate		immiscible	
[TBA][C ₁₂ ESO ₄]	tetra-n-butylammonium lauryl ether sulfate		miscible in all proportions	

Fig. 1. Abbreviations, names, structures (where "n" is approximately six $-O-CH_2-$ groups), water solubility and appearances of the synthesized SAILs.

Molecular dynamics simulations were conducted by the PM7-MD method [57–60]. Each sample system consisted of an ion pair and one CO₂ molecule. The CO₂ molecule was able to sample phase space near the ion pair finding the most energetically favorable location. The constant temperature, 300 K, was maintained by velocity rescaling every 100 time-steps. The initial distribution of linear velocities over degrees of freedom was provided by Maxwell distribution. Each system was sampled during 200 ps with an integration time-step of 0.1 fs.

2.5. Dilution of surface active ionic liquids

The synthesized SAILs were mixed with water to obtain four weight fractions: 80, 60, 40, and 20 wt% SAIL for viscosity assay. The concentrations of the prepared solutions were confirmed by TGA. Table 1 shows concentration in mol·L⁻¹ and weight fractions of each aqueous solution.

3. Results and discussion

3.1. Aspect

The images of the synthesized SAILs – (I) [bmim][C₁₂SO₄] and (II) [bmim][C₁₂ESO₄] – are shown in Fig. 2. Both SAILs are light yellow translucent viscous liquids. Upon mixing with water (80, 60, and 40 wt% SAIL), gels are formed. The gel formation was detected by absence of observable flow upon inversion [36].

Table 1

Correspondence between weight fractions and molarities of the aqueous mixtures of the synthesized SAILs.

x, %	[bmim][C ₁₂ SO ₄]	[bmim][C ₁₂ ESO ₄]	[TBA][C ₁₂ SO ₄]	[TBA][C ₁₂ ESO ₄]
80	1.98 M	1.49 M	Insoluble	1.25 M
60	1.48 M	1.12 M		0.93 M
40	0.99 M	0.75 M		0.62 M
20	0.49 M	0.37 M		0.31 M

[TBA][C₁₂SO₄] is immiscible with water. Consequently, all characterizations for this SAIL were performed with the pure SAIL sample. [TBA][C₁₂ESO₄] is a viscous colorless liquid (Fig. 1), presenting the same aspect when mixed with water over an entire concentration range.

3.2. Thermogravimetry

The thermogram of synthesized SAILs corroborates the concentration of the prepared dilutions by the first mass loss event (~100 °C). This event is related to the elimination of the added water in order to obtain the aqueous mixtures. The thermogravimetric analyses of the [bmim][C₁₂SO₄] SAIL reveals three weight loss events (Fig. 3, I). The first one, 101 °C–146 °C (weight loss 10.2%, T_{max} = 120 °C), is attributed to water evaporation. The high temperature needed to withdraw water is attributed to the water which is trapped in the SAIL structure (remained from synthesis step). This event is also observed in the aqueous mixtures containing 80, 60, and 40 wt% of SAIL. For the water mixture containing 20 wt% of SAIL this event is not visible probably due to the high water content added in order to obtain the solution. However, the water content into the aqueous mixtures (80, 60, 40 and 20 wt% SAIL) are more elevated due (uncertainty of ~1.5%) to the moisture contents in SAILs corroborated by Karl Fischer analyses. The second one, 182 °C–297 °C (weight loss 17.3%, T_{max} = 273 °C), is attributed to a partial degradation of the hydrocarbon chain of the anion. The third one, 302 °C–435 °C (weight loss 67.8%, T_{max} = 366 °C), is attributed to a complete ion degradation.

In turn, the thermogravimetric analysis of the [bmim][C₁₂ESO₄] SAIL presents two weight loss events (Fig. 3, II). The first one, 188 °C–287 °C (weight loss 8.6%, T_{max} = 267 °C), corresponds to the degradation of the side chain of the anion. The second one, 293 °C–435 °C (weight loss 85.3%, T_{max} = 376 °C) corresponds to complete degradation of the ions. [TBA][C₁₂SO₄] presents a single degradation event, 281 °C–321 °C (weight loss 97.3%, T_{max} = 306 °C), corresponding to a simultaneous degradation of the cation and the anion (Fig. 3, III). [TBA][C₁₂ESO₄] presents a single degradation event, 223 °C–376 °C (weight loss 99.4%,

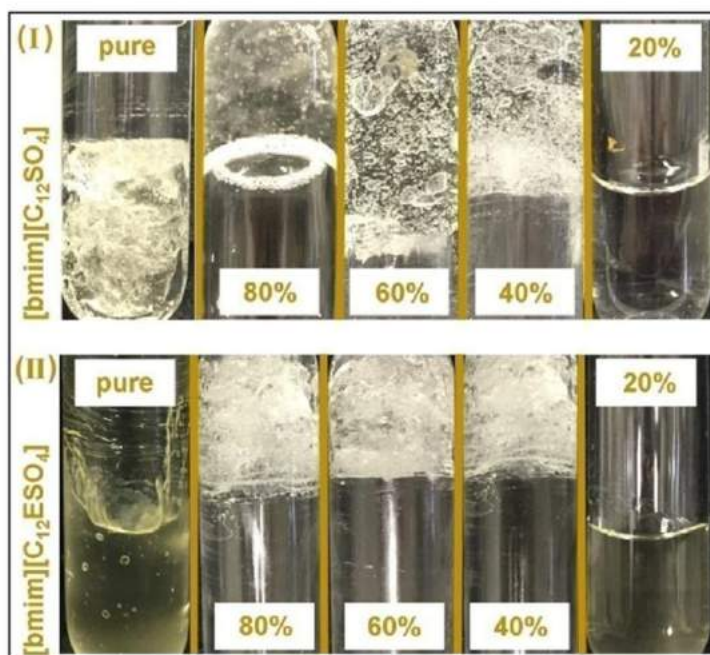


Fig. 2. An appearance of the synthesized SAILs: (I) [bmim][C₁₂SO₄] and (II) [bmim][C₁₂ESO₄] and their aqueous mixtures. Weight percentages are depicted.

$T_{\text{máx}} = 318 \text{ }^\circ\text{C}$) (Fig. 3, IV). The detected degradation temperatures SAIL-water mixture were close to those in pure SAILs. Therefore, water does not alter thermal stabilities of the synthesized SAILs.

3.3. Differential scanning calorimetry analysis

The DSC analysis for the [bmim][C₁₂SO₄] SAIL evinces a melting event, $1.8 \text{ }^\circ\text{C}$, and a crystallization event, $-1.7 \text{ }^\circ\text{C}$. At the first heating cycle, an exothermic peak is located at $155 \text{ }^\circ\text{C}$ for the SAIL-water mixture (80 wt% SAIL) (Fig. 4, I). This peak corresponds to enthalpy 17.1 J g^{-1} , which confirms an important structural interaction of water with SAIL. During heating, one observes reorganization of water molecules, which are more mobile and volatile, as compared to SAILs.

The DSC of the [bmim][C₁₂ESO₄] SAIL reveals a melting temperature, $4.1 \text{ }^\circ\text{C}$, and a crystallization point, $1.2 \text{ }^\circ\text{C}$. Glass transition point of [bmim][C₁₂ESO₄] is $-70 \text{ }^\circ\text{C}$. During the first heating cycle, an exothermic peak appears at $154.6 \text{ }^\circ\text{C}$ (80 wt% SAIL) corresponding to enthalpy 21.3 J g^{-1} (Fig. 4, II). This peak confirms a strong non-covalent interaction of the SAIL with water. The water-SAIL interaction is additionally seen in Fig. 2, II, which shows further structuring of the mixture at 80, 60, and 40 wt% SAIL, up to the point where the mixture does not flow upon inversion of the test tube. The enthalpy involved in the case of [bmim][C₁₂ESO₄] is greater than in the case of [bmim][C₁₂SO₄]. Evidently, presence of the ether moieties in the [bmim][C₁₂ESO₄] SAIL enhances SAIL-water interactions.

The DSC analysis of the [TBA][C₁₂SO₄] SAIL reveals melting, $-22.9 \text{ }^\circ\text{C}$, and crystallization, $-35.6 \text{ }^\circ\text{C}$. Glass transition temperature is $-55.54 \text{ }^\circ\text{C}$. [TBA][C₁₂ESO₄] exhibits the melting point at $-5.0 \text{ }^\circ\text{C}$ and the crystallization point at $-12.2 \text{ }^\circ\text{C}$.

3.4. Viscosity

Pure [bmim][C₁₂SO₄] is extremely viscous due to a long flexible hydrocarbon chain. The 80, 60, and 40 wt% SAIL aqueous mixtures exhibit gel appearances. It was only possible to measure initial viscosities (not shear) at $30 \text{ }^\circ\text{C}$ ($13,200 \text{ Pa}\cdot\text{s}$). The flow curves at $30 \text{ }^\circ\text{C}$ for the SAIL-

water mixtures are presented in Fig. 5, I. Note that viscosity decreases exponentially upon water addition. Compare, at 80 wt% SAIL, initial viscosity is $4203 \text{ Pa}\cdot\text{s}$; at 60 wt% SAIL, initial viscosity is $1070 \text{ Pa}\cdot\text{s}$; at 40 wt% SAIL, initial viscosity is $113 \text{ Pa}\cdot\text{s}$. The [bmim][C₁₂SO₄]-water mixtures (80, 60, and 40 wt% SAIL) exhibits a rheological behavior of pseudoplastic fluids, i.e. viscosity is dependent on the shear rate. In turn, at 20 wt% SAIL, viscosity is much lower, $0.3 \text{ Pa}\cdot\text{s}$. This mixture demonstrates Newtonian behavior. The flow curves at $60 \text{ }^\circ\text{C}$ for the [bmim][C₁₂SO₄]-water mixtures are presented in Fig. 5, II. The viscosity of pure SAIL decreases significantly with temperature increase ($53 \text{ Pa}\cdot\text{s}$) with non-Newtonian behavior. No phase transformation occurs in the $30\text{--}60 \text{ }^\circ\text{C}$ temperature range. Interestingly, the SAIL-water mixtures exhibit higher viscosities, as compared to the pure SAIL. At $60 \text{ }^\circ\text{C}$, water addition to [bmim][C₁₂SO₄] fosters structuring. The initial viscosities are $1784 \text{ Pa}\cdot\text{s}$ (80 wt% SAIL), $969 \text{ Pa}\cdot\text{s}$ (60 wt% SAIL), $335 \text{ Pa}\cdot\text{s}$ (40 wt% SAIL), $25 \text{ Pa}\cdot\text{s}$ (20 wt% SAIL). The viscosities of the SAIL-rich mixtures (80 and 60 wt% SAIL) are systematically higher at $30 \text{ }^\circ\text{C}$ than at $60 \text{ }^\circ\text{C}$. This behavior is reversed in the SAIL-water mixtures (40 and 20 wt% SAIL), in which the viscosities at $60 \text{ }^\circ\text{C}$ are higher than at those at $30 \text{ }^\circ\text{C}$. The described behavior is in drastic contrast with that of conventional fluids.

The [bmim][C₁₂ESO₄] SAIL is viscous and fluid at room temperature. At 80, 60, and 40 wt% SAIL concentrations, the aqueous mixtures have gel appearances. The flow curves at $30 \text{ }^\circ\text{C}$ for SAIL and SAIL-water mixtures are shown in Fig. 5, III. Pure [bmim][C₁₂ESO₄] is a Newtonian fluid with initial viscosity of $0.5 \text{ Pa}\cdot\text{s}$. However, the SAIL-water mixtures (80, 60, and 40 wt%) are pseudoplastic fluids. At 80 wt% SAIL, initial viscosity is $2430 \text{ Pa}\cdot\text{s}$; at 60 wt% SAIL, initial viscosity is $781 \text{ Pa}\cdot\text{s}$; at 40 wt% SAIL, initial viscosity is $201 \text{ Pa}\cdot\text{s}$. The shear values in the viscosity tests remained higher for these SAIL-water mixtures. The rheological behavior observed confirmed the hypothesis that water strongly interacts with the synthesized SAILs, increasing viscosities at lower aqueous contents and decreasing viscosities at higher water contents. The SAIL-water interaction engenders an organized structure causing a three orders of magnitude increasing of the pure SAIL viscosity in the 80 wt% SAIL mixture. The ether groups may be responsible for such a behavior.

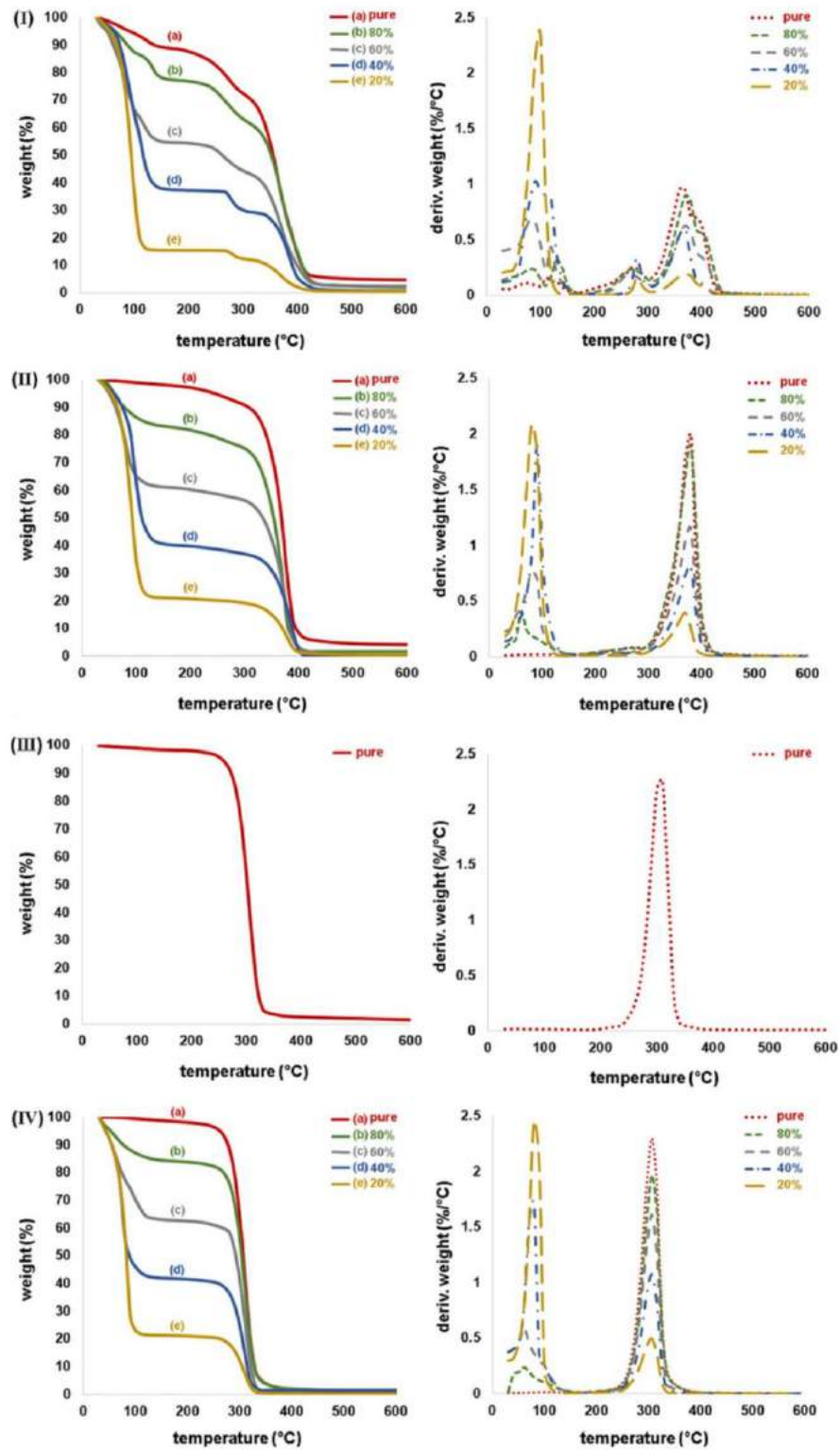


Fig. 3. Thermograms of (I) [bmim][C₁₂SO₄], (II) [bmim][C₁₂ESO₄], (III) [TBA][C₁₂SO₄], (IV) [TBA][C₁₂ESO₄].

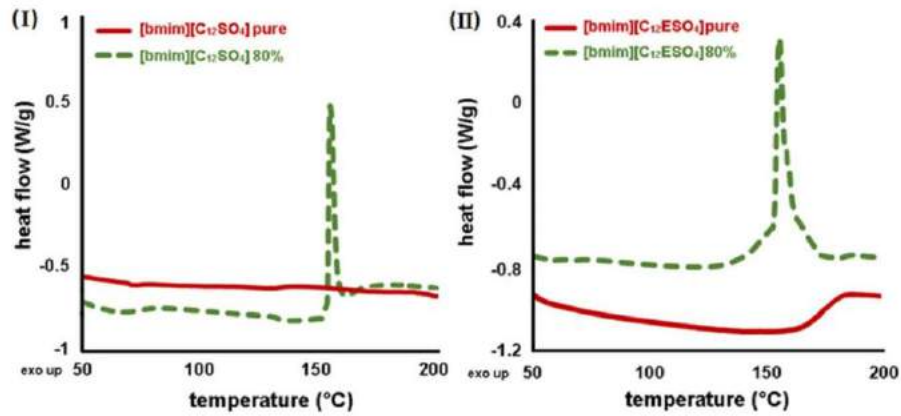


Fig. 4. The first DSC cycle confirming interaction with water of (I) [bmim][C₁₂SO₄] and (II) [bmim][C₁₂ESO₄].

The ether groups are moderately polar and, therefore, favor interactions with water allows the creation of local structures in the mixture. At 20 wt% SAIL, the rheological behavior is Newtonian with a much lower initial viscosity, 0.1 Pa·s, when compared to other SAIL contents. The rheological tests for [bmim][C₁₂ESO₄] at 60 °C (Fig. 5, IV) show that the pure SAIL is a Newtonian fluid with a relatively low initial viscosity,

0.02 Pa·s. At 80 wt% SAIL, the mixture behavior is also Newtonian, whereas initial viscosity is 0.04 Pa·s. Unlike what happens at 30 °C, addition of water does not restructure the SAIL. This behavior is observed only at 60 and 40 wt% SAIL (pseudoplastic fluid). In the 60 wt% SAIL, an initial viscosity, 588 Pa·s, corresponds to a nearly 3000 times increase, as compared to the pure SAIL. In the 40 wt% SAIL mixture, an initial

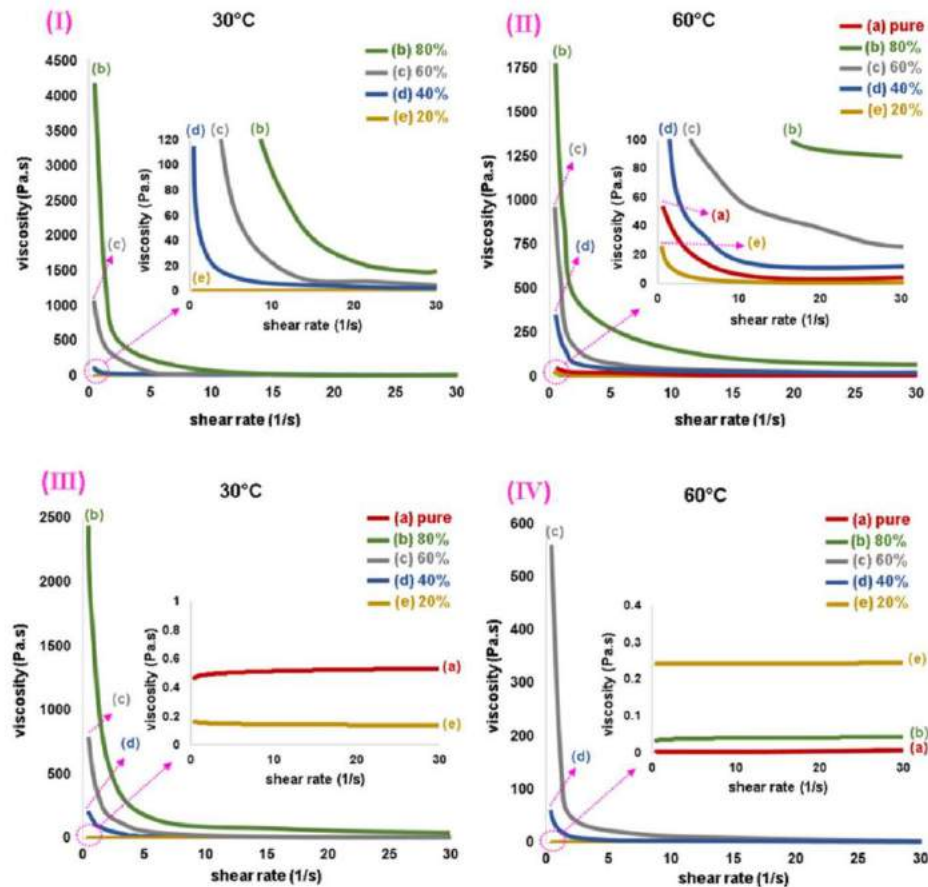


Fig. 5. Flow curves of (I) [bmim][C₁₂SO₄] at 30 °C, (II) [bmim][C₁₂SO₄] at 60 °C, (III) [bmim][C₁₂ESO₄] at 30 °C, (IV) [bmim][C₁₂ESO₄] at 60 °C.

viscosity, 60 Pa·s, is 300 times higher than that of the pure SAIL. The 20 wt% SAIL mixture behaves like Newtonian fluid, with 0.25 Pa·s viscosity. At 60 °C, all SAIL-water mixtures exhibit higher viscosities than the pure SAIL.

[TBA][C₁₂SO₄] is Newtonian fluid both at 30 °C (Fig. 6, I) and 60 °C (Fig. 6, II), viscosities being ~3 Pa·s and ~0.3 Pa·s, respectively. In [TBA][C₁₂ESO₄] at 30 °C (Fig. 6, III), viscosity decreases at higher dilutions. An average viscosity of the pure SAIL is 1.0 Pa·s, whereas an average viscosity at 20 wt% SAIL is 0.02 Pa·s. The same trend is observed at 60 °C (Fig. 6, IV).

3.5. Polarizing optical microscopy

The polarized optical microscopy (POM) images (Fig. 7) provide additional information on the gelatinous structure of the synthesized SAILS.

The polarized micrographs of the SAILS gel samples [bmim][C₁₂SO₄] (80, 60, 40 wt% SAIL, Fig. 7, I) and [bmim][C₁₂ESO₄] (80, 60, 40 wt% SAIL, Fig. 7, II) evince similar structures with scattered maltese crosses.

The amount of these structures is related to the SAIL contents. In particular, samples that are more concentrated provide more maltese crosses structure. This structure suggests LC formation in the gel phase [27,33,36]. We also note some bright areas related to a less organized gelatinous structure [27,33,36]. Much more intense and organized LCs

were observed in [bmim][C₁₂ESO₄] than in [bmim][C₁₂SO₄] (both 80 wt% SAIL). Formation of LCs reflects peculiar structural organization of the mixtures and can be correlated with viscosities. In fact, the three-dimensional structuring of the [bmim][C₁₂ESO₄] when water is added is very significant (viscosity 80 wt% SAIL > pure SAIL) when compared to the [bmim][C₁₂SO₄] (viscosity pure SAIL > 80 wt% SAIL), thus indicating a higher formation of LCs in the [bmim][C₁₂ESO₄].

3.6. Hydrophilicity/hydrophobicity balance

The [bmim⁺] cation is hydrophilic, thanks to its acidic hydrogen in the imidazole ring, which maintains a weak hydrogen bond with water molecule. In turn, most salts of [TBA⁺] are poorly soluble in water requiring less polar solvents, such as acetonitrile. The anions, both [C₁₂SO₄⁻] and [C₁₂ESO₄⁻], are amphiphilic, in which the sulfate group is hydrophilic, whilst the hydrocarbon chain is hydrophobic. The ether groups are more hydrophilic, being responsible for moderate aqueous solubility of most ethers. To characterize hydrophilicity/hydrophobicity balance of the synthesized SAILS, we computed Gibbs free energies of their transfer from water to n-octanol (Fig. 8). Due to the presence of the sulfate groups, these compounds are expected to exhibit surfactant behaviors. The cations, [bmim⁺] and [TBA⁺], are located near the head group (sulfate) of the anions, whereas hydrocarbon tails are directed towards the vapor-liquid interface. [bmim][C₁₂SO₄] and

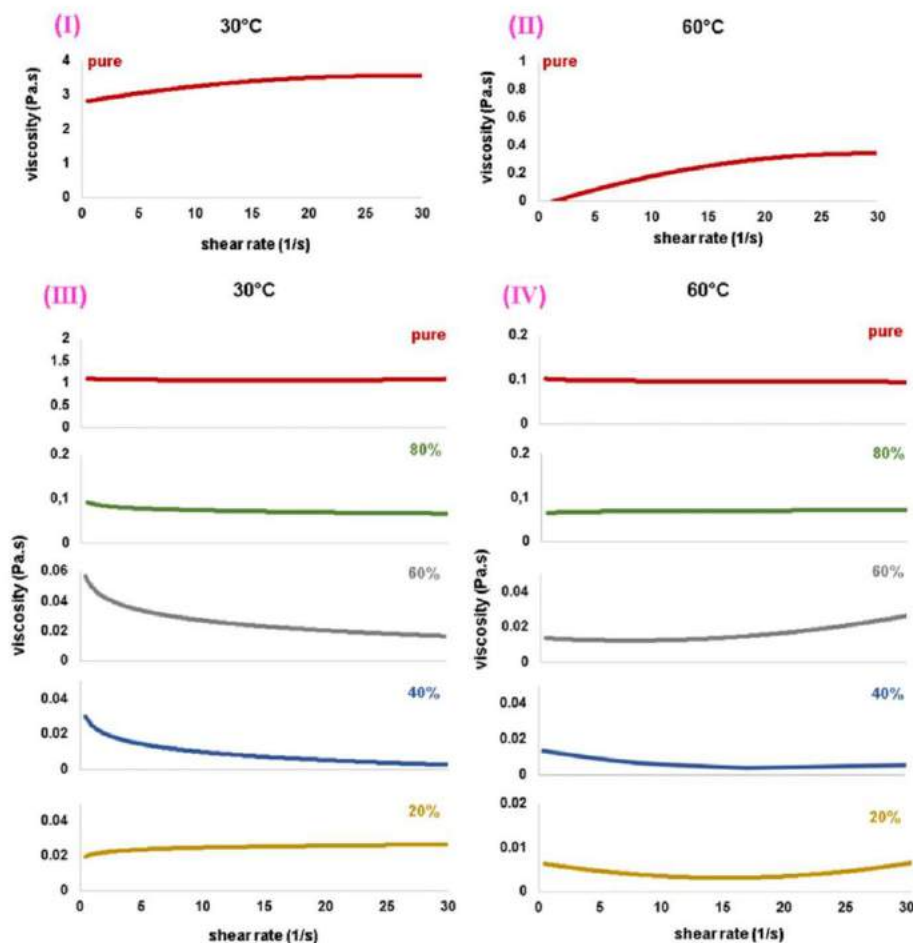


Fig. 6. Flow curves of (I) [TBA][C₁₂SO₄] at 30 °C, (II) [TBA][C₁₂SO₄] at 60 °C, (III) [TBA][C₁₂ESO₄] at 30 °C, (IV) [TBA][C₁₂ESO₄] at 60 °C.

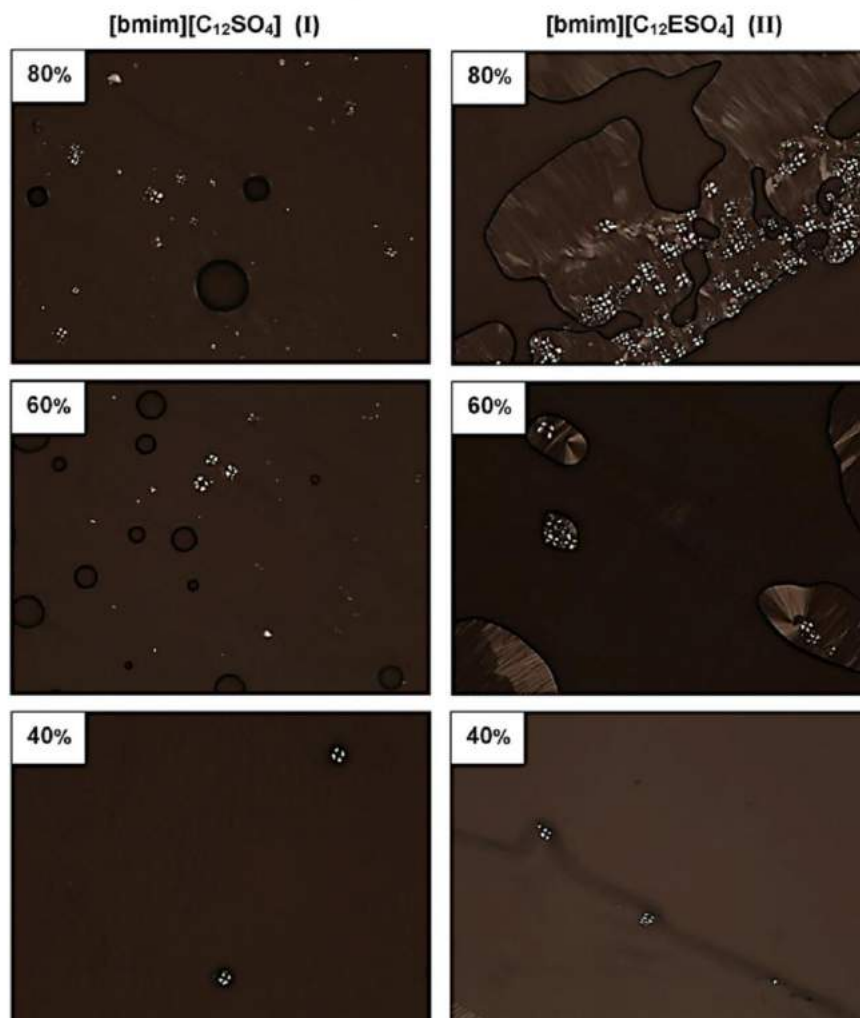


Fig. 7. Polarized optical micrographs of the gel phase of the aqueous mixtures of (I) [bmim][C₁₂SO₄] and (II) [bmim][C₁₂ESO₄] at 80, 60, 40 wt% SAIL.

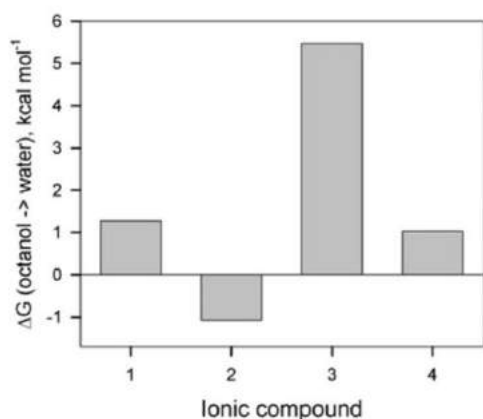


Fig. 8. Free energies of transfer, ΔG (octanol \rightarrow water), of the synthesized SAILs: [1] [bmim][C₁₂SO₄], [2] [bmim][C₁₂ESO₄], [3] [TBA][C₁₂SO₄], [4] [TBA][C₁₂ESO₄].

[bmim][C₁₂ESO₄] are more hydrophilic, as compared to [TBA][C₁₂SO₄] and [TBA][C₁₂ESO₄]. The ether groups of the [C₁₂ESO₄] anion, approximately six $-\text{O}-\text{CH}_2-$ groups per anion, increase hydrophilicity somewhat.

This behavior is experimental corroborated: [bmim][C₁₂SO₄], [bmim][C₁₂ESO₄] and [TBA][C₁₂ESO₄] are water miscible while [TBA][C₁₂SO₄] is immiscible. Partition coefficients can be approximately assessed from $K = \exp(-\Delta G/RT)$, where K is computed from molar concentrations. One concludes that all synthesized ILS exhibit relatively modest hydrophilicities, which are in line with their surfactant-like structures. Likewise, the SAIL [bmim][C₁₂ESO₄] which presents the low partition coefficients, proved experimentally, to be the one which most improved viscosity (~ 5000 times at 80 wt% SAIL) in aqueous solution when compared to the pure SAIL.

3.7. Interactions with carbon dioxide

According to PM7-MD simulations at 300 K, the sulfate group is essential not only to improve aqueous solubility, but to fix CO₂ molecules

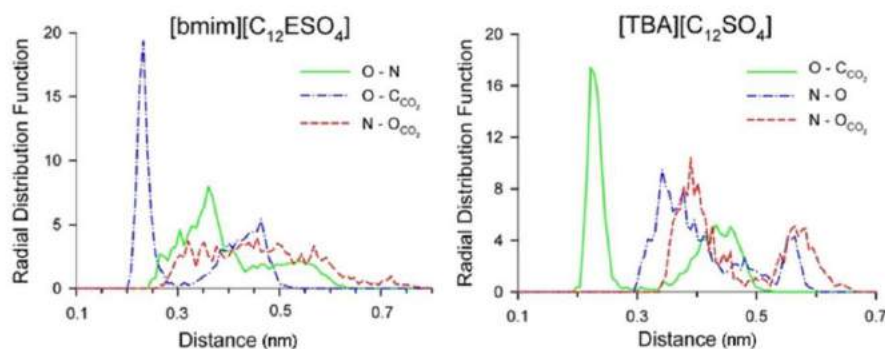


Fig. 9. Radial distribution functions for (left) [bmim][C₁₂ESO₄] and CO₂ and (right) [TBA][C₁₂SO₄] and CO₂. The "N" site belongs to the cation, the "O" site belongs to the anion. See legend for designation of pairwise correlations.

(Fig. 9). High and sharp peaks were obtained for the interaction of the carbon atom of CO₂ and the oxygen atom of –O–SO₃ at 0.22–0.25 nm. The performance of –O–SO₃ is better than that of the imidazole ring. CO₂ also exhibits a relatively strong interaction with the [TBA⁺] cation.

Since the working group in both [C₁₂SO₄[−]] and [C₁₂ESO₄[−]] is –O–SO₃, the CO₂ capture of [bmim][C₁₂SO₄] and [bmim][C₁₂ESO₄] are equal per mole of sorbent. RDFs for [bmim][C₁₂SO₄] and [TBA][C₁₂SO₄] are qualitatively the same as those for [bmim][C₁₂ESO₄] and [TBA][C₁₂ESO₄]. However, the molecular mass of [C₁₂ESO₄[−]] is higher. Therefore, the performance of 1 g of [bmim][C₁₂SO₄] must be accordingly higher. The revealed affinity of –O–SO₃ to CO₂ deserves further experimental investigation to introduce new low-cost SAILs for CO₂ capture.

4. Conclusion

Comparing two cations described in this study, [bmim⁺] and [TBA⁺], it is important to emphasize that [bmim⁺] fosters gel structure formation when combined with the anions tested in this study. The two anions, [C₁₂SO₄[−]] and [C₁₂ESO₄[−]], when combined to [bmim⁺] in aqueous mixtures result in gels with interesting physicochemical properties. This behavior was not observed neither in [TBA][C₁₂SO₄] nor in [TBA][C₁₂ESO₄]. We suppose that binding of [bmim⁺] to water is stronger in both SAILs than binding of [TBA⁺], thanks to an acidic hydrogen atom. The latter gives rise to H-bonding. In turn, H-bonding is responsible for gel and LC formation. [C₁₂SO₄[−]] and [C₁₂ESO₄[−]] differ by only the presence of ether groups. The ether groups improve interactions with water. In [bmim][C₁₂ESO₄], the ether groups increase viscosity by ~5000 times at 80 wt% SAIL aqueous solution when compared to the pure SAIL. In [TBA][C₁₂ESO₄], the ether groups are responsible for better miscibility in water. In turn, [TBA][C₁₂SO₄] is immiscible with water. The simulation results corroborated that the ether groups somewhat increase hydrophilicity. The synthesized SAILs are prospective inexpensive CO₂ scavengers due to a strong electrostatic attraction between the sulfate groups of the anions and the CO₂ molecule. Systematic investigation of CO₂ capture by [bmim][C₁₂SO₄], [bmim][C₁₂ESO₄], [TBA][C₁₂SO₄], and [TBA][C₁₂ESO₄] constitutes an important future direction of the presently initiated work. The synthesized SAILs can also be used to modulate surface tensions of the polar solvents.

Acknowledgments

The authors would like to thank Petrobras (0050.0096056.15.9) for financial support, M.O.V. and W.F.M. thank CAPES for the doctoral fellowship and S.E. thanks CNPq for the researcher scholarship. We thank Dr. Vinicius Duval da Silva (PUCRS, Porto Alegre, Brazil) for the polarized optical microscopy analysis.

References

- [1] I. Goodchild, L. Collier, S.L. Millar, I. Prokeš, J.C.D. Lord, C.P. Butts, J. Bowers, J.R.P. Webster, R.K. Heenan, Structural studies of the phase, aggregation and surface behavior of 1-alkyl-3-methylimidazolium halide + water mixtures, *J. Colloid Interface Sci.* 307 (2007) 455–468.
- [2] R. Aranowski, I. Cichowska-Kopczyńska, B. Dębski, P. Jasiński, Conductivity and viscosity changes of imidazolium ionic liquids induced by H₂O and CO₂, *J. Mol. Liq.* 221 (2016) 541–546.
- [3] H.R. Rafiee, F. Frouzesh, Volumetric properties of ionic liquids, 1-ethyl-3-ethylimidazolium chloride [emim][Cl] and 1-ethyl-3-methylimidazolium hydrogen sulfate [emim][HSO₄] in sucrose aqueous solutions at T = (293.15–313.15) K and ambient pressure, *Fluid Phase Equilib.* 425 (2016) 120–126.
- [4] M. Barycki, A. Sosnowska, A. Gajewicz, M. Bobrowski, D. Wilenska, P. Skurski, A. Geldon, C. Czaplowski, S. Uhl, E. Laux, T. Journot, L. Jeandupeux, H. Keppner, T. Puzyn, Temperature-dependent structure-property modeling of viscosity for ionic liquids, *Fluid Phase Equilib.* 427 (2016) 9–17.
- [5] M.T. Zafarani-Moattar, H. Shekaari, E.M.H. Agha, Vapor-liquid equilibria study of the ternary systems containing sucrose in aqueous solutions of ionic liquids, 1-butyl-3-methylimidazolium bromide and 1-hexyl-3-methylimidazolium bromide at 298.15 K and atmospheric pressure, *Fluid Phase Equilib.* 429 (2016) 45–54.
- [6] B. Yoo, W. Afzal, J.M. Praunzt, Solubility Parameters for nine ionic liquids, *Eng. Chem. Res.* 51 (29) (2012) 9913–9917.
- [7] A. Marciniak, The solubility parameters of ionic liquids, *Int. J. Mol. Sci.* 11 (2010) 1973–1990.
- [8] T. Letcher, A. Marciniak, M. Marciniak, Determination of activity coefficients at infinite dilution of solutes in the ionic liquid 1-butyl-3-methylimidazolium octyl sulfate using gas-liquid chromatography at a temperature of 298.15 K, 313.15 K, or 328.15 K, *J. Chem. Eng. Data* 50 (2005) 1294–1298.
- [9] C. Herrera, G.C. Costa, M. Atilhan, L.T. Costa, S. Aparicio, A theoretical study on aminoacid-based ionic liquids with acid gases and water, *J. Mol. Liq.* 225 (2017) 347–356.
- [10] L. Chen, M. Sharifzadeh, N.M. Dowell, T. Welton, N. Shah, J.P. Hallett, Inexpensive ionic liquids: [HSO₄][−]-based solvent production at bulk scale, *Green Chem.* 16 (2014) 3098–3106.
- [11] A. George, A. Brandt, K. Tran, S.M.S. Nizan, S. Zahari, D. Klein-Marcuschamer, N. Sun, N. Sathitsuksanoh, J. Shi, V. Stavila, R. Parthasarathi, S. Singh, B.M. Holmes, T. Welton, B.A. Simmons, J.P. Hallett, Design of low-cost ionic liquids for lignocellulosic biomass pretreatment, *Green Chem.* 17 (2015) 1728–1734.
- [12] B. Dong, N. Li, L. Zheng, L. Yu, T. Inoue, Surface adsorption and micelle formation of surface active ionic liquids in aqueous solution, *Langmuir* 23 (2007) 4178–4182.
- [13] F. Geng, L. Zheng, J. Liu, L. Yu, C. Tung, Interactions between a surface active imidazolium ionic liquid and BSA, *Colloid Polym. Sci.* 287 (2009) 1253–1259.
- [14] U. Preiss, C. Jungnickel, J. Thoming, I. Krossing, J. Luczak, M. Diedenhofen, A. Klamt, Predicting the critical micelle concentrations of aqueous solutions of ionic liquids and other ionic surfactants, *Chem. Eur. J.* 15 (2009) 8880–8885.
- [15] X. Li, Y. Gao, J. Liu, L. Zheng, B. Chen, L. Wub, C. Tung, Aggregation behavior of a chiral long-chain ionic liquid in aqueous solution, *J. Colloid Interface Sci.* 343 (2010) 94–101.
- [16] F. Geng, L. Zheng, L. Yu, G. Li, C. Tung, Interaction of bovine serum albumin and long-chain imidazolium ionic liquid measured by fluorescence spectra and surface tension, *Process Biochem.* 45 (2010) 306–311.
- [17] A. Di Crescenzo, M. Aschi, E. Del Canto, S. Giordani, D. Demurtas, A. Fontana, Structural modifications of ionic liquid surfactants for improving the water dispersibility of carbon nanotubes: an experimental and theoretical study, *Phys. Chem. Chem. Phys.* 13 (2011) 11373–11383.
- [18] K.S. Rao, T.J. Trivedi, A. Kumar, Aqueous biamphiphilic ionic liquid system: self-assembly and synthesis of gold nanocrystals/nanoplates, *J. Phys. Chem. B* 116 (2012) 14363–14374.
- [19] I.A. Sedov, B.N. Solomonov, Thermodynamic description of the solvophobic effect in ionic liquids, *Fluid Phase Equilib.* 425 (2016) 9–14.

- [20] J. Jingjing, H. Bing, L. Meijia, C. Ni, Y. Li, L. Min, Salt-free cationic surface active ionic liquids 1-alkyl-3-methylimidazolium alkylsulfate: aggregation behavior in aqueous solution, *J. Colloid Interface Sci.* 412 (2013) 24–30.
- [21] A. Gong, X. Zhu, Surfactant/ionic liquid aqueous two-phase system extraction coupled with spectrofluorimetry for the determination of dutasteride in pharmaceutical formulation and biological samples, *Fluid Phase Equilib.* 374 (2014) 70–78.
- [22] P.B. Kumar, G. Aniruddha, G. Nidhil, Deciphering the interaction of a model transport protein with a prototypical imidazolium room temperature ionic liquid: effect on the conformation and activity of the protein, *J. Photochem. Photobiol. B* 133 (2014) 99–107.
- [23] P. Bharmoria, K.S. Rao, T.J. Trivedi, A. Kumar, Biamphiphilic ionic liquid induced folding alterations in the structure of bovine serum albumin in aqueous medium, *J. Phys. Chem. B* 118 (2014) 115–124.
- [24] P. Bharmoria, M.J. Mehta, I. Pancha, A. Kumar, Structural and functional stability of cellulase in aqueous-biamphiphilic ionic liquid surfactant solution, *J. Phys. Chem. B* 118 (2014) 9890–9899.
- [25] J. Saien, S. Asadabadi, Alkyl chain length, counter anion and temperature effects on the interfacial activity of imidazolium ionic liquids: comparison with structurally related surfactants, *Fluid Phase Equilib.* 386 (2015) 134–139.
- [26] T. Tsukatani, H. Katano, H. Tatsumi, M. Deguchi, N. Hirayama, Halogen-free water-immiscible ionic liquids based on tetraoctylammonium cation and dodecylsulfate and dodecylbenzenesulfonate anions, and their application as chelate extraction solvent, *Anal. Sci.* 22 (2006) 199–200.
- [27] L. Shi, M. Zhao, L. Zheng, Lyotropic liquid crystalline phases formed in ternary mixtures of N-alkyl-N-methylpyrrolidinium bromide/1-decanol/water, *RSC Adv.* 2 (2012) 11922–11929.
- [28] J.M. Obliosca, S.D. Arco, M.H. Huang, Synthesis and optical properties of 1-alkyl-3-methylimidazolium lauryl sulfate ionic liquids, *J. Fluoresc.* 17 (2007) 613–618.
- [29] S.M. Tawfik, Ionic liquids based gemini cationic surfactants as corrosion inhibitors for carbon steel in hydrochloric acid solution, *J. Mol. Liq.* 216 (2016) 624–635.
- [30] J.H. Porada, M. Mansueto, S. Laschat, C. Stubenrauch, Microemulsions with hydrophobic ionic liquids: influence of the structure of the anion, *J. Mol. Liq.* 227 (2017) 202–209.
- [31] A. Selwent, J. Łuczak, Micellar aggregation of Triton X-100 surfactant in imidazolium ionic liquids, *J. Mol. Liq.* 221 (2016) 557–566.
- [32] M.A. Firestone, M.L. Dietz, S. Seifert, S. Trasobares, D.J. Miller, N.J. Zaluzec, Ionogel-templated synthesis and organization of anisotropic gold nanoparticle, *Small* 754 (2005) 25–27.
- [33] H. Kaper, B.Z. Smarsly, Templating and phase behaviour of the long chain ionic liquid C16mimCl, *Phys. Chem.* 220 (2006) 1455–1471.
- [34] T.W. Wang, H. Kaper, M. Antonietti, B. Smarsly, Templating behavior of a long-chain ionic liquid in the hydrothermal synthesis of mesoporous silica, *Langmuir* 23 (2007) 1489–1495.
- [35] B.A. Coldren, H. Warriner, R. van Zanten, J.A. Zasadzinski, E.B. Sirota, Lamellar gels and spontaneous vesicles in cationic surfactant mixtures, *Langmuir* 22 (2006) 2465–2473.
- [36] Y. Zhao, X. Chen, B. Jing, X. Wang, F. Ma, Novel gel phase formed by mixing a cationic surfactive ionic liquid C16mimCl and an anionic surfactant SDS in aqueous solution, *J. Phys. Chem. B* 113 (2009) 983–988.
- [37] K.P. Ananthapadmanabhan, Interactions of Surfactants with Polymers and Proteins, in: E.D. Goddard, K.P. Ananthapadmanabhan (Eds.), CRC Press, Inc, London, U.K., 1993 (Chapter 8).
- [38] M.N. Jones, Surfactant interactions with biomembranes and proteins, *Chem. Soc. Rev.* 21 (1992) 127–136.
- [39] D.G. Dalgleish, in: J. Sjöblom (Ed.), Emulsions and Emulsion Stability, Marcel Dekker, New York, 1996 (Chapter 5).
- [40] M. Mavaddat, S. Riahi, A molecular structure based model for predicting optimal salinity of anionic surfactants, *Fluid Phase Equilib.* 409 (2016) 354–360.
- [41] H. Wu, E.J. Maginn, Water solubility and dynamics of CO₂ capture ionic liquids having aprotic heterocyclic anions, *Fluid Phase Equilib.* 368 (2014) 72–79.
- [42] A.S. Aquino, F.L. Bernard, M.O. Vieira, J.V. Borges, M.F. Rojas, F.D. Vecchia, R. Ligabue, M. Seferin, S. Menezes, S. Einloft, A new approach to CO₂ capture and conversion using imidazolium based-ionic liquids as sorbent and catalyst, *J. Braz. Chem. Soc.* 25 (2014) 2251–2257.
- [43] S.N. Khan, S.M. Hailegiorgis, Z. Man, A.M. Shariff, S. Garg, Thermophysical properties of concentrated aqueous solution of N-methyldiethanolamine (MDEA), piperazine (PZ), and ionic liquids hybrid solvent for CO₂ capture, *J. Mol. Liq.* 229 (2017) 221–229.
- [44] Z. Bazargani, F. Sabzi, Thermodynamic modeling of CO₂ absorption in 1-butyl-3-methylimidazolium-based ionic liquids, *J. Mol. Liq.* 223 (2016) 235–242.
- [45] M. Zoubeik, M. Mohamedali, A. Henni, Experimental solubility and thermodynamic modeling of CO₂ in four new imidazolium and pyridinium-based ionic liquids, *Fluid Phase Equilib.* 419 (2016) 67–74.
- [46] R. Hayes, G.C. Warr, R. Atkin, Structure and nanostructure in ionic liquids, *Chem. Rev.* 115 (2015) 6357–6426.
- [47] M.O. Vieira, A.S. Aquino, M.K. Schütz, F.D. Vecchia, R. Ligabue, M. Seferin, S. Einloft, Chemical conversion of CO₂: evaluation of different ionic liquids as catalysts in dimethyl carbonate synthesis, *Energy Procedia* (2017) <http://dx.doi.org/10.1016/j.egypro.2017.03.1876> (in press).
- [48] Z. Fenga, F. Cheng-Gang, W. You-Ting, W. Yuan-Tao, L. Ai-Mina, Z. Zhi-Bing, Absorption of CO₂ in the aqueous solutions of functionalized ionic liquids and MDEA, *Chem. Eng. J.* 160 (2010) 691–697.
- [49] M.M. Taib, T. Murugesan, Solubilities of CO₂ in aqueous solutions of ionic liquids (ILs) and monoethanolamine (MEA) at pressures from 100 to 1600 kPa, *Chem. Eng. J.* 181–182 (2012) 56–62.
- [50] A. Haghtalab, A. Afsharpoor, Solubility of CO₂ + H₂S gas mixture into different aqueous N-methyldiethanolamine solutions blended with 1-butyl-3-methylimidazolium acetate ionic liquid, *Fluid Phase Equilib.* 406 (2015) 10–20.
- [51] T. Welton, Room temperature ionic liquids – solvents for synthesis and catalysis, *Chem. Rev.* 99 (1999) 2071–2083.
- [52] N. Jain, A. Kumar, S. Chauhan, S. Chauhan, Chemical and biochemical transformations in ionic liquids, *Tetrahedron* 61 (2005) 1015–1060.
- [53] P. Wasserscheid, T. Welton, *Ionic Liquids in Synthesis*, 368, Wiley-VCH Verlags GmbH & Co., Weinheim, 2008.
- [54] A.V. Marenich, C.J. Cramer, D.G. Truhlar, Universal solvation model based on solute electron density and on a continuum model of the solvent defined by the bulk dielectric constant and atomic surface tensions, *J. Phys. Chem. B* 113 (2009) 6378–6396.
- [55] C.T. Lee, W.T. Yang, R.G. Parr, Development of the Colle-Salvetti correlation-energy formula into a functional of the electron-density, *Phys. Rev. B* 37 (1988) 785–789.
- [56] A.D. Becke, Density-functional exchange-energy approximation with correct asymptotic-behavior, *Phys. Rev. A* 38 (1988) 3098–3100.
- [57] J.J.P. Stewart, Optimization of parameters for semiempirical methods VI: more modifications to the NDDO approximations and re-optimization of parameters, *J. Mol. Model.* 19 (2013) 1–32.
- [58] A.S. Aquino, F.L. Bernard, J.V. Borges, L. Mafra, F.D. Vecchia, M.O. Vieira, R. Ligabue, M. Seferin, V.V. Chaban, E.J. Cabrita, S. Einloft, Rationalizing the role of the anion in CO₂ capture and conversion using imidazolium-based ionic liquid modified mesoporous silica, *RSC Adv.* 5 (2015) 64220–64227.
- [59] V. Chaban, Hydrogen fluoride capture by imidazolium acetate ionic liquid, *Chem. Phys. Lett.* 625 (2015) 110–115.
- [60] V. Chaban, The thiocyanate anion is a primary driver of carbon dioxide capture by ionic liquids, *Chem. Phys. Lett.* 618 (2015) 89–93.

4.3. Capítulo III

Este segundo artigo utiliza os oito líquidos iônicos sintetizados nesta tese ([bmim][C₁₂SO₄], [bmim][C₁₂ESO₄], ([bmim][C₁₂BSO₃], [bmim][C₁₂SAR], [TBA][C₁₂SO₄], [TBA][C₁₂ESO₄], ([TBA][C₁₂BSO₃] e [TBA][C₁₂SAR]) como catalisadores na síntese do carbonato de propileno (PC). Foi realizado um estudo de termodinâmica a fim de encontrar a melhor condição reacional, além de um estudo teórico determinando as energias de formação que comprovou o mecanismo proposto para esta reação catalítica.

Este artigo intitulado “*Surface Active Ionic Liquids as Catalyst for CO₂ Conversion to Propylene Carbonate*”, DOI: 10.1007/s10562-017-2212-4, foi publicado em 2018 na revista *Catalysis Letters*, ISSN: 1011-372X.

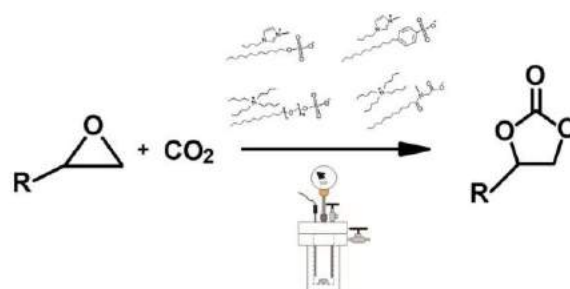
Surface Active Ionic Liquids as Catalyst for CO₂ Conversion to Propylene Carbonate

Michele O. Vieira¹ · Wesley F. Monteiro¹ · Bruna S. Neto² · Rosane Ligabue¹ · Vitaly V. Chaban³ · Sandra Einloft¹ 

Received: 26 July 2017 / Accepted: 29 September 2017 / Published online: 14 October 2017
© Springer Science+Business Media, LLC 2017

Abstract CO₂ capture is an efficient possibility to mitigate environmental impacts. An efficient transformation of CO₂ into useful chemicals is a need from environmental protection and resource utilization viewpoint. Cyclic carbonates, such as propylene carbonate is used in numerous technologies. We hereby report eight surface active ionic liquids (SAILs) composed of the well-known cations ([bmim⁺] and [TBA⁺]) and long-alkyl-chain anions ([C₁₂SO₄⁻], [C₁₂ESO₄⁻], [C₁₂BSO₃⁻] and [C₁₂SAR⁻]). In this work, we have studied catalytic activities of SAILs for cyclic carbonate synthesis. The work demonstrates that [TBA⁺] is more active as a catalyst because the higher molecular volume increases the distance cation/anion, consequently, a weaker electrostatic interaction cation/anion results in a more nucleophilic anion. The [TBA][C₁₂SO₄] was the SAIL that presented better catalytic activity, reaching 79.2% of conversion and 87.7% of selectivity, besides the high capacity of recycles and possible use for the catalysis of other cyclic carbonates.

Graphical Abstract



Keywords Ionic liquid · Propylene carbonate · Cycloaddition · Catalysis · Carbon dioxide

1 Introduction

Carbon dioxide (CO₂) is one of the main greenhouse gases responsible for climate change. However, CO₂ can be useful as an inexpensive C1 block, nontoxic, nonflammable and abundant carbon source [1, 2]. Global efforts to reduce CO₂ production and emission levels are underway. These efforts may drastically alter the development of countries that use coal as a primary energy source, since 1 kWh of produced energy results in production of 950 g CO₂ [3, 4].

CO₂ capture is an efficient possibility to mitigate environmental impacts [5–7]. Currently, only 0.62% of atmospheric CO₂ is used industrially, in the form of fire extinguishers, soft drinks carbonation, supercritical fluid, and advanced oil recovery (EOR) [8]. One strategy is CO₂ capture and conversion into value-added products. The CO₂ captured from stationary sources can be used as reagent and/or reaction medium for chemical syntheses [9–12].

✉ Sandra Einloft
einloft@pucrs.br

¹ Post-Graduation Program in Materials Engineering and Technology, Pontifical Catholic University of Rio Grande do Sul, PUCRS, Porto Alegre, Brazil

² School of Engineering, Pontifical Catholic University of Rio Grande do Sul, PUCRS, Porto Alegre, Brazil

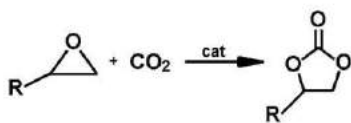
³ P.E.S., Vasilievsky Island, Saint Petersburg, Leningrad Oblast, Russian Federation

An efficient transformation of CO₂ into useful chemicals is a need from environmental protection and resource utilization viewpoint and has attracted much attention in recent years [13–17]. Cyclic carbonates, such as ethylene carbonate, dimethyl carbonate, styrene carbonate and propylene carbonate (PC), are used in numerous technologies [18–21]. Among possibilities, one can highlight usage as aprotic polar solvents, monomers for polycarbonate synthesis, electrolytes for batteries, intermediates in pharmaceuticals and fine chemicals synthesis [22]. Reaction of CO₂ with epoxide forming five-membered cyclic carbonates (Scheme 1) has been extensively studied because it is a 100% atom-economical process [22].

In the past years, various catalysts were developed for chemical fixation of CO₂ to form carbonates, e.g. metal complexes, silicas, zeolites, cellulose, carbon and titanate nanotubes, functionalized polymers, etc [23–25]. Ionic liquids (ILs) exhibit catalytic activity in cyclic carbonates syntheses. The catalytic performance of ILs depends both on the cation and the anion [36–40]. Literature describes the use of [C₈mim][HSO₄] as a catalyst for PC synthesis with a yield of 68 and 97% of selectivity [41].

Surface active ionic liquids (SAILs) constitute a particular class of ILs [42–52]. SAILs contain significantly long hydrophobic chains in cation, anion or both. The most reported cations to form SAILs are imidazolium, pyrrolidinium, pyridinium, and quaternary ammonium. The side chain of these cations may change from C₆ to C₁₆ while retaining substantial surface activity [42–47]. The anions may have C₂₀ in their chain and are usually derived from anionic surfactants making these products potentially interesting for industrial use due to a relatively low cost [48–52]. The large carbon chains of SAILs structures provide self-organizing properties allowing micelle formation, facilitating microemulsions and liquid crystals preparation [52–57]. Although several studies have been done with SAILs in several technological segments, these are insufficiently investigated in the context of catalysis.

We hereby report eight SAILs based on imidazolium ([bmim⁺]) and tetrabutylammonium ([TBA⁺]) cations combined with four different anions (C₁₂ chain) derived from the surfactants: sodium lauryl sulfate ([C₁₂SO₄⁻]), sodium lauryl ether sulfate ([C₁₂ESO₄⁻]), sodium lauryl benzene sulfonate ([C₁₂BSO₃⁻]) and sodium lauroyl sarcosinate ([C₁₂SAR⁻]).



Scheme 1 Catalytic synthesis of cyclic carbonates from epoxides and CO₂

The major advantages of these SAILs compared to other ionic liquids traditionally reported in literature is mainly related to production costs. SAILs anions are derived from surfactant salts largely available in the market. Besides, the absence of fluorinate, phosphonate and heavy metals in their structure help in toxicity prevention.

Finally, these synthesized SAILs were tested as possible catalysts for CO₂ cycloaddition to propylene oxide to produce PC. Recycle tests were performed for the SAIL presenting the highest catalytic activity.

2 Methodology

Structural formulas of the synthesized SAILs are shown in Fig. 1.

2.1 Materials

1-chlorobutane (Acros Organics, 99.0%), 1-methylimidazole (Sigma-Aldrich, 99.0%), acetophenone (Merck, 98.0%), acetone (Vetec, 99.5%), carbon dioxide (Air liquids, 99.998%), dichloromethane (Vetec, 99.5%), diethyl ether (Dinâmica, 99.0%), epichlorohydrin (Sigma-Aldrich, 99.0%), glycidyl isopropyl ether (Sigma-Aldrich, 98.0%), methanol HPLC (99.9%), propylene oxide (Sigma-Aldrich, 99.0%), sodium dodecylbenzenesulfonate (Synth, 50.0%), sodium lauryl ether sulfate (Synth, 50.0%), sodium lauryl sulfate (Synth, 90.0%), sodium *N*-lauryl sarcosine (Merck, 95.0%), styrene oxide (Sigma-Aldrich, 97.0%), tetra-*n*-butylammonium bromide (Panreac, 98.0%), toluene (Merck, 99.9%), zinc bromide (Sigma-Aldrich, 98.0%) were used as purchased.

2.2 Syntheses and Characterization SAILs

The surface active ionic liquids were synthesized following procedures described elsewhere [50–52, 58].

The obtained compounds were characterized by universal attenuated total reflectance Fourier transform infrared spectroscopy (UATR-FTIR) in the range of 4000–650 cm⁻¹ with Perkin-Elmer spectrophotometer 100 FT-IR Spectrum. Nuclear magnetic resonance (NMR) measurements were performed in Bruker Spectrophotometer, operating at 600 MHz, using DMSO-*d*₆ as solvent and glass tubes of diameter 5 mm.

2.2.1 [bmim][C₁₂SO₄]

FTIR ν (cm⁻¹): 3178–3126 (C–H aromatic), 2970 (C–H of CH₂), 2897 (C–H of CH₃), 1628 (C=N aromatic), 1579–1471 (C=C aromatic), 1286 (C–N aromatic), 1172 (C–N alifatic), 1042 (S=O). ¹H-NMR (600 MHz, DMSO-*d*₆) δ (ppm): 9.10 [s, 1H]; 7.75 [d, 1H]; 7.69–7.67 [d, 1H];

Abbreviation	Name	Structure	Abbreviation	Name	Structure
[bmim][C ₁₂ SO ₄]	1 - butyl - 3 - methylimidazolium lauryl sulfate		[TBA][C ₁₂ SO ₄]	tetra - n - butylammonium lauryl sulfate	
[bmim][C ₁₂ ESO ₄]	1 - butyl - 3 - methylimidazolium lauryl ether sulfate		[TBA][C ₁₂ ESO ₄]	tetra - n - butylammonium lauryl ether sulfate	
[bmim][C ₁₂ BSO ₃]	1 - butyl - 3 - methylimidazolium lauryl benzene sulfonate		[TBA][C ₁₂ BSO ₃]	tetra - n - butylammonium lauryl benzene sulfonate	
[bmim][C ₁₂ SAR]	1 - butyl - 3 - methylimidazolium lauroyl sarcosinate		[TBA][C ₁₂ SAR]	tetra - n - butylammonium lauroyl sarcosinate	

Fig. 1 Abbreviations, names and structures of the synthesized SAILs

4.16 [t, 2H, J=6.9 Hz]; 3.85 [s, 3H]; 3.86 [t, 2H, J=6.3 Hz]; 1.82–1.68 [m, 2H, J=14.9; 7.5 Hz]; 1.48 [dt, 2H, J=14.7; 7.3 Hz]; 1.24 [s, 20H]; 0.95–0.81 [m, 6H]. Water miscible [52].

2.2.2 [bmim][C₁₂ESO₄]

FTIR ν (cm⁻¹): 3158–3120 (C–H aromatic), 2966 (C–H of CH₂), 2882 (C–H of CH₃), 1628 (C=N aromatic), 1568–1459 (C=C aromatic), 1282 (C–N aromatic), 1215 (C–O), 1170 (C–N alifatic), 1019 (S=O). ¹H-NMR (600 MHz, DMSO-d₆) δ (ppm): 9.11 [s, 1H]; 7.77 [d, 1H]; 7.70 [d, 1H]; 4.17 [t, 2H, J=6.8 Hz]; 3.78 [s, 3H]; 3.86 [t, 2H, J=15.7 Hz]; 3.54–3.41 [dt, 4H]; 1.82–1.70 [m, 2H, J=13.4; 7.5 Hz]; 1.47 [dt, 2H, J=12.8; 6.8 Hz]; 1.24 [s, 24H]; 0.93–0.79 [m, 6H]. Water miscible [52].

2.2.3 [bmim][C₁₂BSO₃]

FTIR ν (cm⁻¹): 3163–3120 (C–H aromatic), 2966 (C–H of CH₂), 2872 (C–H of CH₃), 1627 (C=N aromatic), 1602 (C=C aromatic), 1574 (C=C aromatic), 1492 (C=C aromatic), 1466 (C=C aromatic), 1285 (C–N aromatic), 1169 (C–N alifatic), 1221 (C–O), 1019 (S=O), 830 (aromatic ring). ¹H-NMR (600 MHz, DMSO-d₆) δ (ppm): 9.15 [s, 1H]; 7.78 [d, 1H, J=1.7 Hz]; 7.71 [d, 1H, J=1.7 Hz]; 7.59–7.48 [m, 2H]; 7.48–7.05 [m, 2H]; 4.16 [t, 2H, J=7.2 Hz]; 3.85 [s, 3H]; 3.64 [t, 2H, J=6.0 Hz]; 2.2 [t, 2H]; 1.82–1.71 [m, 2H, J=14.9; 7.6 Hz]; 1.35 [dt, 2H, J=14.8; 7.5 Hz]; 1.32–1.21 [m, 18H]; 0.97 [t, 3H, J=7.6 Hz]; 0.85 [t, 3H]. Water miscible.

2.2.4 [bmim][C₁₂SAR]

FTIR ν (cm⁻¹): 3432 (N–C=O), 3137–3045 (C–H aromatic), 2957 (C–H of CH₂), 2871 (C–H of CH₃), 1670 (C=O), 1634 (C=N aromatic), 1567–1463 (C=C aromatic), 1231 (C–N aromatic), 1281–1167 (C–N alifatic). ¹H-NMR (600 MHz, DMSO-d₆) δ (ppm): 9.21 [s, 1H]; 7.77 [d, 1H, J=1.6 Hz]; 7.68 [d, 1H, J=1.7 Hz]; 4.23 [t, 2H, J=7.1 Hz]; 3.84 [s, 3H]; 3.48 [s, 2H, J=10.1 Hz]; 2.75 [m, 20H]; 2.51 [s, 3H]; 1.82–1.70 [m, 2H, J=14.7; 7.5 Hz]; 1.31 [dt, 2H, J=14.6; 7.4 Hz]; 1.23 [t, 3H]; 0.95 [t, 3H, J=7.6 Hz]. Water miscible.

2.2.5 [TBA][C₁₂SO₄]

FTIR ν (cm⁻¹): 2962 (C–H of CH₂), 2877 (C–H of CH₃), 1280 (N–C alifatic), 1216 (C–O), 1023 (S=O). ¹H-NMR (600 MHz, DMSO-d₆) δ (ppm): 3.67 [t, 2H, J=6.1 Hz]; 3.23–3.12 [m, 8H]; 1.54 [m, 8H]; 1.44 [m, 8H, J=7.2 Hz]; 1.37–1.21 [m, 20H]; 0.94 [m, 12H]; 0.86 [t, 3H]. Water immiscible [52].

2.2.6 [TBA][C₁₂ESO₄]

FTIR ν (cm⁻¹): 2969 (C–H of CH₂), 2872 (C–H of CH₃), 1269 (N–C alifatic), 1216 (C–O), 1020 (S=O). ¹H-NMR (600 MHz, DMSO-d₆) δ (ppm): 3.79 [t, 2H]; 3.67 [t, 2H, J=6.0 Hz]; 3.49 [t, 2H, J=17.2 Hz]; 3.23–3.11 [m, 8H];

1.58 [m, 8H]; 1.36–1.19 [m, 8H, J = 5.8 Hz]; 0.94 [s, 26H]; 0.85 [t, 12H, J = 6.1 Hz]. Water miscible [52].

2.2.7 [TBA][C₁₂BSO₃]

FTIR ν (cm⁻¹): 2960 (C–H of CH₂), 2878 (C–H of CH₃), 1600 (C=C aromatic), 1570 (C=C aromatic), 1492 (C=C aromatic), 1460 (C=C aromatic), 1280 (N–C alifatic), 1216 (C–O), 1023 (S=O), 832 (aromatic ring). ¹H-NMR (600 MHz, DMSO-d₆) δ (ppm): 7.62–7.51 [m, 2H]; 7.37–7.01 [m, 2H]; 3.61 [t, 2H, J = 5.9 Hz]; 3.22–3.08 [m, 8H]; 2.2 [t, 2H]; 1.56 [m, 8H]; 1.46–1.32 [m, 18H]; 1.28 [m, 8H, J = 6.4 Hz]; 0.91 [t, 12H, J = 7.2 Hz]; 0.88 [t, 3H]. Water miscible.

2.2.8 [TBA][C₁₂SAR]

FTIR ν (cm⁻¹): 3428 (N–C=O), 2960 (C–H of CH₂), 2875 (C–H of CH₃), 1681 (C=O), 1280–1186 (N–C alifatic). ¹H-NMR (600 MHz, DMSO-d₆) δ (ppm): 3.50 [s, 2H, J = 10.1 Hz]; 3.20–3.08 [m, 8H]; 2.70 [m, 20H]; 2.48 [s, 3H]; 1.62 [m, 8H]; 1.36 [m, 8H, J = 6.5 Hz]; 1.20 [t, 3H]; 0.94 [t, 12H, J = 7.1 Hz]. Water miscible.

SAILs moisture contents were determined by coulometric Karl Fischer titration method using a KF-1000 Analyzer (Brazil) and Karl Fischer reagent without pyridine (Merck) as titrating solution and methanol as solvent. The sodium (Na⁺) content was determined by atomic absorption spectroscopy (AAS) by Varian AAS 55 spectrometer with an air/acetylene flame (99.99% Air Products). The chloride (Cl⁻) content was performed in a portable Vernier LabQuest system with a specific sensor for this ion. Results of SAILs synthesis residual contaminants are presented in Table 1.

The thermogravimetric analysis (TGA) was carried out in TA Instruments Q600 with a heating rate of 20 °C min⁻¹, from 25 to 1000 °C in the nitrogen atmosphere.

Table 1 Residual contaminants in the synthesized SAILs

SAIL	Moisture contents (%)	Residual [Na ⁺] (%)	Residual [Cl ⁻] (%)
[bmim][C ₁₂ SO ₄] [52]	1.43	0.20	0.08
[bmim][C ₁₂ ESO ₄] [52]	0.42	ND	0.05
[bmim][C ₁₂ BSO ₃]	0.81	0.13	0.11
[bmim][C ₁₂ SAR]	0.24	ND	ND
[TBA][C ₁₂ SO ₄] [52]	0.19	ND	ND
[TBA][C ₁₂ ESO ₄] [52]	0.46	0.07	ND
[TBA][C ₁₂ BSO ₃]	0.67	ND	ND
[TBA][C ₁₂ SAR]	0.30	ND	ND

ND not detected

2.3 Cycloaddition Reaction

PC syntheses from CO₂ and propylene oxide (PO) were carried out in presence of [bmim⁺] and [TBA⁺] cation-based SAILs combined to different anions [C₁₂SO₄⁻], [C₁₂ESO₄⁻], [C₁₂BSO₃⁻] and [C₁₂SAR⁻]. These compounds were tested in presence of metallic halide (ZnBr₂) as a cocatalyst. The use of SAIL [bmim][C₁₂ESO₄] was evaluated for the determination of the reaction parameters (amount of catalyst, temperature, pressure and time) and the best catalyst was tested for kinetics and cycles.

All cycloaddition reactions were performed in a stainless steel autoclave of 120 cm³ equipped with magnetic stirring. For a typical reaction, 100 mmol of propylene oxide, 0.25 mmol of cocatalyst (ZnBr₂) and 1 mmol of SAIL were used. The syntheses were performed without any additional solvent. The autoclave was pressurized with CO₂ and heated to the desired working temperature. After the reaction completion, the reactor was cooled to room temperature and slowly depressurized.

Catalyst separation from PC was performed by a simple distillation under inert atmosphere (N₂). CO₂ cycloaddition reaction conversion was determined by gravimetric technique from isolated product. To determine the selectivity, the resulting liquid mixtures were analyzed using a gas chromatograph Shimadzu CG-2014 equipped with a flame ionization detector and a 100% dimethyl polysiloxane column (30 m × 0.53 mm ID) using acetophenone as external standard and dimethyl ether as solvent. The turnover number (TON) and turnover frequency (TOF) were calculated according to equations (1) and (2).

$$\text{TON} = \frac{\text{mmol of product}}{\text{mmol of catalyst}} \quad (1)$$

$$\text{TOF} = \frac{\text{TON}}{\text{time (h)}} \quad (2)$$

2.4 Computational Methodology

Electronic structure of the simulated species was optimized by the hybrid density functional theory Becke-3-Lee-Yang-Parr (B3LYP) [59, 60]. The atom-centered split-valence double-zeta polarized basis set 6-31G(d) was used to approximate the wave function. All elements, except hydrogen, were equipped with additional polarization functions to improve accuracy of simulation of ions. The wave function convergence criterion was set to 2×10^4 kJ mol⁻¹. The steepest descent geometry optimization criterion was set to 0.1 kJ mol⁻¹. The reaction coordinates were sampled with a step of 0.05 Å in all cases.

GAMESS US 2013 was used to conduct electronic structure calculations [61]. Gabedit 2.8 was used to prepare input molecular structures and visualize the results [62].

3 Results and Discussion

3.1 Influence of Reaction Parameters

The best parameters for CO₂ cycloaddition to propylene oxide were preliminarily tested using the SAIL [bmim][C₁₂ESO₄] as a catalyst. An effect of catalyst concentration was investigated by varying the amount of SAIL from 0.5 to 2.5 mmol (using initial pressure 4.0 MPa, temperature 383 K and duration 6 h). Results can be seen in Fig. 2a. The conversion increases with the increase of the catalyst amount [13]. Compare conversion 46.6% with 0.5 mmol of catalyst with conversion 65.0% with 1.0 mmol of catalyst. Further addition of catalyst to the reaction media leads to a more modest conversion increase. Note 68.6% with

2 mmol and 73.3% with 2.5 mmol. Based on these results, the amount of 1.0 mmol of catalyst was chosen for all further investigations reported below.

The temperature influence was investigated using 1.0 mmol of SAIL at the initial pressure of 4.0 MPa and reaction duration of 6 h. The results can be seen in Fig. 2b. We discovered the highest-performance temperature for this reaction amounting to 383 K, at which the conversion reaches 65.0%. Further temperature increase results in a gradually deteriorated performance (64.1% at 393 K and 63.4% at 403 K), but practically insignificant (~1.5% by 20 K). This behavior is not related to catalyst degradation as one can see in Fig. 3 shows [bmim][C₁₂ESO₃] thermogram. Two weight loss events occurs, the first one at 188–287 °C (weight loss 8.6%), corresponds to the degradation of the side chain of the anion and the second one at 293–435 °C (weight loss 85.3%) corresponds to complete degradation of the ions [52]. The conversion reduction is probably related to propylene oxide isomerization, the interaction between of propylene oxide and water [13, 39]

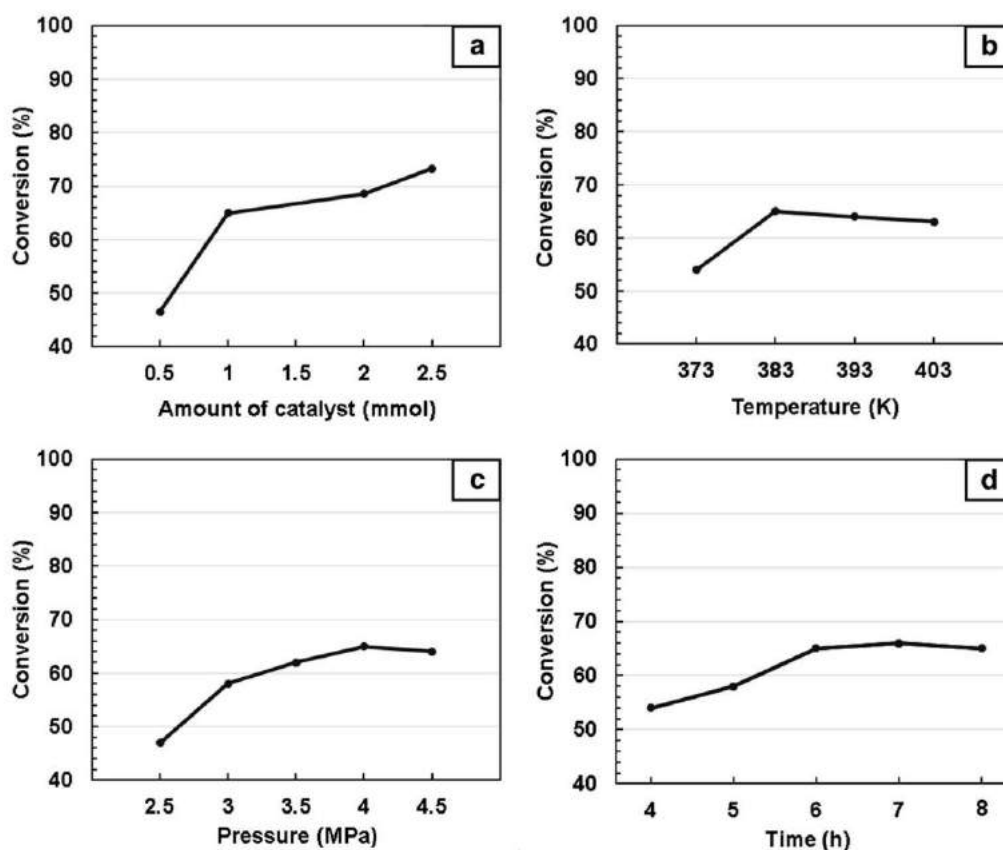


Fig. 2 The effect of amount of catalyst (a), temperature (b), pressure (c) and time (d) on the PC synthesis using [bmim][C₁₂ESO₄] as a catalyst

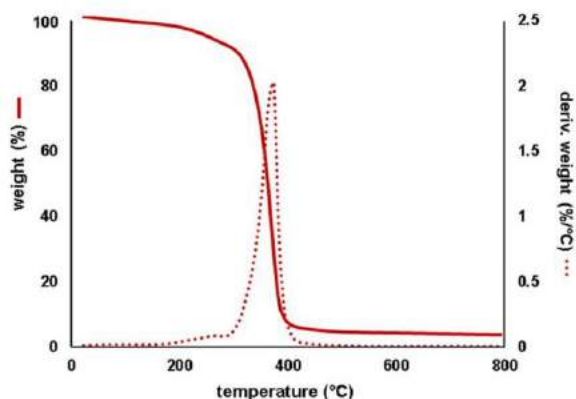


Fig. 3 Thermogram of [bmim][C₁₂ESO₄]

and initiation of secondary reversible reactions of epoxide [22, 37, 63].

Pressure effect (Fig. 2c) was studied by varying pressure from 2.5 to 4.5 MPa, keeping the other parameters as follows: 1.0 mmol of catalyst, temperature 383 K, duration 6 h. The conversion percentage increases up to 4.0 MPa. Compare conversion 47.2% at 2.5 MPa with 65.0% at 4.0 MPa and 64.0% at 4.5 MPa. Such a trend was also observed in other studies [37, 63]. This behaviour is due to a stoichiometric rate of propylene oxide/CO₂, so that one does not inhibit the role of the other. Yet, the propylene oxide remains liquid up to 4.0 MPa, favoring interaction with the catalyst. Above this pressure propylene oxide passes to the gaseous state, decreasing the contact with SAIL that remains in the liquid state in contact only with the reaction products [64].

Finally, the reaction time effect (Fig. 2d) was evaluated with the best parameters determined so far (1 mmol of catalyst, 383 K of temperature and 4.0 MPa of pressure). As

depicted in Fig. 2d, one can see that the conversion percentage evolves gradually during 6 h. Above this temperature there is no significant change in conversion values.

To recapitulate, the better reaction conditions for CO₂ cycloaddition to propylene oxide are 1.0 mmol catalyst, 383 K temperature, 4.0 MPa pressure, duration 6 h.

3.2 An Effect of SAIL

It is important to highlight that no product was detected when the reaction was performed without a catalytic system (catalyst/cocatalyst), therefore, the reaction of PO + CO₂ is not spontaneous. When only the SAIL was used (entry 3) or only the cocatalyst was used (entry 4), there is no significant conversion to the PC [23]. Consequently, presence of a Lewis acid as a cocatalyst is fundamental for the activity of SAILs for the cyclic carbonate syntheses [65]. Table 2 presents the results obtained for cycloaddition of CO₂ to epoxide using SAILs as catalysts combined with ZnBr₂. Comparing [bmim⁺] (entries 1–6) with [TBA⁺] (entries 7–10) one can see that [TBA⁺] is more active as a catalyst. The higher [TBA⁺] molecular volume increases the distance cation/anion, consequently, a weaker electrostatic interaction cation/anion results in a more nucleophilic anion. The latter increases catalytic activity [13]. A previous study [66] also indicates that at high temperature [TBA⁺] generates a degradation product, trialkylammonium, which may be a key component for favoring catalysis that require basic sites in the catalyst, thus making [TBA⁺] more efficient than [bmim⁺]. SAIL [TBA][C₁₂SO₄] (entry 7) presented better conversion and selectivity results, 79.2% of conversion and 87.7% of selectivity. This compound is the only tested SAIL that is largely hydrophobic (0.19% of moisture content, Table 1). This characteristic may contribute to the observed good conversion, since the presence of moisture

Table 2 Catalytic performances of SAILs for the cycloaddition of CO₂ to form PC^a

Entry	Catalyst	Conversion (%)	Selectivity (%)	TON	TOF (h ⁻¹)
1	[bmim][C ₁₂ SO ₄]	16.5	57.6	9.5	1.6
2	[bmim][C ₁₂ ESO ₄]	65.0	79.1	51.3	8.5
3	[bmim][C ₁₂ ESO ₄] ^b	Trace	–	–	–
4	ZnBr ₂ ^c	–	–	–	–
5	[bmim][C ₁₂ BSO ₃]	45.3	55.5	25.1	4.2
6	[bmim][C ₁₂ SAR]	70.9	28.9	20.5	3.4
7	[TBA][C ₁₂ SO ₄]	79.2	87.7	69.4	11.6
8	[TBA][C ₁₂ ESO ₄]	34.6	67.1	23.2	3.9
9	[TBA][C ₁₂ BSO ₃]	65.7	76.3	50.1	8.4
10	[TBA][C ₁₂ SAR]	82.4	26.9	22.2	3.7

^aReaction conditions: PO 100 mmol, catalyst 1.0 mmol, 0.25 mmol of ZnBr₂, T = 383 K, initial CO₂ pressure 4.0 MPa, t = 6 h. TON = mmol of products/mmol of catalyst. TOF = TON/time (h)

^bReaction without cocatalyst ZnBr₂

^cReaction using only ZnBr₂ as catalyst

may deactivate the catalyst [67] and hydrolyze the product [68]. Corroborating this result compare [bmim][C₁₂SO₄] (entry 1), the one with the highest amount of moisture contents, (1.43%), presented values of 16.5% of conversion and 57.6% of selectivity.

Low PC selectivity of the catalyst can be explained by a nucleophilic attack (by water) in the cyclic ester group of PC [69]. Another possibility is the reaction between propylene oxide and residual water (moisture), producing by-products (mainly propane-1,2-diol) since water molecule competes with CO₂ molecule in the attack to the less hindered carbon of epoxy ring according to literature [68–71]. Propane-1,2-diol selectivity was of 31.6% ([bmim][C₁₂SO₄]; entry 1).

The presence of ether functional group in [bmim][C₁₂ESO₄] (entry 2) suggests a better interaction with propylene oxide exhibiting conversion of 65.0% and selectivity of 79.1% superior when compared to the cation without the presence of this functional group (entry 1). This effect is no longer observed with [TBA][C₁₂ESO₄] (entry 8), where the presence of the ether reveals a significant loss of catalytic capacity. This result suggests that the greater distance cation–anion that occurs in [TBA⁺] deactivates a possible nucleophilic effect that oxygen may be exerting. The moisture contents of these two SAILs are quite similar.

Comparing SAILs containing a very large aromatic group in their chain [bmim][C₁₂B_{SO}₃] and [TBA][C₁₂B_{SO}₃] (entries 5 and 9) we see an influence of the possible amount of moisture contents present in the SAILs. While [bmim][C₁₂B_{SO}₃] (0.81% moisture contents) presented conversion of 45.3% and selectivity of 55.5%, [TBA][C₁₂B_{SO}₃] (0.67% moisture contents) presented 65.7% of conversion and 76.3% of selectivity. Another determining factor for these results is the anion volume, many studies indicate that voluminous molecules hinder the steric interaction between catalyst and substrate [36, 72, 73].

Finally, comparing the two SAILs with nitrogenous anions, [bmim][C₁₂SAR] (entry 6) and [TBA][C₁₂SAR] (entry 10) we have a high catalytic activity with low selectivity for PC in both cases. This is due to the presence of the nitrogenous base which enhances basic sites of the environment and increases the nucleophilicity of the medium leading to a high conversion [74, 75]. Previous studies indicate that more acidic catalysts favor the epoxide ring opening resulting in high selectivity, since they act as Lewis acids, and may even dispense the use of cocatalyst [74, 75]. The terminal acetate anion may decentralize this electronic charge and activate the catalytic potential.

The two most basic anions [C₁₂SAR⁻] and [C₁₂B_{SO}₃⁻] do not present good catalytic results. Thus, acidic sites are preferable for epoxide cycloaddition.

A plausible mechanism for cycloaddition of CO₂ to epoxide catalyzed by SAILs is presented in Fig. 4. Mechanism involves a metal halide (ZnBr₂) acting as a Lewis acid,

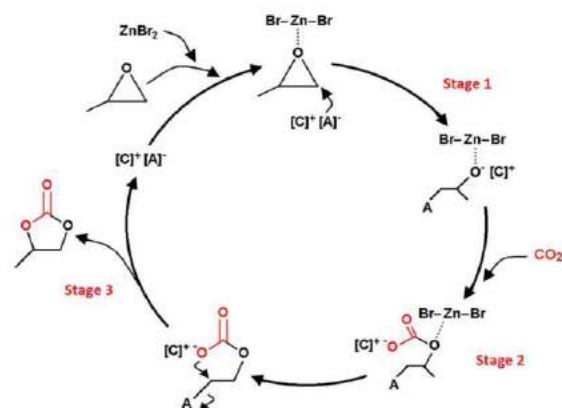


Fig. 4 Proposed mechanism for the synthesis of propylene carbonate from propylene oxide and CO₂

interacting with the oxygen atom of the epoxide, so that the basic anion of SAIL carries out the attack on the least impeded carbon atom of the epoxy ring.

As mentioned previously, there is no significant conversion without the presence of the metal halide. This can be attributed to the non-nucleophilic natures of the anions used in this work [76]. In the next step, a species of oxyanion is formed. The CO₂ carbon atom interacts with the anionic species producing an anionic alkylcarbonate. The latter is converted into the cyclic carbonate by intermolecular cyclic elimination and finally the SAIL is regenerated.

3.3 Computer Simulations

The simulation of energetics of PC formation along the proposed reaction coordinates for the three stages (Fig. 4) of the catalyzed PC synthesis is presented in Figs. 5 and 6. The goal of these simulations was to identify possible energetic barriers and overall reaction energetics in the case of different catalysts employed. An initial breakage of the epoxide molecule is essentially barrier-free and brings over 100 kJ mol⁻¹. This stage does depend on the anion chosen (Fig. 5), but this effect is modest as compared to other energy alterations in the course of PC synthesis. Note, ZnBr₂ simplifies opening of the epoxide ring drastically. Previous simulations [77] revealed a high and very different by shape barrier when only a salt catalyst was selected. Both our and earlier simulations are confirmed by the hereby reported syntheses, which indicate negligible transformation in the absence of ZnBr₂. The most favorable anion out of the large set benchmarked is chloride. All sulfate-based anions exhibit similar performances to [C₁₂SO₄⁻]. The alkylcarbonate formation exhibits a small barrier of 13 kJ mol⁻¹ and brings ~20 kJ mol⁻¹. At this stage, the oxygen-zinc bond is ruined and ZnBr₂ floats away.

Fig. 5 Energy profiles describing stages 1 and 2 of PC formation catalyzed by ZnBr₂ and ionic liquid catalysts (tetra-*n*-butylammonium chloride and tetra-*n*-butylammonium lauryl sulfate). Arrows show directions of the considered chemical reactions

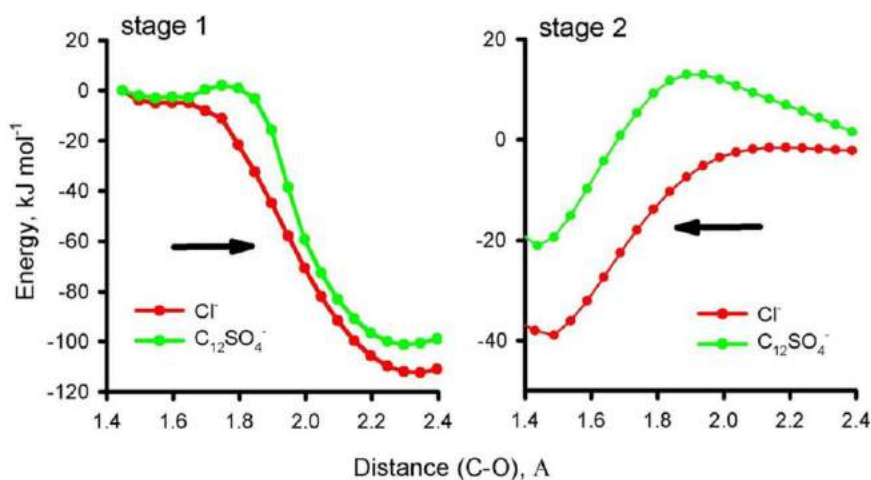
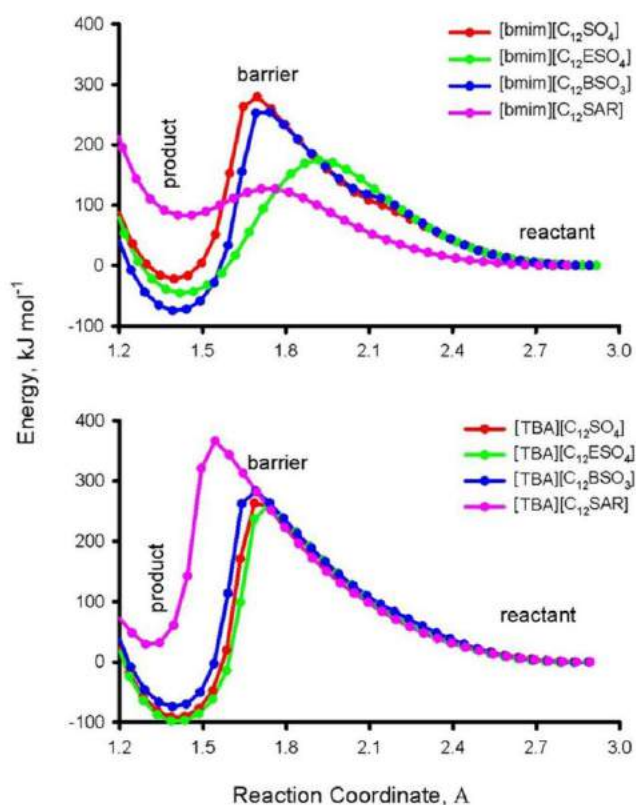


Fig. 6 Energy profiles describing the closure of the PC ring (stage 3). The reaction coordinate is a distance between oxygen and carbon of PC forming a covalent bond



An energy barrier is associated with the closure of the ring (Fig. 6), which is quite dependent on the SAIL catalyst. To overcome this particular barrier, heating of the reactants is necessary. The sulfate containing anions behave differently from the SAR⁻ anion. The role of the cation is significant. A strong cation–anion attraction in the case of

the imidazolium-based SAILs is favorable to detach the anion from alkylcarbonate and, therefore, engender the carbon–oxygen covalent bond (Fig. 4) of the emerging PC. A weaker interaction of [TBA⁺] with the same anions results in somewhat higher barriers for the sulfate containing SAILs and a much larger barrier for [TBA][C₁₂SAR].

The conducted simulations suggest that ionic catalysts with stronger cation–anion attraction are preferable for the PC synthesis upon its last stage. In the considered SAILs, this effect is, however, blocked by a higher hydrophilicity (represented by moisture content by Karl Fischer) of the imidazolium-based ionic liquids than that of the tetrabutylammonium-based ionic liquids.

3.4 Catalyst Recycling

As important as catalyst catalytic activity is its regeneration capacity. For this test, the SAIL with best performance as catalyst for this reaction ($[\text{TBA}][\text{C}_{12}\text{SO}_4] + \text{ZnBr}_2$) was chosen (1 mmol, 383 K, 4.0 MPa and 6 h). The procedure used to separate the catalytic system $[\text{SAIL} + \text{ZnBr}_2]$ from PC was the same used in all syntheses, a simple distillation in the inert atmosphere. The recycle was tested for five times without any catalyst or cocatalyst addition (Fig. 7).

The SAIL slightly decreases its catalytic activity in the first cycle. Initial values are 79.2% of conversion and 87.7% of selectivity. In the first cycle, these values decrease to 75.6 and 84.7%, respectively. From this point, the decay between the recycles is quite subtle, arriving in the fifth recycle in values of 73.1% of conversion and 83.1% of selectivity. The high thermal stability of SAILs is mainly responsible for these results. Under these reaction conditions, there is no catalyst decomposition. FTIR analysis was performed in catalyst after the fifth recycle and no structural change was observed, as shown in Fig. 8. The $[\text{TBA}][\text{C}_{12}\text{SO}_4]$ proved to be efficient for this reaction.

3.5 Application to Other Cyclic Carbonates

Catalytic behaviour of the best SAIL $[\text{TBA}][\text{C}_{12}\text{SO}_4]$ was investigated. Other terminal epoxides can be converted to

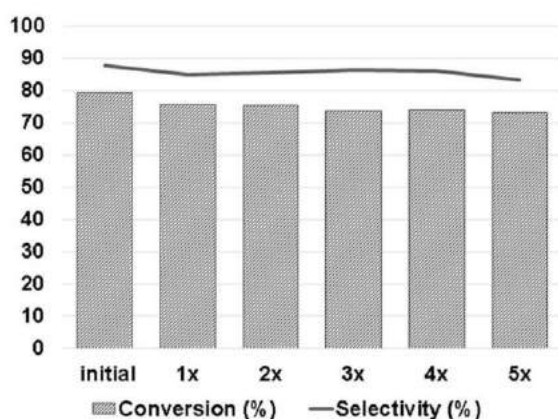


Fig. 7 Recycling experiments of $[\text{TBA}][\text{C}_{12}\text{SO}_4]$

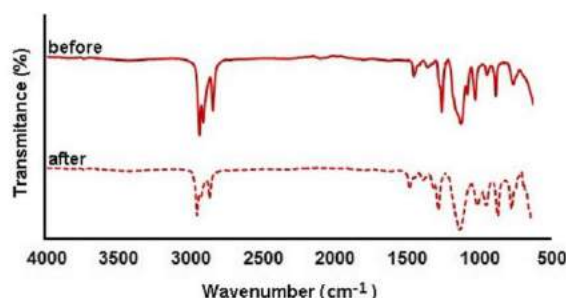


Fig. 8 FTIR analysis before and after 5 uses of $[\text{TBA}][\text{C}_{12}\text{SO}_4]$

cyclic carbonates with possible commercial applications (Table 3).

SAIL $[\text{TBA}][\text{C}_{12}\text{SO}_4]$ shows good catalytic activity for all tested epoxides. The styrene oxide (entry 11) presented very similar results compared to the PC synthesis (Table 2, entry 7). SAIL activity is good even in presence of aromatic ring, a voluminous group.

The presence of functional groups in the monosubstituted epoxides, such as glycidyl isopropyl ether (entry 12) and epichlorohydrin (entry 13), results in higher conversions and selectivities even relative to PC (Table 2, entry 7) and styrene carbonate (entry 11) [25, 78].

Table 3 Application of $[\text{TBA}][\text{C}_{12}\text{SO}_4]$ to catalyze syntheses of other cyclic carbonates

Entry	Substrate	Product	Conversion (%)	Selectivity (%)
11 ^a			74.5	87.8
12 ^b			86.5	92.6
13 ^c			92.1	94.7

^aReaction conditions: SO 50 mmol, catalyst 0.5 mmol, 0.125 mmol of ZnBr_2 , $T = 353 \text{ K}$, initial CO_2 pressure 4.0 MPa, $t = 4 \text{ h}$

^bReaction conditions: GIE 50 mmol, catalyst 0.5 mmol, 0.125 mmol of ZnBr_2 , $T = 393 \text{ K}$, initial CO_2 pressure 3.0 MPa, $t = 3 \text{ h}$

^cReaction conditions: epichlorohydrin 100 mmol, catalyst 1.0 mmol, 0.15 mmol of ZnBr_2 , $T = 393 \text{ K}$, initial CO_2 pressure 3.0 MPa, $t = 2 \text{ h}$

4 Conclusion

Several SAILs were synthesized and characterized to be used as catalysts in the CO₂ cycloaddition to epoxides and showed catalytic efficiency. The best reaction condition for the synthesis of propylene carbonate was 383 K of temperature, 6 h of time at 4.0 MPa of pressure. The [TBA][C₁₂SO₄] was the SAIL that presented better catalytic activity, reaching 79.2% of conversion and 87.7% of selectivity, besides the high capacity of recycles and possible use for the catalysis of other cyclic carbonates.

Acknowledgements M.O.V. and W.F.M. thank CAPES for the doctoral fellowships, B.S.N. thanks FAPERGS for scholarship and S.E. thanks CNPq for the researcher scholarship.

References

- Kuwahara Y, Yamashita H (2013) *J. CO₂ Util* 1:50
- Zhao G, Zhang Y, Li J, Gao S (2015) *J Energy Chem* 24:353
- Darensbourg DJ (2010) *Inorg Chem* 49:10765
- Aresta M, Dibenedetto A (2007) *Dalton Trans* 28:2975
- Masoumi S, Rahimpour MR, Mehdipour M (2016) *J. CO₂ Util* 16:42
- Chowdhury S, Balasubramanian R (2016) *J CO₂ Util* 13:50
- Manoranjan N, Won DH, Kimb J, Woo SI (2016) *J. CO₂ Util* 16:486
- Aresta M, Dibenedetto A (2013) *Chem Rev* 114:1709
- Barbarossa V, Barzagli F, Mani F, Lai S, Vanga G (2015) *J CO₂ Util* 10:50
- Meylan FD, Moreau V, Erkman S (2015) *J. CO₂ Util* 12:101
- Cuellar-Franca RM, Azapagic A (2015) *J CO₂ Util* 9:82
- Duraccio V, Gnoni MG, Elia V (2015) *J. CO₂ Util* 10:23
- Ju HY, Manju MD, Kim KH, Park SW, Park DW (2008) *J Ind Eng Chem* 14:157
- Zhang X, Su D, Xiao L, Wu W (2017) *J CO₂ Util* 17:37
- Meng Q, Cheng R, Li J, Wang T, Liu B (2016) *J CO₂ Util* 16:86
- Pan X, Liu Z, Cheng R, Yang Y, Zhong L, He X, Liu B (2013) *J CO₂ Util* 2:39
- Song QW, Zhou ZH, He LN (2017) *Green Chem* 19:p 3707
- Bobink FD, Dyson PJ (2016) *J Catal* 343:52
- Zhang X, Geng W, Yue C, Wu W, Xiao L (2016) *J Environ Chem Eng* 4:2565
- Hwang GY, Roshan R, Ryu HS, Jeong HM, Ravi S, Kim MI, Park DW (2016) *J CO₂ Util* 15:123
- Dai W, Yang W, Zhang Y, Wang D, Luo X, Tu X (2017) *J CO₂ Util* 17:256
- Sakakura T, Choi JC, Yasuda H (2007) *Chem Rev* 107:2365
- Monteiro WF, Vieira MO, Aquino AS, Souza MO, Lima J, Einloft S, Ligabue R (2017) *Appl Catal A* 544:46
- Zhang H, Kong X, Cao C, Pang G, Shi Y (2016) *J CO₂ Util* 14:76
- Buonerba A, Nisi AD, Grassi A, Milione S, Capacchione C, Vagine S, Rieger B (2015) *Catal Sci Technol* 5:118
- Zhong S, Liang L, Liu B, Sun J (2014) *J. CO₂ Util* 6:75
- Liu M, Liu B, Liang L, Wang F, Shi L, Sun J (2016) *J Mol Catal A* 418:78
- Fuentes SG, Contreras R, Isaacs M, Honores J, Quezada D, Landaeeta E, Toledo RO (2016) *J CO₂ Util* 16:114
- Liu M, Lan J, Liang L, Sun J, Arai M (2017) *J Catal* 347:138
- Peng J, Yang HJ, Geng Y, Wei Z, Wang L, Guo CY (2017) *J. CO₂ Util* 17:243
- Xie Y, Wang TT, Liu XH, Zou K, Deng WQ (2013) *Nat Commun* 4:1
- Zhong S, Liang L, Liu M, Liu B, Sun J (2015) *J. CO₂ Util* 9:58
- Wu X, Wang M, Xie Y, Chena C, Li K, Yuan M, Zhao X, Hou Z (2016) *Appl Catal A* 519:146
- Bhin KM, Tharun J, Roshan KR, Kim DW, Chung Y, Park DW (2017) *J CO₂ Util* 17:112
- Werner T, Tenhumberg N (2014) *J CO₂ Util* 7:39
- Vieira MO, Aquino AS, Schütz MK, Vecchia FD, Ligabue R, Seferin M, Einloft S (2017) *Energy Proced* 114:7141
- Aquino AS, Bernard FL, Vieira MO, Borges JV, Rojas MF, Vecchia FD, Ligabue RA, Seferin M, Menezes S, Einloft S (2014) *J Braz Chem Soc* 25:2251
- Aquino AS, Bernard FL, Borges JV, Mafra L, Vecchia FD, Vieira MO, Ligabue R, Seferin M, Chaban VV, Cabrita EJ, Einloft S (2015) *RSC Adv* 5:64220
- Xiao L, Su D, Yue C, Wu W (2014) *J. CO₂ Util* 6:1
- Vekariya RL (2017) *J Mol Liq* 227:44
- Jasiak K, Siewniak A, Kopczynska K, Chrobok A, Baj S (2016) *J Chem Technol Biotechnol* 91:2827
- Sedov IA, Solomonov BN (2016) *Fluid Phase Equilib* 425:9
- Geng F, Zheng L, Yu L, Li G, Tung C (2010) *Process Biochem* 45:306
- Jingjing J, Bing H, Meijia L, Ni C, Li Y, Min L (2013) *J Colloid Interface Sci* 412:24
- Li X, Gao Y, Liu J, Zheng L, Chen B, Wub L, Tung C (2010) *J Colloid Interface Sci* 343:94
- Vekariya RL, Dhar A, Lunagariya J (2017) *Compos Interfaces* 24:801
- Meng Y, Liu J, Li Z, Wei H (2014) *J Chem Eng Data* 59:2186
- Obliosca JM, Arco SD, Huang MH (2007) *J Fluoresc* 17:613
- Bharmoria P, Rao KS, Trivedi TJ, Kumar A (2014) *J Phys Chem B* 118:115
- Rao KS, Tushar JT, Kumar A (2012) *J Phys Chem B* 116:14363
- Bharmoria P, Mehta MJ, Pancha I, Kumar A (2014) *J Phys Chem B* 118:9890
- Vieira MO, Monteiro WF, Ligabue R, Seferin M, Chaban VV, Andreeva NA, Nascimento JF, Einloft S (2017) *J Mol Liq* 241:64
- Shi L, Zhao M, Zheng L (2012) *RSC Adv* 2:11922
- Porada JH, Mansueto M, Laschat S, Stubenrauch C (2017) *J Mol Liq* 227:202
- Selwent A, Łuczak J (2016) *J Mol Liq* 221:557
- Kaper H, Smarsly BZ (2006) *Phys Chem* 220:1455
- Zhao Y, Chen X, Jing B, Wang X, Ma F (2009) *J Phys Chem B* 113:983
- Vekariya RL, Kumar NS (2017) *Colloid Surf. A* 529:203
- Becke AD (1988) *Phys Rev A* 38:3098
- Lee CT, Yang WT, Parr RG (1988) *Phys Rev B* 37:785.
- Schmidt MW, Baldrige KK, Boat JA, Elbert ST, Gordon MS, Jensen JH, Koseki S, Matsunaga N, Nguyen KA, Su S, Windus TL, Dupuis M, Montgomery JA (1993) *J Comput Chem* 14:1347
- Allouche AR (2011) *J Comput Chem* 32:174
- Sun J, Cheng WG, Fan W, Wang YH, Meng ZY, Zhang SJ (2009) *Catal Today* 148:361
- Xiao LF, Yue QF, Xia CG, Xu LW (2008) *J Mol Catal A Chem* 279:230
- Kim HS, Kim JJ, Kim H, Jang HG (2003) *J Catal* 220:44
- North M, Pasquale R (2009) *Angew Chem* 121:2990
- Lan DH, Yang FM, Luo SL, Au CT, Yin SF (2014) *Carbon* 73:351
- Sun J, Ren J, Zhang S, Cheng W (2009) *Tetrahedron Lett* 50:423
- Jin X, Bobba P, Reding N, Song Z, Thapa PS, Prasad G, Subramaniam B, Chaudhari RV (2017) *Chem Eng Sci* 168:189
- Kilic A, Ulusoy M, Durgun M, Aytar E (2014) *Inorg Chim Acta* 411:17
- Li DW, Bi J, Lian LS, Biao LX, Man TX, Tong AC (2014) *Appl Catal A* 470:183

-
72. Ju HY, Manju MD, Kim KH, Park SW, Park DW (2007) *Korean J Chem Eng* 24:917
73. Ju HY, Manju MD, Park DW, Choe Y, Park SW (2007) *React Kinet Catal Lett* 90:3
74. Kim J, Kim SN, Jang HG, Seo G, Ahn WS (2013) *Appl Catal A* 453:175
75. Kim YJ, Park DW (2013) *J Nanosci Nanotechnol* 13:2307
76. Sun J, Fujita S, Arai M (2005) *J Organomet Chem* 690:3490
77. Wang JQ, Dong K, Cheng WG, Sun J, Zhang SJ (2012) *Catal Sci Technol* 2:1480
78. Yang ZZ, He LN, Miao CX, Chanfreau S (2010) *Adv Synth Catal* 352:2233

4.4. Capítulo IV

Este terceiro artigo utiliza, novamente, os oito líquidos iônicos sintetizados nesta tese ([bmim][C₁₂SO₄], [bmim][C₁₂ESO₄], ([bmim][C₁₂BSO₃], [bmim][C₁₂SAR], [TBA][C₁₂SO₄], [TBA][C₁₂ESO₄], ([TBA][C₁₂BSO₃] e [TBA][C₁₂SAR]) como catalisadores na síntese do carbonato de estireno (SC), carbonato de glicidil isopropil éter (GC) e carbonato de epiclorigrina (EC). Foi realizado um estudo de termodinâmica para determinar as melhores condições reacionais para cada um dos produtos, além de um estudo teórico que definiu a nucleofilicidade de cada ânion testados a fim de corroborar na discussão dos resultados de catálise.

Este artigo intitulado *“Chemical fixation of CO₂: The influence of linear amphiphilic anions on surface active ionic liquids (SAILs) as catalysts for synthesis of cyclic carbonates under solvent-free conditions”*, foi submetido em revista internacional especializada na área.

1 **Chemical fixation of CO₂: The influence of linear amphiphilic anions**
2 **on surface active ionic liquids (SAILs) as catalysts for synthesis of**
3 **cyclic carbonates under solvent-free conditions**

4
5 Michele O. Vieira¹; Wesley F. Monteiro¹; Bruna S. Neto²; Vitaly V. Chaban³; Rosane
6 Ligabue^{1,4}; Sandra Einloft^{1,2*}

7
8 ¹Post-Graduation Program in Materials Engineering and Technology, Pontifical Catholic
9 University of Rio Grande do Sul - PUCRS, Brazil

10 ²School of Technology, Pontifical Catholic University of Rio Grande do Sul - PUCRS, Brazil

11 ³P.E.S., Vasilievsky Island, Saint Petersburg, Leningrad Oblast, Russian Federation

12 ⁴School of Sciences, Pontifical Catholic University of Rio Grande do Sul - PUCRS, Brazil

13 *Corresponding author. Tel.: +55 51 33203558. E-mail addresses: einloft@pucls.br

14

15 **Abstract.** Carbon dioxide (CO₂) conversion is an efficient option to mitigate
16 environmental impacts caused by CO₂ high concentration in the atmosphere. In this
17 work are described catalytic activities of surface active ionic liquids (SAILs) composed
18 of well-known cations 1-butyl-3-methylimidazolium ([bmim⁺]) and tetra-n-
19 butylammonium ([TBA⁺]) and long alkyl chain anions: lauryl sulfate ([C₁₂SO₄⁻]), lauryl
20 ether sulfate ([C₁₂ESO₄⁻]), lauryl benzene sulfonate ([C₁₂BSO₃⁻]) and lauroyl sarcosinate
21 ([C₁₂SAR⁻]) for cyclic carbonate synthesis. Results evidenced that [TBA⁺] is more
22 active as catalyst due to its higher molecular volume resulting in a more nucleophilic
23 anion. The [TBA][C₁₂BSO₃] SAIL presented better catalytic activity for styrene
24 carbonate (SC) synthesis, reaching 81.4% of conversion and 87.0% of selectivity,
25 besides the high recycle capacity and possible application as catalyst for the syntheses
26 of different cyclic carbonates: glycidyl isopropyl ether carbonate (GC) and
27 epichlorohydrin carbonate (EC).

28

29 **Keywords:** carbon dioxide; catalysis; cycloaddition; ionic liquid; cyclic carbonate.

30

31 **1. Introduction**

32

33 Greenhouse gas (GHG) concentration in the atmosphere is increasing due to
34 anthropogenic sources emissions. CO₂ is a greenhouse gas with important

35 environmental impact [1]. Approximately 116 million tons of CO₂ are used annually for
36 value-added products production, 94% of which are used only for urea production [2].
37 However, this CO₂ use is still insignificant (~0.1%) [3]. In this way, research
38 development involving CO₂ conversion is a current issue and of paramount importance
39 for climate change mitigation [4,5].

40 Cyclic carbonates are used in numerous industrial sectors such as aprotic polar
41 solvents, monomers for polycarbonate synthesis and electrolytes for batteries [6,7,8].
42 CO₂ reaction with epoxide forming cyclic carbonates has been extensively studied using
43 different catalysts [9,10,11,12,13,14].

44 Surface active ionic liquids (SAILs) contain significantly long hydrophobic chains in
45 the cation (C₆ to C₁₆), in the anion (up to C₂₀) or both [15,16]. The most reported cations
46 to form SAILs are imidazolium, pyridinium and quaternary ammonium. Anions are
47 usually derived from anionic surfactants and SAILs performance depends both on the
48 cation and the anion [17,18,19]. Although several studies have been performed with
49 SAILs in several scientific segments (micelle formation, facilitating microemulsions
50 and liquid crystals preparation) [20,21,22], these are poorly investigated in catalysis
51 context [23,24].

52 In a previous work, we described SAILs use for cycloaddition of CO₂ in propylene
53 epoxide (PC) [24]. Literature describes the use of solvent in SC synthesis [25]. Unlike,
54 additional solvent in SC synthesis is not required when SAILs are used as catalysts. In
55 addition, SAILs are derived from surfactants, low cost and abundant materials. SAILs
56 utilization as catalysts is still little explored. For this reason, a more detailed study of
57 cycloaddition is proposed.

58 In this work we describe the use of imidazolium ([bmim⁺]) and tetrabutylammonium
59 ([TBA⁺]) cations based SAILs combined with different anions derived from the
60 surfactants: sodium lauryl sulfate ([C₁₂SO₄⁻]), sodium lauryl ether sulfate ([C₁₂ESO₄⁻]),
61 sodium lauryl benzene sulfonate ([C₁₂BSO₃⁻]) and sodium lauroyl sarcosinate
62 ([C₁₂SAR⁻]) as catalysts for CO₂ cycloaddition to styrene oxide (SO) in order to produce
63 styrene carbonate (SC). We also tested recycle capacity and the possibility of using
64 these SAILs in other cyclic carbonates production: glycidyl isopropyl ether carbonate
65 (GC) and epichlorohydrin carbonate (EC).

66

67 **2. Methodology**

68

69 Synthesis of 1-butyl-3-methylimidazolium lauryl sulfate ([bmim][C₁₂SO₄]; yield =
70 47%), 1-butyl-3-methylimidazolium lauryl ether sulfate ([bmim][C₁₂ESO₄]; yield =
71 76%), 1-butyl-3-methylimidazolium lauryl benzene sulfonate ([bmim][C₁₂BSO₃]; yield =
72 81%), 1-butyl-3-methylimidazolium lauroyl sarcosinate ([bmim][C₁₂SAR]; yield = 63%),
73 tetra-n-butylammonium lauryl sulfate ([TBA][C₁₂SO₄]; yield = 87%), tetra-n-
74 butylammonium lauryl ether sulfate ([TBA][C₁₂ESO₄]; yield = 90%), tetra-n-
75 butylammonium lauryl benzene sulfonate ([TBA][C₁₂BSO₃]; yield = 92%) and tetra-n-
76 butylammonium lauroyl sarcosinate ([TBA][C₁₂SAR]; yield = 79%) was performed with
77 an equimolar mixture of [bmim][Cl] or [TBA][Br] and the sodium salt of anion of
78 interesting was dissolved in sufficient water and kept at 333.15 K for 18 h. Water was
79 removed from the reaction mixture after completion of reaction in vacuum in the same
80 temperature. The product was dissolved with dichloromethane and was washed with
81 water several times. The dichloromethane was removed with vacuum at room
82 temperature and the remaining product is the pure ionic liquid which is stored under
83 inert atmosphere.

84 Characterization of synthesized SAILs are presented in supplementary material.

85

86 2.1. Cycloaddition reaction

87 Styrene carbonate (SC) syntheses from CO₂ and styrene oxide (SO) were carried
88 out in presence of surface active ionic liquids (SAILs) used as catalyst. These
89 compounds were tested in presence of metallic halide (ZnBr₂) as a cocatalyst. All
90 cycloaddition reactions were performed in a stainless steel autoclave of 120 cm³
91 equipped with magnetic stirring. For a typical reaction, 50 mmol of styrene oxide, 0.5
92 mmol of SAIL and 0.125 mmol of cocatalyst (ZnBr₂) were used. All reactions were
93 performed using catalyst content of 1 mol% relative to epoxide.

94 Syntheses were performed without any additional solvent. Autoclave was
95 pressurized with CO₂ and heated to the desired working temperature. After the reaction
96 completion, the reactor was cooled to room temperature and slowly depressurized.

97 Catalyst separation from SC was performed by a simple distillation under inert
98 atmosphere (N₂). To determine the conversion and selectivity of CO₂ cycloaddition
99 reaction, the resulting liquid mixtures were analyzed using a gas chromatograph
100 Shimadzu CG-2014 equipped with a flame ionization detector (FID) and a 100%
101 dimethyl polysiloxane column (30 m x 0.53 mm ID) using acetophenone as internal
102 standard and diethyl ether as solvent.

103 The [TBA][C₁₂SO₄] was chosen for reaction parameters (temperature, time and
104 pressure) determination because it showed better catalytic results in the propylene
105 carbonate (PC) synthesis as previously reported [24].

106 The best catalyst was reused for 5 times without any catalyst or cocatalyst addition.
107 The procedure used to separate the catalytic system [SAIL + ZnBr₂] from SC was the
108 same used in all syntheses, a simple distillation in inert atmosphere.

109 For the other cycloaddition reactions (GC and EC), the assays were performed in the
110 same way, also using the [TBA][C₁₂SO₄] to determine the optimum reaction
111 parameters.

112

113 2.2. Determination of nucleophilicities

114 The geometries of ions were optimized using the steepest descent algorithm with
115 an energy threshold of 10⁻⁴ Hartree. The hybrid density functional Becke-3-Lee-Yang-
116 Parr (B3LYP) was employed [26,27]. The wave functions of the simulated ions were
117 constructed from the atom-centered split-valence triple-zeta polarized basis set 6-
118 311+G*. Diffuse functions were deliberately supplemented to allow for high-quality
119 reproduction of the electron density on organic anions. All electrons of the simulated
120 ions were treated explicitly. The wave function convergence criterion was set to 10⁻⁷
121 Hartree. Hirshfeld charges localized on the oxygen atoms of the head groups were used
122 as a measure of respective nucleophilicities [28]. The reported quantum mechanical
123 calculations were conducted in US GAMESS 2014 [29].

124

125 3. Results and Discussion

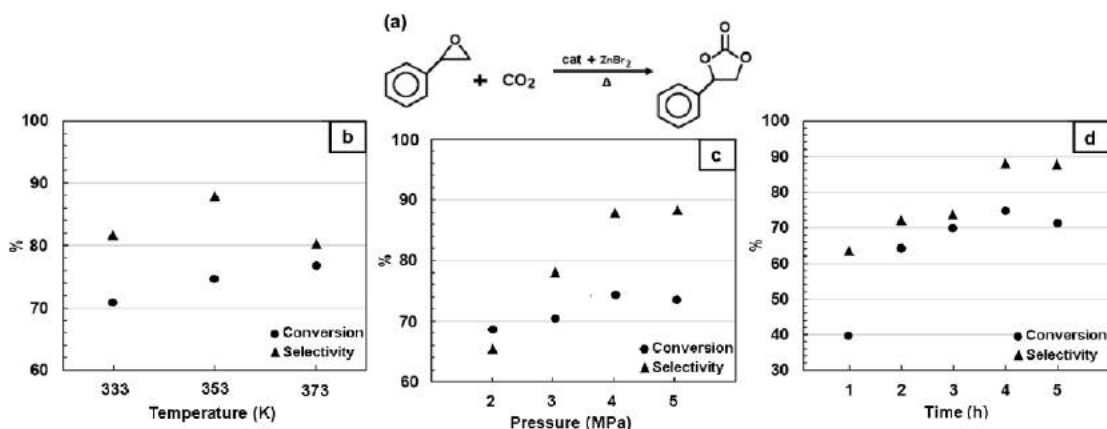
126

127 3.1. Influence of reaction parameters

128 We first performed reaction parameters (temperature, pressure and time)
129 optimization for SC formation reaction from styrene oxide and CO₂ (Figure 1). The
130 detailing of these reactions (entries 1-10) are presented in Table 1.

131 Temperature optimization (Fig. 1b) was performed varying temperature from 333
132 to 373 K (4.0 MPa of CO₂ and 4 h). Progressive reaction temperature increase slightly
133 increased styrene oxide conversion with selectivity loss in SC at 373 K. The best results
134 (entry 2: 74.5% of conversion and 87.8% of selectivity) were obtained at 353 K of
135 temperature and are in agreement with literature [30]. It was evidenced that the ideal
136 temperature for the styrene oxide cycloaddition is 353 K using [TBA][C₁₂SO₄] as

137 catalysts [31,32,33]. The selectivity decrease with increasing temperature is related to
 138 products formation derived from styrene carbonate hydrolysis, like diols [34,35].
 139



140

141 **Figure 1.** The reaction scheme (a), the effect of temperature (b), pressure (c) and time
 142 (d) on the SC synthesis using [TBA][C₁₂SO₄] as a catalyst. Reaction conditions: styrene
 143 oxide 50 mmol, catalyst 0.5 mmol, 0.125 mmol of ZnBr₂.

144

145 The CO₂ pressure (Fig. 1c) was varied from 2.0 to 5.0 MPa (353 K and 4 h). The
 146 best result (entry 2: 74.5% conversion and 87.8% selectivity) was obtained at 4.0 MPa
 147 of pressure. Result improvement in relation to selectivity is proportional to pressure
 148 increase (2.0 MPa < 3.0 MPa < 4.0 MPa < 5.0 MPa). In relation to conversion, there is an
 149 ideal pressure around 4.0 MPa. This tendency was already described in SC synthesis
 150 and attributed to epoxide dissolution by CO₂ excess [32].

151

152 **Table 1.** Effect of reaction parameters using [TBA][C₁₂SO₄] as catalyst for the
 153 cycloaddition of CO₂ to form SC*.

Entry	Time (h)	Temperature (K)	Pressure (MPa)	Conversion (%)	Selectivity (%)
1	4	333	4.0	70.6	81.6
2	4	353	4.0	74.5	87.8
3	4	373	4.0	76.7	80.1
4	4	353	2.0	68.7	65.4
5	4	353	3.0	70.4	78.1
6	4	353	5.0	73.3	88.1
7	1	353	4.0	39.4	63.2

8	2	353	4.0	64.2	71.7
9	3	353	4.0	69.8	73.1
10	5	353	4.0	71.5	86.9

154 * Reaction conditions: styrene oxide 50 mmol, catalyst 0.5 mmol and 0.125 mmol of
 155 ZnBr₂.

156

157 Finally, time (Fig. 1d) was varied from 1 to 5 hours (4.0 MPa of CO₂ and 353 K).
 158 Increasing the time from 1 to 4 hours significantly increases conversion and selectivity.
 159 Previous studies demonstrate that styrene oxide conversion increased up to 4 h of
 160 reaction [32]. In agreement with literature when the time was increased to 5 hours a
 161 decrease in conversion and a slight decrease in selectivity were noticed. Results
 162 evidenced that under these conditions 4 hours is the ideal reaction time.

163

164 3.2. Nucleophilicities of the anions

165 Organic anions constituting SAILs get attached to the reactant to saturate one of the
 166 dangling bonds of epoxide's carbon and get liberated from the product to give rise to the
 167 cyclic carbonate moiety (Figure 2). Therefore, nucleophilicity of the anion is its most
 168 important descriptor that determines catalytic activity of the SAIL. In terms of
 169 electronic density, nucleophilicity is numerically equal to electronic charge on the atom
 170 participating in the reaction. More positive charge (electron-poor site) indicates smaller
 171 nucleophilicity, whilst more negative charge (electron-rich site) indicates larger
 172 nucleophilicity. In principle, nucleophilicity depends both on electronic structure of an
 173 ion and on its chemical environment. In the herein reported simulations, we neglected
 174 an effect of the cation, since they act separately. Indeed, the headgroup of the anion is
 175 covalently bound to an emerging carbonate moiety, whereas the cation does not directly
 176 participate at this stage. The obtained nucleophilicities of the anions are quite similar,
 177 nonetheless, modest differences can be observed: [C₁₂SAR⁻] (-0.45) > [C₁₂BSO₃⁻] (-
 178 0.43) > [C₁₂SO₄⁻] (-0.41) = [C₁₂ESO₄⁻] (-0.41). In the sulfur containing anions, an effect
 179 of the groups (hydrocarbon, methoxy, benzyl) in the attached chain is insignificant and
 180 nucleophilicity is primarily determined by the structure of the head group. A somewhat
 181 larger nucleophilicity of the head group of [C₁₂SAR⁻] is in line with chemical
 182 expectations consideration its structure. Although [C₁₂SAR⁻] is the strongest
 183 nucleophile among the probed anions, it is also an attractive target for polar molecules,
 184 such as those of water vapor.

185

186 3.3. The SAIL effect

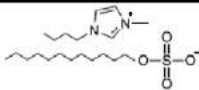
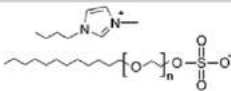
187 Table 2 presents the results of SAILs catalytic performances for cycloaddition of
 188 CO₂ to styrene oxide. In the beginning of the study catalytic performances of two
 189 cations were compared [bmim⁺] (entries 11-14) and [TBA⁺] (entries 4, 15-24). As we
 190 can see the [TBA⁺], for all anions, presented better catalytic activity. The higher
 191 molecular volume of [TBA⁺] increases the cation-anion distance making the
 192 electrostatic interaction weaker, promoting in a more nucleophilic anion [36]. There is
 193 evidence that higher temperatures generate a degradation product of the [TBA⁺], called
 194 trialkylammonium [37], providing basic sites resulting in a more effective catalyst.

195 Analyzing [C₁₂SO₄⁻] anion one observes that [bmim][C₁₂SO₄] (entry 11) presents
 196 the lower catalytic activity. This result is possibly related to the high amount of water
 197 (1.43%) imprisoned in SAIL structure, comparing to other SAILs which present
 198 significantly lower moisture content [24]. Water can deactivate the catalyst decreasing
 199 conversion [35]. Yet, water can compete with CO₂ in SO interaction or even
 200 hydrolyzing the SC forming undesirable by-products, usually diols [34]. This water
 201 interference is no longer perceived in the single hydrophobic SAIL [18,24]
 202 ([TBA][C₁₂SO₄], entry 2) presenting 74.5% of conversion and 87.8% of selectivity,
 203 quite satisfactory results.

204 In a previous study [TBA][C₁₂SO₄] was described as the best catalytic system for
 205 propylene carbonate (PC) synthesis compared to other SAILs [24]. Even if the reaction
 206 mechanism for PC synthesis is close to that of SC synthesis, a different behavior was
 207 observed concerning the catalyst activity. Styrene oxide is a far bulkier molecule than
 208 propylene oxide, so a stereo impediment was already expected. Despite the similar
 209 mechanism, a catalyst to promote the geometric fit is needed.

210

211 **Table 2.** Catalytic performances of SAILs for the cycloaddition of CO₂ to form SC *.

Entry	SAIL	Structure SAIL	Conversion (%)	Selectivity (%)
11	[bmim][C ₁₂ SO ₄]		25.4	77.4
12	[bmim][C ₁₂ ESO ₄]		73.6	80.5

13	[bmim][C ₁₂ BSO ₃]		79.2	81.3
14	[bmim][C ₁₂ SAR]		83.4	46.9
2	[TBA][C ₁₂ SO ₄]		74.5	87.8
15	[TBA][C ₁₂ SO ₄]**		Trace	-
16	***	-	-	-
17	[TBA][C ₁₂ ESO ₄]		76.3	85.6
18	[TBA][C ₁₂ BSO ₃]		81.4	87.0
19	[TBA][C ₁₂ BSO ₃]1x		85.3	87.9
20	[TBA][C ₁₂ BSO ₃]2x		82.1	83.5
21	[TBA][C ₁₂ BSO ₃]3x		81.4	81.1
22	[TBA][C ₁₂ BSO ₃]4x		78.3	80.9
23	[TBA][C ₁₂ BSO ₃]5x		74.1	80.1
24	[TBA][C ₁₂ SAR]		87.9	44.1

212 * Reaction conditions: SO 50 mmol, catalyst 0.5 mmol, 0.125 mmol of ZnBr₂, T = 353

213 K, initial CO₂ pressure 4.0 MPa and t = 4 h.

214 ** Reaction without cocatalyst ZnBr₂.

215 *** Reaction only ZnBr₂.

216

217 Addition of an ether functional group to the anion, [bmim][C₁₂ESO₄] (entry 12)
 218 and [TBA][C₁₂ESO₄] (entry 17), in both cations improved the conversion when
 219 compared to the anion without this group ([C₁₂SO₄⁻]). This result is very pronounced in
 220 the cation [bmim⁺]. The organic functional group "ether" is a group with polar affinities;
 221 it may be that any moisture contained in the medium is interacting with this group,
 222 avoiding the interaction with catalyst active sites. The [TBA][C₁₂SO₄] (entry 2) and
 223 [TBA][C₁₂ESO₄] (entry 17) evidenced the similar catalytic activity. We see that, from
 224 the theoretical computational study, taking into account only the anion, the
 225 nucleophilicities values of the [C₁₂SO₄⁻] and [C₁₂ESO₄⁻] are practically the same (-0.41),
 226 corroborating with the activity presented in the catalytic tests.

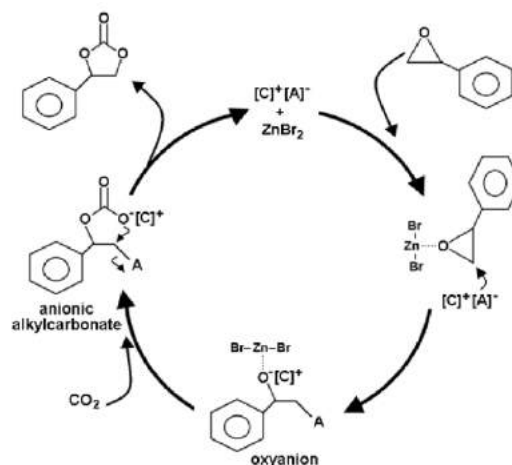
227 The anion $[\text{C}_{12}\text{BSO}_3^-]$ presented the best results when combined with both
228 cations $[\text{bmim}^+]$ and $[\text{TBA}^+]$. SAIL $[\text{TBA}][\text{C}_{12}\text{BSO}_3]$ (entries 18-23) was the one with
229 the best catalytic activity. This behavior is related to the anion containing an aromatic
230 ring. The substrate being a styrene oxide, producing styrene carbonate (both containing
231 aromatic ring in the structure), and the anion of the catalyst in question being aromatic
232 ($[\text{C}_{12}\text{BSO}_3^-]$) an interaction between these aromatic rings may be occurring during the
233 catalytic cycle. Aromatic rings π - π stacking increase the formed oxyanion stabilization
234 (see Fig. 2) not displacing electronic charge contained in the structure, facilitating
235 interaction with CO_2 . This anion has higher nucleophilicity (-0.43) as compared to
236 $[\text{C}_{12}\text{SO}_4^-]$ and $[\text{C}_{12}\text{ESO}_4^-]$, also justifying better catalytic activity.

237 The anion $[\text{C}_{12}\text{SAR}^-]$ presents some peculiarities justifying its behavior of high
238 conversion and low selectivity (entries 14 and 24). Among all tested SAILs containing
239 $[\text{bmim}^+]$ as cation, the $[\text{bmim}][\text{C}_{12}\text{SAR}]$ was the catalyst that presented the highest
240 conversion (83.4%) and lower selectivity (46.9%), the same was observed with $[\text{TBA}^+]$
241 cation, where $[\text{TBA}][\text{C}_{12}\text{SAR}]$ presented the highest conversion result (87.9%) and
242 lower selectivity (44.1%). The higher conversion results when compared to others tested
243 anions are justified by the higher nucleophilicity of this anion (-0.45). Another fact that
244 deserves attention, justifying the low selectivity, is the presence of resonance in the
245 anion amide group. This displacement of electrons between oxygen and nitrogen (amide
246 group) can cause an early anion release in the anionic alkylcarbonate step (see Fig. 2).
247 Yet, a bonding of this anion in the epoxide to a place other than the carboxylate can
248 occur favoring other species formation in addition to styrene carbonate.

249 That reaction (CO_2 cycloaddition to SO to produce SC) is not spontaneous,
250 therefore no product was detected when the reaction was performed without a catalytic
251 system (catalyst/cocatalyst). When only the SAIL was used (entry 15) or only the
252 cocatalyst was used (entry 16), there is no significant conversion to SC [9,24].

253 The presence of a Lewis acid as a cocatalyst (ZnBr_2) is essential for SAILs
254 activity [38,39]. The ZnBr_2 interact with the oxygen atom of the epoxide, so that the
255 basic anion of SAIL carries out the attack on the least impeded carbon atom of the
256 epoxy ring. Figure 2 presents a possible mechanism for the cyclic carbonate synthesis.
257 The CO_2 carbon atom interacts with the anionic species producing an anionic
258 alkylcarbonate. The latter is converted into the cyclic carbonate by intermolecular cyclic
259 elimination and finally the SAIL is regenerated.

260



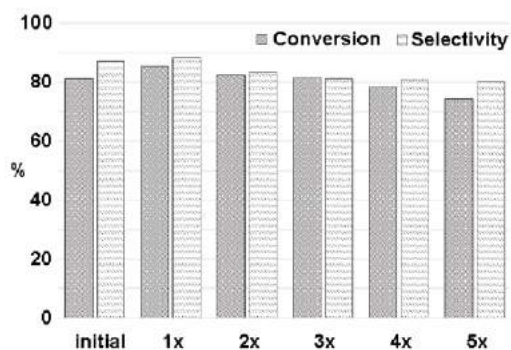
261

262 **Figure 2.** Proposed mechanism for the synthesis of styrene carbonate from styrene
263 oxide and CO_2 .

264

265 For industrial application, it is desired that catalyst stay active for several cycles
266 of use. To evaluate the SAILs stability we performed several catalytic cycles using the
267 system with highest catalytic activity ($[TBA][C_{12}BSO_3]$) (Table 2, entries 19-23).
268 Figure 3 presents the behavior of SAIL during recycle tests. In the first recycle (entry
269 19) one observed an increase in conversion (from 81.4% to 85.3%) and selectivity (from
270 87.0% to 87.9%). This catalytic activity increase in the first recycle is not rare, since
271 after the first reaction any possible impurity have been washed away from the catalytic
272 system [12,33]. Residual moisture removal of the catalyst is also possible. Therefore,
273 the $[TBA][C_{12}BSO_3]$ maintains significant activity after 3 replicates with good
274 reproducibility. From recycle 4, there is little gradual activity loss.

275



276

277 **Figure 3.** SC recycling experiments of $[TBA][C_{12}BSO_3]$.

278

279 3.4. Application to other cyclic carbonates

280 It is very usual in most current publications, the use of the best catalytic system for
 281 propylene oxide and styrene oxide cycloaddition to obtain other cyclic carbonates
 282 [40,41,42,43,44]. A few works further study the formation reaction of glycidyl
 283 isopropyl ether carbonate (GC) and epichlorohydrin carbonate (EC) [45,46], being,
 284 often, optimization study of reactional parameters not described. Here we performed the
 285 study of the better reaction conditions for glycidyl isopropyl ether carbonate (GC)
 286 (Table 3, entries 25-32) and epichlorohydrin carbonate (EC) (Table 4, entries 34-41).
 287 The [TBA][C₁₂SO₄] was elected as catalyst. Figure 4 shows the results of Table 3 and 4.
 288

289 **Table 3.** Effect of the reaction parameters using [TBA][C₁₂SO₄] as catalyst and
 290 performances of the best SAILs ([TBA][C₁₂BSO₃]) for the cycloaddition of CO₂ to
 291 form GC*.

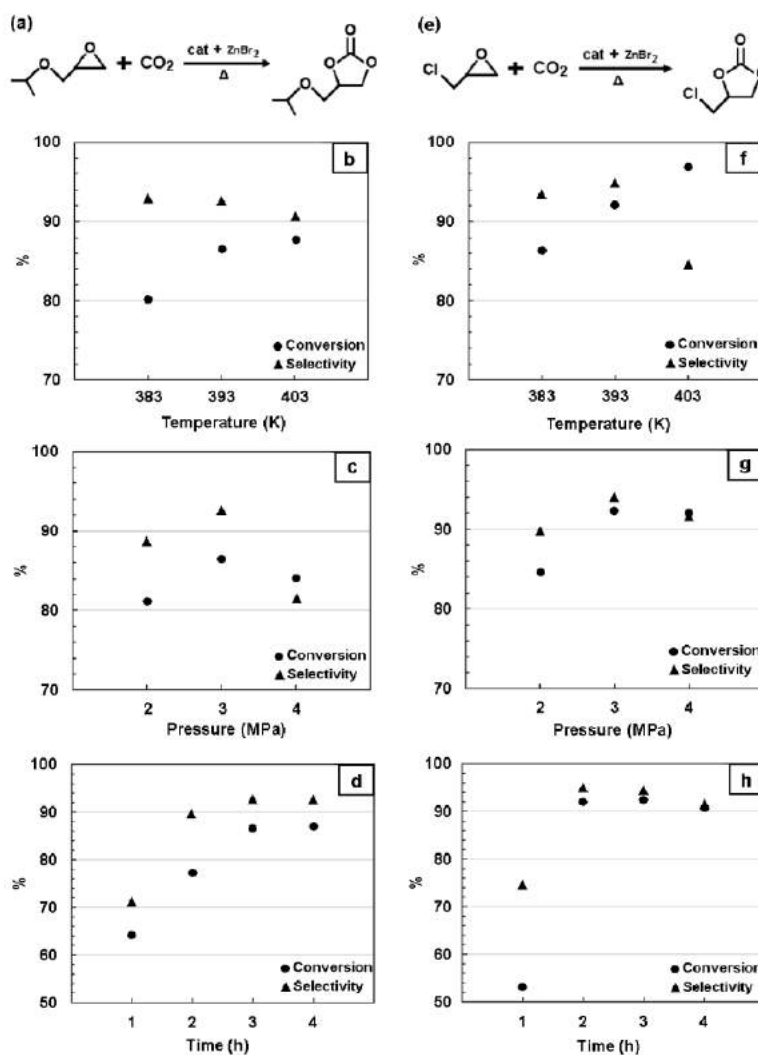
Entry	SAIL	Time (h)	Temperature (K)	Pressure (MPa)	Conversion (%)	Selectivity (%)
25	[TBA][C ₁₂ SO ₄]	3	383	3.0	80.1	92.9
26	[TBA][C ₁₂ SO ₄]	3	393	3.0	86.5	92.6
27	[TBA][C ₁₂ SO ₄]	3	403	3.0	87.7	90.4
28	[TBA][C ₁₂ SO ₄]	3	393	2.0	81.2	88.6
29	[TBA][C ₁₂ SO ₄]	3	393	4.0	84.0	81.5
30	[TBA][C ₁₂ SO ₄]	1	393	3.0	64.2	71.0
31	[TBA][C ₁₂ SO ₄]	2	393	3.0	77.3	89.4
32	[TBA][C ₁₂ SO ₄]	4	393	3.0	87.1	92.4
33	[TBA][C ₁₂ BSO ₃]	3	393	3.0	87.2	84.6

292 * Reaction conditions: glycidyl isopropyl ether 50 mmol, catalyst 0.5 mmol and 0.125
 293 mmol of ZnBr₂.

294

295 It is important to mention that without ZnBr₂ as cocatalyst there is no significant
 296 conversion of GC and EC. Temperature optimization (entries 25-27 for GC – Fig. 4b)
 297 (entries 24-36 for EC – Fig. 4f) was performed varying temperature from 383 K to 403
 298 K. The progressive increase of the reaction temperature significantly increased the
 299 conversion of GC and EC. In addition, a loss of selectivity at 403 K for GC and a
 300 marked loss of selectivity for the EC were observed. Selectivity loss for EC with
 301 increasing temperature is probably due to decomposition of the product into 1-
 302 chloroethane-1,2-diol [35,47].

303



304

305 **Figure 4.** The reaction scheme on the GC synthesis (a): the effect of temperature (b),
 306 pressure (c) time (d); and the reaction scheme on the EC synthesis (e): the effect of
 307 temperature (f), pressure (g), time (h) both using [TBA][C₁₂SO₄] as catalyst and ZnBr₂
 308 as cocatalyst.

309

310 The influence of pressure in selectivity and conversion (entries 26, 28-29 for GC
 311 – Fig. 4c) (entries 35, 37-38 for EC – Fig. 4g) was evaluated from 2.0 MPa to 4.0 MPa.
 312 An increase in conversion and selectivity up to 3.0 MPa was observed for both
 313 carbonates. For pressure values superior to 3.0 MPa a decrease in both conversion and
 314 selectivity was observed, being more pronounced in GC. This behavior is due to an
 315 ideal stoichiometric rate of epoxide/CO₂, so that one does not inhibit the role of the
 316 other and/or the CO₂ acts as epoxide diluent [47].

317 Finally, time influence in selectivity and conversion (entries 35, 39-41 for GC –
 318 Fig. 4d) (entries 35, 39-41 for EC – Fig. 4h) was performed varying from 1 to 4 hours of
 319 reaction time. Increasing the time up to 3 hours significantly increases the conversion
 320 and selectivity to GC. For EC the increases in conversion and selectivity was observed
 321 up to 2 hours. Increasing reaction time do not improve selectivity and conversion since
 322 the reaction was already at equilibrium and product decomposition could occur in
 323 longer times (entry 41) [36,46,47].

324

325 **Table 4.** Effect of the reaction parameters using [TBA][C₁₂SO₄] as catalyst and
 326 performances of the best SAILs ([TBA][C₁₂BSO₃]) for the cycloaddition of CO₂ to
 327 form EC*.

Entry	SAIL	Time (h)	Temperature (K)	Pressure (MPa)	Conversion (%)	Selectivity (%)
34	[TBA][C ₁₂ SO ₄]	2	383	3.0	86.3	93.4
35	[TBA][C ₁₂ SO ₄]	2	393	3.0	92.1	94.7
36	[TBA][C ₁₂ SO ₄]	2	403	3.0	96.8	84.3
37	[TBA][C ₁₂ SO ₄]	2	393	2.0	84.6	89.8
38	[TBA][C ₁₂ SO ₄]	2	393	4.0	92.0	91.7
39	[TBA][C ₁₂ SO ₄]	1	393	3.0	53.3	74.2
40	[TBA][C ₁₂ SO ₄]	3	393	3.0	92.4	93.9
41	[TBA][C ₁₂ SO ₄]	4	393	3.0	90.7	91.1
42	[TBA][C ₁₂ BSO ₃]	2	393	3.0	81.5	93.5

328 * Reaction conditions: epichlorohydrin 50 mmol, catalyst 0.5 mmol and 0.125 mmol of
 329 ZnBr₂.

330

331 The presence of functional groups in the starting epoxide, such as ether in
 332 glycidyl isopropyl ether (entries 26 and 33) and chlorine in epichlorohydrin (entries 35
 333 and 42) resulted in higher conversions and selectivities when compared to SC, both for
 334 [TBA][C₁₂SO₄] (entry 2) and [TBA][C₁₂BSO₃] (entry 18) because of the less significant
 335 steric hindrance.

336 After these studies, an ideal condition was determined for glycidyl isopropyl
 337 ether carbonate (GC) synthesis, being: 393 K of temperature, 3 hours and 3.0 MPa of
 338 initial pressure of CO₂. For the epichlorohydrin carbonate (EC) it was: 393 K of
 339 temperature, 2 hours and 3.0 MPa of initial pressure of CO₂. The use of the best

340 catalytic system elected previously, [TBA][C₁₂BSO₃] was evaluated obtaining
341 interesting results for GC (Table 3, entry 33; selectivity 84.6% and conversion 87.2%)
342 and EC (Table 4, entry 42; selectivity 93.5% and conversion 81.5%) syntheses.

343

344 **4. Conclusion**

345

346 Several SAILs were used as catalysts in the CO₂ cycloaddition to styrene oxide
347 and showed catalytic efficiency. The best reaction condition for the synthesis of styrene
348 carbonate (SC) was 353 K of temperature, 4 h of time at 4.0 MPa of pressure. The
349 [TBA][C₁₂BSO₃] was the SAIL that presented better catalytic activity, reaching 81.4%
350 of conversion and 87.0% of selectivity and these results increasing after the first
351 recycle. The best reaction condition for glycidyl isopropyl ether carbonate (GC)
352 synthesis was 393 K of temperature, 3 h of time at 3.0 MPa of pressure and finally, the
353 best reaction condition for the synthesis of epichlorohydrin carbonate (EC) was 393 K
354 of temperature, 2 h of time at 3.0 MPa of pressure.

355

356 **Acknowledgments**

357

358 This study was financed in part by the Coordenação de Aperfeiçoamento de Pessoal de
359 Nível Superior – Brasil (CAPES) – Finance Code 001. SE thanks CNPq for research
360 scholarship.

361

362 **References**

-
1. Zoundi Z (2017) CO₂ emissions, renewable energy and the Environmental Kuznets Curve, a panel cointegration approach. *Renew Sust Energ Rev* 72:1067-1075.
 2. Otto A, Grube T, Schiebahn S, Stolten D (2015) Closing the loop: captured CO₂ as a feedstock in the chemical industry. *Energy Environ Sci* 8:3283-3297.
 3. Rafiee A, Khalilpour RK, Milani D, Panahi M (2018) Trends in CO₂ conversion and utilization: A review from process systems perspective. *J Environ Chem Eng* 6:5771–5794.
 4. Song QW, Zhou ZH, He LN (2017) Efficient, selective and sustainable catalysis of carbon dioxide. *Green Chem* 19:3707-3728.

-
5. Vieira MO, Aquino AS, Schütz MK, Vecchia FD, Ligabue R, Seferin M, Einloft S (2017) Chemical Conversion of CO₂: Evaluation of Different Ionic Liquids as Catalysts in Dimethyl Carbonate Synthesis. *Energy Procedia* 114:7141-7149.
 6. Bobbink FD, Dyson PJ (2016) Synthesis of carbonates and related compounds incorporating CO₂ using ionic liquid-type catalysts: State-of-the-art and beyond. *J Catal* 343:52-61.
 7. Zhang X, Geng W, Yue C, Wu W, Xiao L (2016) Multilayered supported ionic liquids bearing a carboxyl group: Highly efficient catalysts for chemical fixation of carbon dioxide. *J Environ Chem Eng* 4(2):2565-2572.
 8. Ji L, Luo Z, Zhang Y, Wang R, Ji Y, Xia F, Gao G (2018) Imidazolium ionic liquids/organic bases: Efficient intermolecular synergistic catalysts for the cycloaddition of CO₂ and epoxides under atmospheric pressure. *Mol Catal* 446:124–130.
 9. Aquino AS, Bernard FL, Vieira MO, Borges JV, Rojas MF, Vecchia FD, Ligabue RA, Seferin M, Menezes S, Einloft S (2014) A New Approach to CO₂ Capture and Conversion Using Imidazolium Based-Ionic Liquids as Sorbent and Catalyst. *J Braz Chem Soc* 25(12):2251-2257.
 10. Zhu Z, Zhang Y, Wang K, Fu X, Chen F, Jing H (2016) Chiral oligomers of spiro-salencobalt(III)X for catalytic asymmetric cycloaddition of epoxides with CO₂. *Catal Commun* 81:50-53.
 11. Feng C, Guo C, Hu D, Guo J, Cao X, Akram N, Wang J (2018) Catalytic performance of Co 1,3,5-benzenetricarboxylate in the conversion of CO₂ to cyclic carbonates. *Reac Kinet Mech Cat* 125(2):633-645.
 12. Monteiro WF, Vieira MO, Aquino AS, Souza MO, Lima J, Einloft S, Ligabue R (2017) CO₂ conversion to propylene carbonate catalyzed by ionic liquid containing organosilane groups supported on titanate nanotubes/nanowires. *Appl Catal A-Gen* 544:46-54.
 13. Nourian M, Zadehahmadi F, Kardanpour R, Tangestaninejad S, Moghadam M, Mirkhani V, Baltork IM, Bahadori M (2017) Chemical fixation of carbon dioxide catalyzed by magnetically recoverable NH₂-MIL-101(Al) as an elegant nanoreactor. *Catal Commun* 94:42-46.
 14. Karamé I, Zaher S, Eid N, Christ L (2018) New zinc/tetradentate N₄ ligand complexes: Efficient catalysts for solvent-free preparation of cyclic carbonates by CO₂/epoxide coupling. *Mol. Catal.* 456:87–95.

-
15. Bharmoria P, Mehta MJ, Pancha I, Kumar A (2014) Structural and Functional Stability of Cellulase in Aqueous-Bi-amphiphilic Ionic Liquid Surfactant Solution. *J Phys Chem B* 118(33):9890-9899.
 16. Vekariya RL, Dhar A, Lunagariya J (2017) Synthesis and characterization of double -SO₃H functionalized Brønsted acidic hydrogensulfate ionic liquid confined with silica through sol-gel method. *Compos Interfaces* 24:801-816.
 17. Vekariya RL, Kumar NS (2017) Micellization behaviour of surface active N-alkyl pyridinium dodecylsulphate task-specific ionic liquids in aqueous solutions. *Colloid Surf A-Physicochem Eng Asp* 529:203-209.
 18. Vieira MO, Monteiro WF, Ligabue R, Seferin M, Chaban VV, Andreeva NA, Nascimento JF, Einloft S (2017) Ionic liquids composed of linear amphiphilic anions: Synthesis, physicochemical characterization, hydrophilicity and interaction with carbon dioxide. *J Mol Liq* 241:64-73.
 19. Müller E, Zahnweh L, Estrine B, Zech O, Allolio C, Heilmann J, Kunz W (2018) Oligoether carboxylate counterions: An innovative way towards surfactant ionic liquids. *J Mol Liq* 251:61-69.
 20. Zhao Y, Chen X, Jing B, Wang X, Ma F (2009) Novel Gel Phase Formed by Mixing a Cationic Surfactive Ionic Liquid C₁₆mimCl and an Anionic Surfactant SDS in Aqueous Solution. *J Phys Chem B* 113(4):983-988.
 21. Selwent A, Luczak J (2016) Micellar aggregation of Triton X-100 surfactant in imidazolium ionic liquids. *J Mol Liq* 221:557-566.
 22. Porada JH, Mansueto M, Laschat S, Stubenrauch C (2017) Microemulsions with hydrophobic ionic liquids: Influence of the structure of the anion. *J Mol Liq* 227:202-209.
 23. Jasiak K, Siewniak A, Kopczynska K, Chrobok A, Baj S (2016) Hydrogensulphate ionic liquids as an efficient catalyst for the synthesis of cyclic carbonates from carbon dioxide and epoxides. *J Chem Technol Biotechnol* 91:2827-2833.
 24. Vieira MO, Monteiro WF, Neto BS, Ligabue R, Chaban VV, Einloft S (2018) Surface Active Ionic Liquids as Catalyst for CO₂ Conversion to Propylene Carbonate. *Catal Lett* 148:108-118.
 25. Jawad A, Rezaei F, Rownaghi AA (2017) Porous polymeric hollow fibers as bifunctional catalysts for CO₂ conversion to cyclic carbonates. *J CO₂ Util* 21:589-596.

-
26. Lee C, Yang W, Parr RG (1988) Development of the Colic-Salvetti correlation-energy formula into a functional of the electron density. *Phys Rev B* 37(2):785-789.
 27. Becke AD (1988) Density-functional exchange-energy approximation with correct asymptotic behavior. *Phys Rev A* 38(6):3098-3100.
 28. Hirshfeld FL (1977) Bonded-atom fragments for describing molecular charge densities. *Theor Chim Acta* 44(2):129-138.
 29. Schmidt MW, Baldridge KK, Boatz JA, Elbert ST, Gordon MS, Jensen JH, Koseki S, Matsunaga N, Nguyen KA, Su S, Windus TL, Dupuis M, Jr JAM (1993) General atomic and molecular electronic structure system. *J Comput Chem* 14(11):1347-1363.
 30. Zhu M, Srinivas D, Bhogeswararao S, Ratnasamy P, Carreon MA (2013) Catalytic activity of ZIF-8 in the synthesis of styrene carbonate from CO₂ and styrene oxide. *Catal Commun* 32:36-40.
 31. Sun J, Fujita S, Bhanage BM, Arai M (2004) One-pot synthesis of styrene carbonate from styrene in tetrabutylammonium bromide. *Catal Today* 93:383-388.
 32. Montoya CA, Paninho AB, Felix PM, Zakrzewska ME, Vital J, Visak VN, Nunes AVM (2015) Styrene carbonate synthesis from CO₂ using tetrabutylammonium bromide as a non-supported heterogeneous catalyst phase. *J Supercrit Fluids* 100:155-159.
 33. Paninho AB, Ventura ALR, Branco LC, Pombeiro AJL, Silva MFCG, Ponte MN, Mahmudov KT, Nunes AVM (2018) CO₂ + ionic liquid biphasic system for reaction/product separation in the synthesis of cyclic carbonates. *J Supercrit Fluids* 132:71-75.
 34. Xiao LF, Yue QF, Xia CG, Xu LW (2008) Supported basic ionic liquid: Highly effective catalyst for the synthesis of 1,2-propylene glycol from hydrolysis of propylene carbonate. *J Mol Catal A-Chem* 279:230-234.
 35. Jin X, Bobba P, Reding N, Song Z, Thapa PS, Prasad G, Subramaniam B, Chaudhari RV (2017) Kinetic modeling of carboxylation of propylene oxide to propylene carbonate using ion-exchange resin catalyst in a semi-batch slurry reactor. *Chem Eng Sci* 168:189-203.
 36. Ju HY, Manju MD, Kim KH, Park SW, Park DW (2008) Catalytic performance of quaternary ammonium salts in the reaction of butyl glycidyl ether and carbon dioxide. *J Ind Eng Chem* 14(2):157-160.
 37. North M, Pasquale R (2009) Mechanism of Cyclic Carbonate Synthesis from Epoxides and CO₂. *Angew Chem* 121:2990-2992.

-
38. Kim HS, Kim JJ, Kim H, Jang HG (2003) Imidazolium zinc tetrahalide-catalyzed coupling reaction of CO₂ and ethylene oxide or propylene oxide. *J Catal* 220(1):44-46.
39. Sun J, Fujita S, Arai M (2005) Development in the green synthesis of cyclic carbonate from carbon dioxide using ionic liquids. *J Organomet Chem* 690(15):3490-3497.
40. Zhang H, Kong X, Cao C, Pang G, Shi Y (2016) An efficient ternary catalyst ZnBr₂/K₂CO₃/[Bmim]Br for chemical fixation of CO₂ into cyclic carbonates at ambient conditions. *J CO₂ Util* 14:76-82.
41. Dai W, Yang W, Zhang Y, Wang D, Luo X, Tu X (2017) Novel isothiuronium ionic liquid as efficient catalysts for the synthesis of cyclic carbonates from CO₂ and epoxides. *J CO₂ Util* 17:256-262.
42. Li B (2018) A novel metal-organic framework as a heterogeneous catalysis for the solvent-free conversion of CO₂ and epoxides into cyclic carbonate. *Inorg Chem Commun* 88:56-59.
43. Wu Y, Song X, Li S, Zhang J, Yang X, Shen P, Gao L, Wei R, Zhang J, Xiao G (2018) 3D-monoclinic M-BTC MOF (M = Mn, Co, Ni) as highly efficient catalysts for chemical fixation of CO₂ into cyclic carbonates. *J Ind Eng Chem* 58:296-303.
44. Zhang X, Chen Z, Yang X, Li M, Chen C, Zhang N (2018) The fixation of carbon dioxide with epoxides catalyzed by cation-exchanged metal-organic framework. *Microporous Mesoporous Mat* 258:55-61.
45. Zhang Y, Tan Z, Liu B, Mao D, Xiong C (2015) Coconut shell activated carbon tethered ionic liquids for continuous cycloaddition of CO₂ to epichlorohydrin in packed bed reactor. *Catal Commun* 68:73-76.
46. Ji L, Luo Z, Zhang Y, Wang R, Ji Y, Xia F, Gao G (2018) Imidazolium ionic liquids/organic bases: Efficient intermolecular synergistic catalysts for the cycloaddition of CO₂ and epoxides under atmospheric pressure. *Mol Catal* 446:124-130.
47. Sogukomerogullari HG, Aytar E, Ulusoy M, Demir S, Dege N, Richeson DS, Sönmez M (2018) Synthesis of complexes Fe, Co and Cu supported by "SNS" pincer ligands and their ability to catalytically form cyclic carbonates. *Inorg Chim Acta* 471:290-296.

Supplementary Material



Click here to access/download
Supplementary Material
Supplementary Material.docx



Supplementary Material

Chemical fixation of CO₂: The influence of linear amphiphilic anions on surface active ionic liquids (SAILs) as catalysts for synthesis of cyclic carbonates under solvent-free conditions

Michele O. Vieira¹; Wesley F. Monteiro¹; Bruna S. Neto²; Vitaly V. Chaban³; Rosane Ligabue^{1,4}; Sandra Einloft^{1,2}

¹Post-Graduation Program in Materials Engineering and Technology, Pontifical Catholic University of Rio Grande do Sul - PUCRS, Brazil

²School of Technology, Pontifical Catholic University of Rio Grande do Sul - PUCRS, Brazil

³P.E.S., Vasilievsky Island, Saint Petersburg, Leningrad Oblast, Russian Federation

⁴School of Sciences, Pontifical Catholic University of Rio Grande do Sul - PUCRS, Brazil

Michele Oliveira Vieira: mov_0702@hotmail.com

Wesley Formentin Monteiro: wesleymonteiro@msn.com

Bruna Silveira Neto: bruna.silveira.006@acad.pucrs.br

Vitaly V. Chaban: vvchaban@gmail.com

Rosane Ligabue: rligabue@pucrs.br

Sandra Einloft: einloft@pucrs.br

Legend of Figures:

Fig. S1. Cations and anions of the synthesized SAILs.

Fig. S2. Characterization of [bmim][C₁₂SO₄].

Fig. S3. Characterization of [bmim][C₁₂ESO₄].

Fig. S4. Characterization of [bmim][C₁₂BSO₃].

Fig. S5. Characterization of [bmim][C₁₂SAR].

Fig. S6. Characterization of [TBA][C₁₂SO₄].

Fig. S7. Characterization of [TBA][C₁₂ESO₄].

Fig. S8. Characterization of [TBA][C₁₂BSO₃].

Fig. S9. Characterization of [TBA][C₁₂SAR].

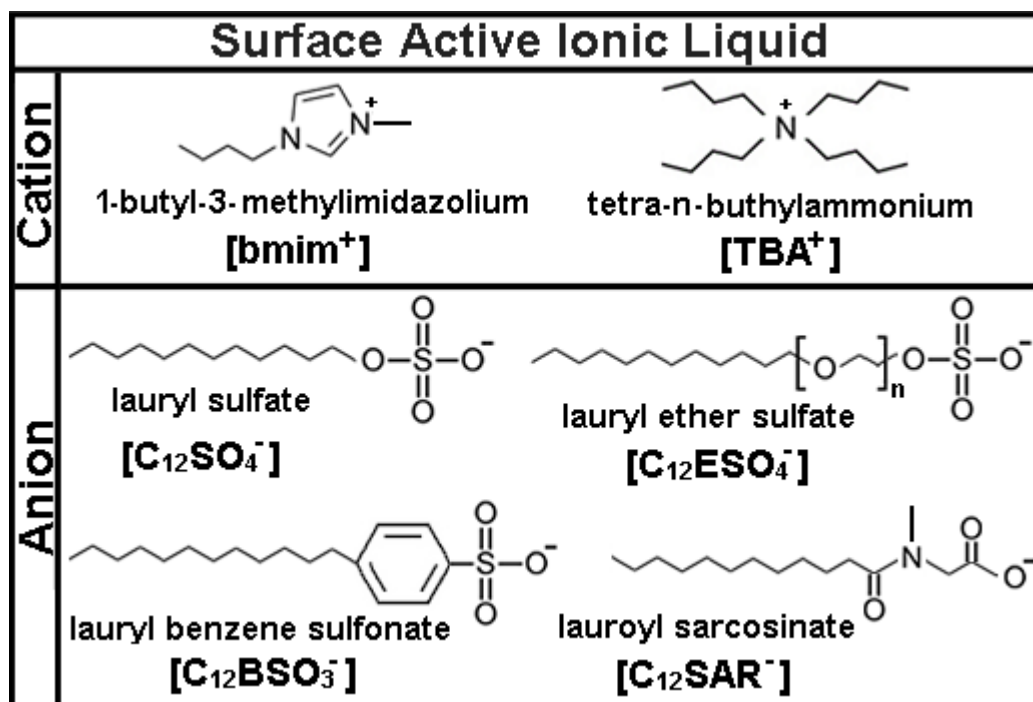


Fig. S1. Cations and anions of the synthesized SAILs.

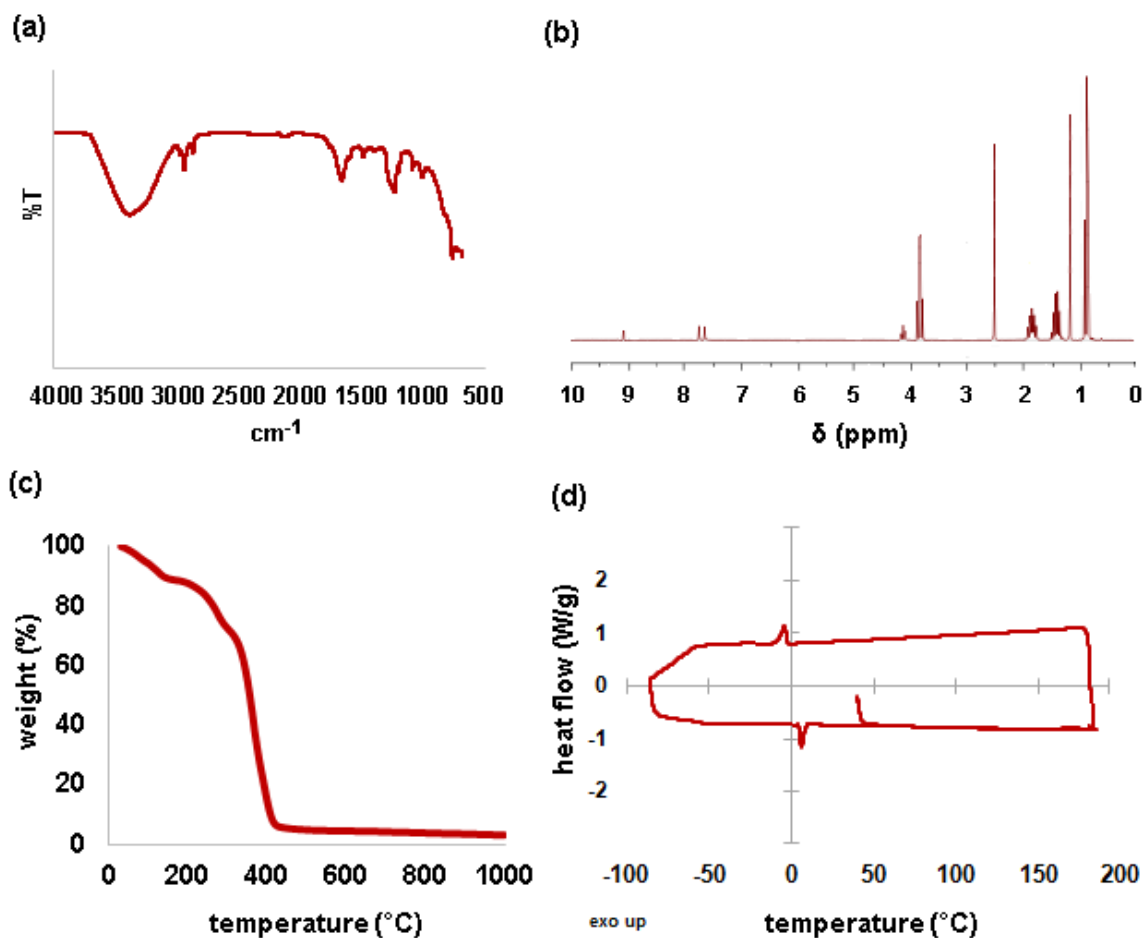


Fig. S2. Characterization of [bmim][C₁₂SO₄]: (a) FTIR, (b) ¹H-NMR; (c) TGA and (d) DSC.

[bmim][C₁₂SO₄] - FTIR ν (cm⁻¹): 3178-3126 (C-H aromatic), 2970 (C-H of CH₂), 2897 (C-H of CH₃), 1628 (C=N aromatic), 1579-1471 (C=C aromatic), 1286 (C-N aromatic), 1172 (C-N alifatic), 1042 (S=O). ¹H-NMR (600 MHz, DMSO-d₆) δ (ppm): 9.10 [s, 1H]; 7.75 [d, 1H]; 7.69-7.67 [d, 1H]; 4.16 [t, 2H, J=6.9 Hz]; 3.85 [s, 3H]; 3.86 [t, 2H, J=6.3 Hz]; 1.82-1.68 [m, 2H, J=14.9; 7.5 Hz]; 1.48 [dt, 2H, J=14.7; 7.3 Hz]; 1.24 [s, 20H]; 0.95-0.81 [m, 6H]. Water miscible, 1.43% moisture content. DSC: 1.8 °C (melting point), -1.7 °C (crystallization), not detected (glass transition). TGA: 101-146 °C (weight loss 10.2%, T_{max} = 120 °C), 182-297 °C (weight loss 17.3%, T_{max} = 273 °C) and 302-435 °C (weight loss 67.8%, T_{max} = 366 °C). Yield = 47%.

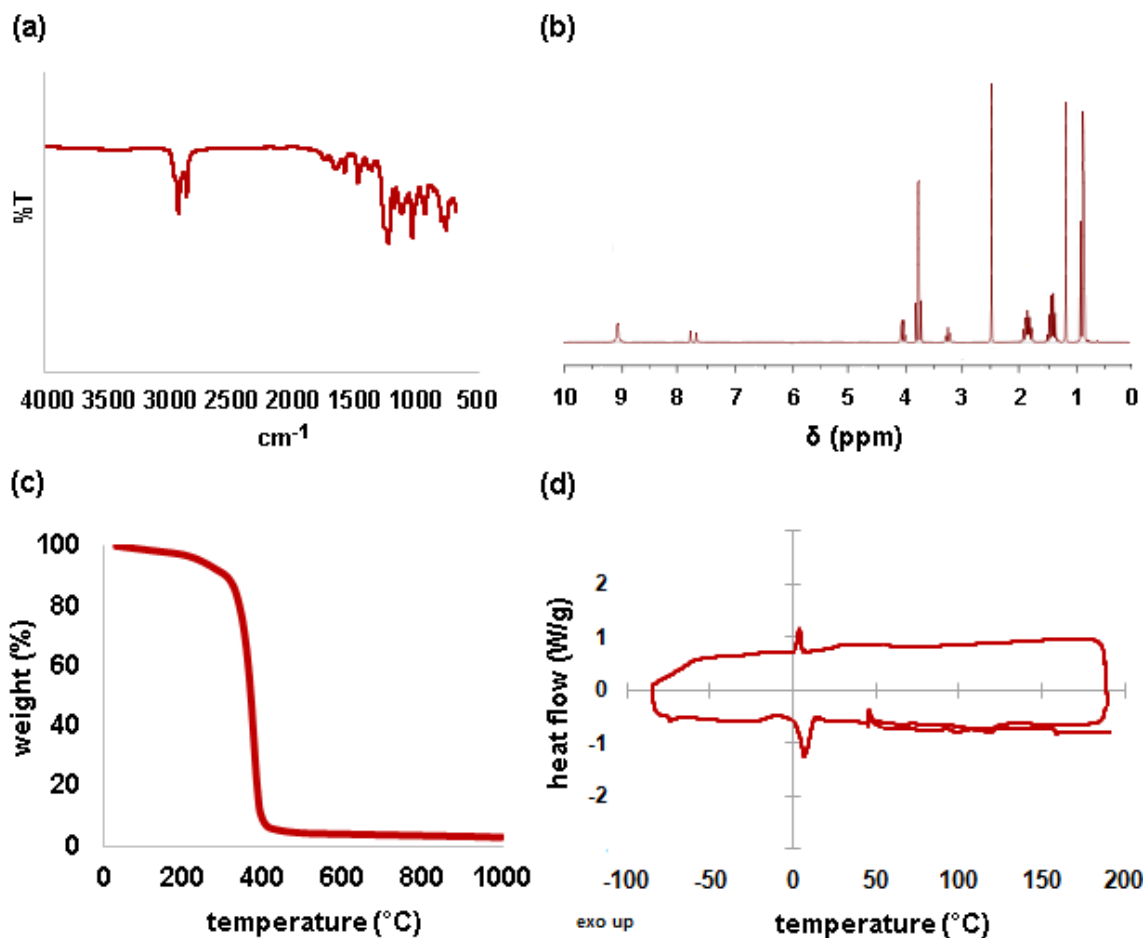


Fig. S3. Characterization of [bmim][C₁₂ESO₄]: (a) FTIR, (b) ¹H-NMR; (c) TGA and (d) DSC.

[bmim][C₁₂ESO₄] - FTIR ν (cm⁻¹): 3158-3120 (C-H aromatic), 2966 (C-H of CH₂), 2882 (C-H of CH₃), 1628 (C=N aromatic), 1568-1459 (C=C aromatic), 1282 (C-N aromatic), 1215 (C-O), 1170 (C-N alifatic), 1019 (S=O). ¹H-NMR (600 MHz, DMSO-d₆) δ (ppm): 9.11 [s, 1H]; 7.77 [d, 1H]; 7.70 [d, 1H]; 4.17 [t, 2H, J=6.8 Hz]; 3.78 [s, 3H]; 3.86 [t, 2H, J=15.7 Hz]; 3.54-3.41 [dt, 4H]; 1.82-1.70 [m, 2H, J=13.4; 7.5 Hz]; 1.47 [dt, 2H, J=12.8; 6.8 Hz]; 1.24 [s, 24H]; 0.93-0.79 [m, 6H]. Water miscible, 0.42% moisture content. DSC: 4.1 °C (melting point), 1.2 °C (crystallization), -70.0 °C (glass transition). TGA: 188-287 °C (weight loss 8.6%, T_{máx} = 267 °C) and 293-435 °C (weight loss 85.3%, T_{máx} = 376 °C). Yield = 76%.

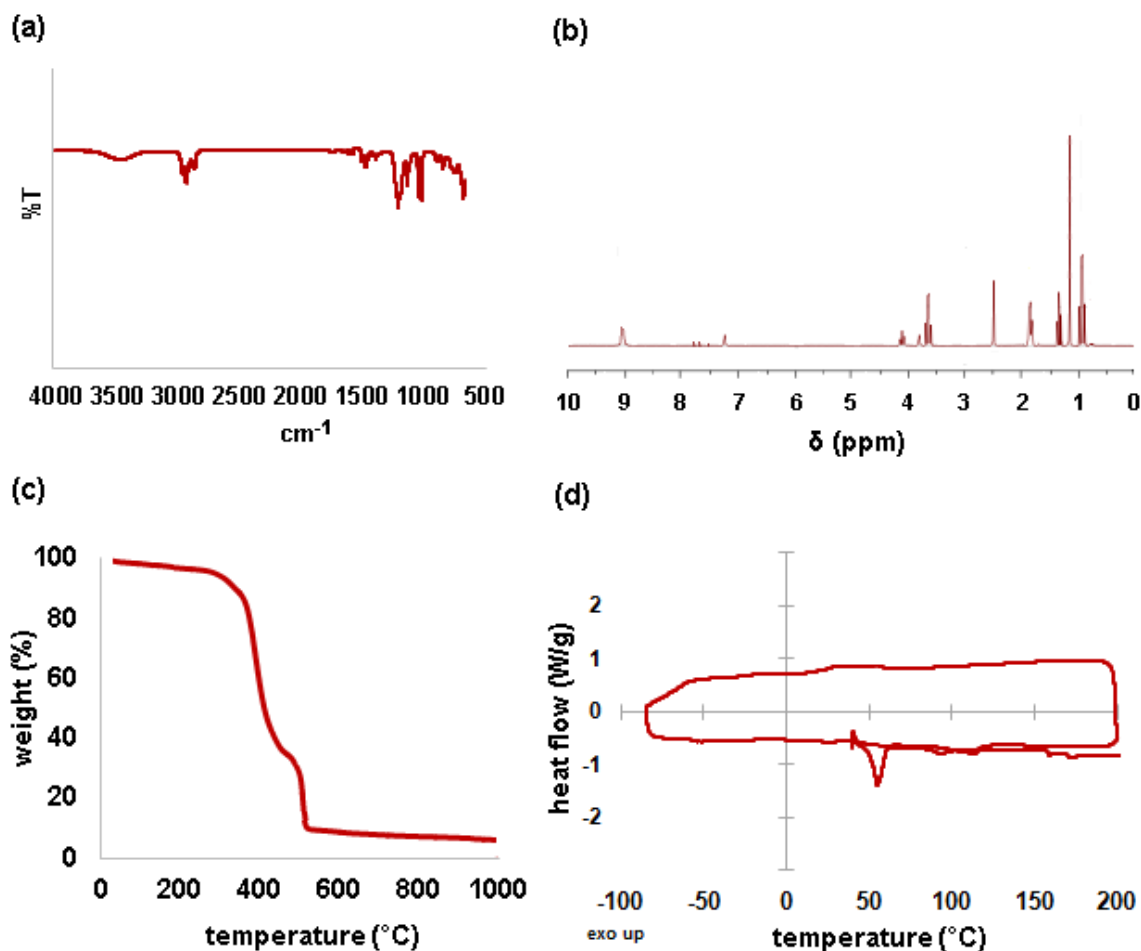


Fig. S4. Characterization of [bmim][C₁₂BSO₃]: (a) FTIR, (b) ¹H-NMR; (c) TGA and (d) DSC.

[bmim][C₁₂BSO₃] - FTIR ν (cm⁻¹): 3163-3120 (C-H aromatic), 2966 (C-H of CH₂), 2872 (C-H of CH₃), 1627 (C=N aromatic), 1602 (C=C aromatic), 1574 (C=C aromatic), 1492 (C=C aromatic), 1466 (C=C aromatic), 1285 (C-N aromatic), 1169 (C-N alifatic), 1221 (C-O), 1019 (S=O), 830 (aromatic ring). ¹H-NMR (600 MHz, DMSO-d₆) δ (ppm): 9.15 [s, 1H]; 7.78 [d, 1H, J=1.7 Hz]; 7.71 [d, 1H, J=1.7 Hz]; 7.59-7.48 [m, 2H]; 7.48-7.05 [m, 2H]; 4.16 [t, 2H, J=7.2 Hz]; 3.85 [s, 3H]; 3.64 [t, 2H, J=6.0 Hz]; 2.2 [t, 2H]; 1.82-1.71 [m, 2H, J=14.9; 7.6 Hz]; 1.35 [dt, 2H, J=14.8; 7.5 Hz]; 1.32-1.21 [m, 18H]; 0.97 [t, 3H, J=7.6 Hz]; 0.85 [t, 3H]. Water miscible, 0.81% moisture content. DSC: 51.0 °C (melting point), not detected (crystallization), -48,1 °C (glass transition). TGA: 385-453 °C (weight loss 63.8%, T_{máx} = 414 °C) and 458-501 °C (weight loss 25.1%, T_{máx} = 484 °C). Yield = 81%.

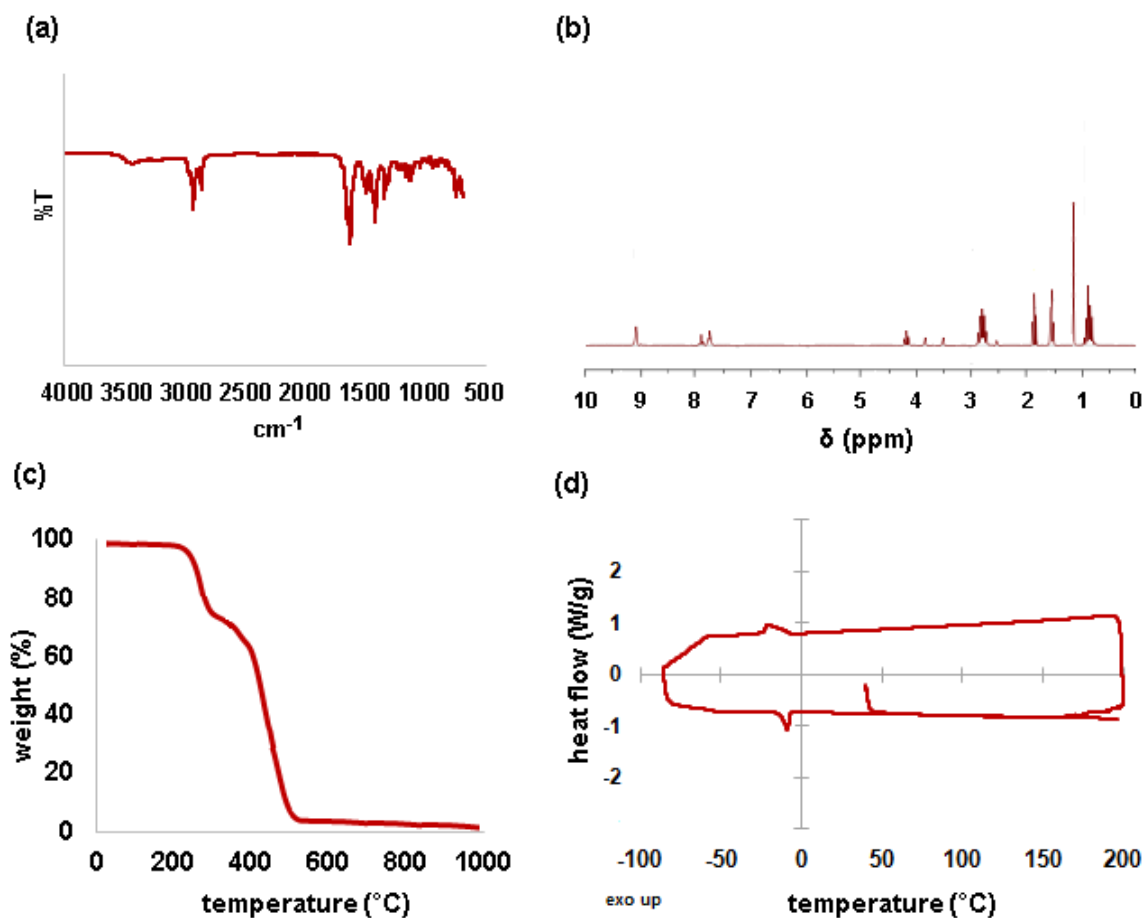


Fig. S5. Characterization of [bmim][C₁₂SAR]: (a) FTIR, (b) ¹H-NMR; (c) TGA and (d) DSC.

[bmim][C₁₂SAR] - FTIR ν (cm⁻¹): 3432 (N-C=O), 3137-3045 (C-H aromatic), 2957 (C-H of CH₂), 2871 (C-H of CH₃), 1670 (C=O), 1634 (C=N aromatic), 1567-1463 (C=C aromatic), 1231 (C-N aromatic), 1281-1167 (C-N alifatic). ¹H-NMR (600 MHz, DMSO-d₆) δ (ppm): 9.21 [s, 1H]; 7.77 [d, 1H, J=1.6 Hz]; 7.68 [d, 1H, J = 1.7 Hz]; 4.23 [t, 2H, J=7.1 Hz]; 3.84 [s, 3H]; 3.48 [s, 2H, J=10.1 Hz]; 2.75 [m, 20H]; 2.51 [s, 3H]; 1.82 – 1.70 [m, 2H, J=14.7; 7.5 Hz]; 1.31 [dt, 2H, J=14.6; 7.4 Hz]; 1.23 [t, 3H]; 0.95 [t, 3H, J=7.6 Hz]. Water miscible, 0.24% moisture content. DSC: -8.2 °C (melting point), -12.1 °C (crystallization), not detected (glass transition). TGA: 227-328 °C (weight loss 27.0%, T_{máx} = 266 °C) and 376-50132 °C (weight loss 58.2%, T_{máx} = 415 °C). Yield = 63%.

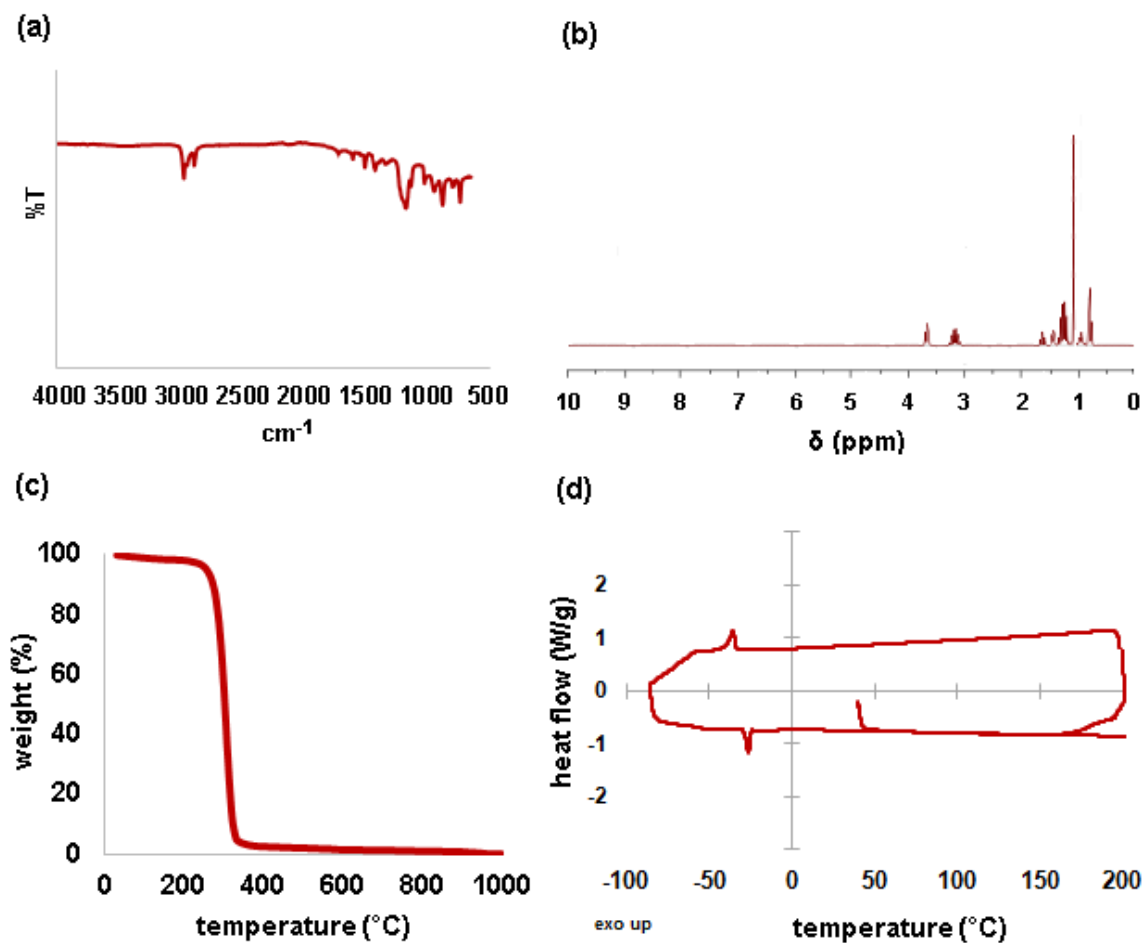


Fig. S6. Characterization of [TBA][C₁₂SO₄]: (a) FTIR, (b) ¹H-NMR; (c) TGA and (d) DSC.

[TBA][C₁₂SO₄] - FTIR ν (cm⁻¹): 2962 (C-H of CH₂), 2877 (C-H of CH₃), 1280 (N-C alifatic), 1216 (C-O), 1023 (S=O). ¹H-NMR (600 MHz, DMSO-d₆) δ (ppm): 3.67 [t, 2H, J=6.1 Hz]; 3.23-3.12 [m, 8H]; 1.54 [m, 8H]; 1.44 [m, 8H, J=7.2 Hz]; 1.37-1.21 [m, 20H]; 0.94 [m, 12H]; 0.86 [t, 3H]. Water immiscible, 0.19% moisture content. DSC: -22,9°C (melting point), -35.6°C (crystallization), -55.5°C (glass transition). TGA: 281-321°C (weight loss 97.3%, T_{máx} = 306°C). Yield = 87%.

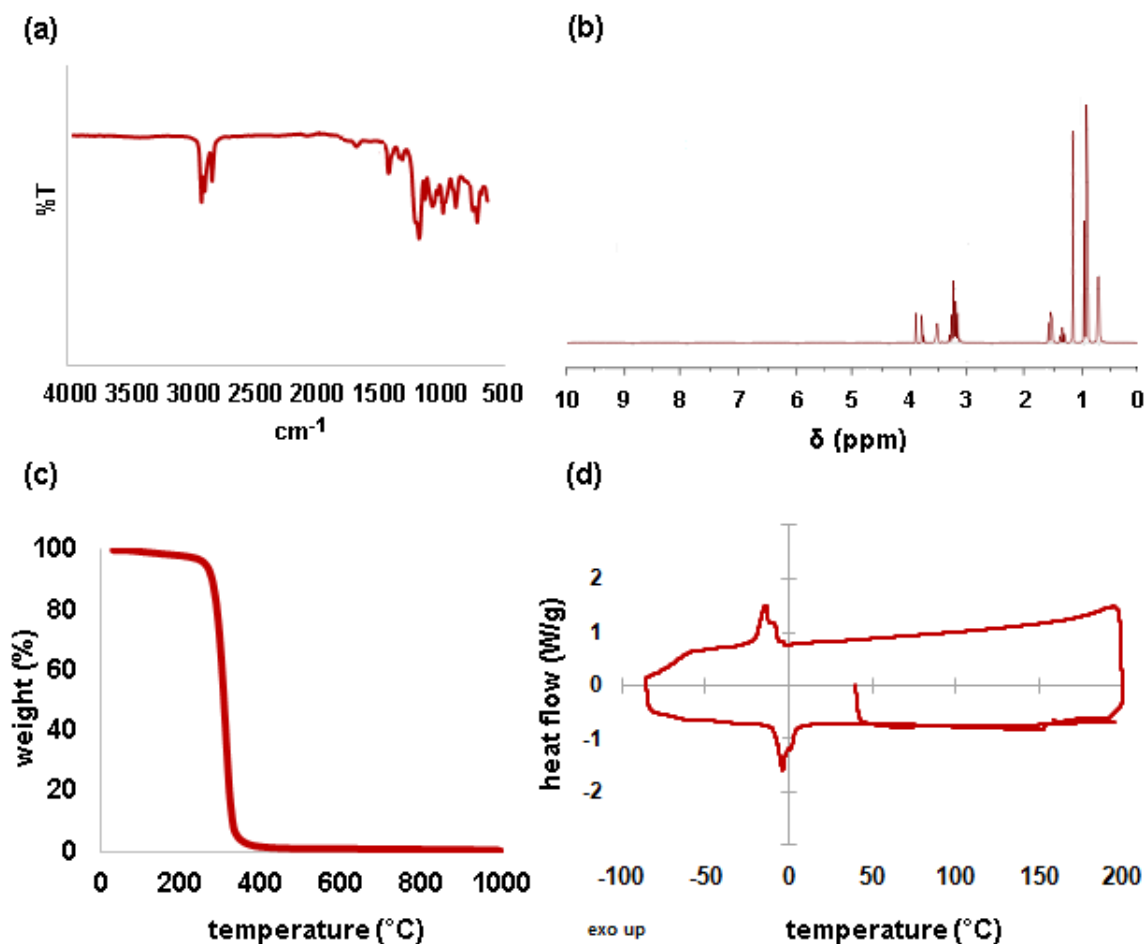


Fig. S7. Characterization of [TBA][C₁₂ESO₄]: (a) FTIR, (b) ¹H-NMR; (c) TGA and (d) DSC.

[TBA][C₁₂ESO₄]- FTIR ν (cm⁻¹): 2969 (C-H of CH₂), 2872 (C-H of CH₃), 1269 (N-C alifatic), 1216 (C-O), 1020 (S=O). ¹H-NMR (600 MHz, DMSO-d₆) δ (ppm): 3.79 [t, 2H]; 3.67 [t, 2H, J=6.0 Hz]; 3.49 [t, 2H, J=17.2 Hz]; 3.23-3.11 [m, 8H]; 1.58 [m, 8H]; 1.36-1.19 [m, 8H, J=5.8 Hz]; 0.94 [s, 26H]; 0.85 [t, 12H, J=6.1 Hz]. Water miscible, 0.46% moisture content. DSC: -5.0°C (melting point), -12.2°C (crystallization), not detected (glass transition). TGA: 223-376°C (weight loss 99.4%, T_{máx} = 318°C). Yield = 90%.

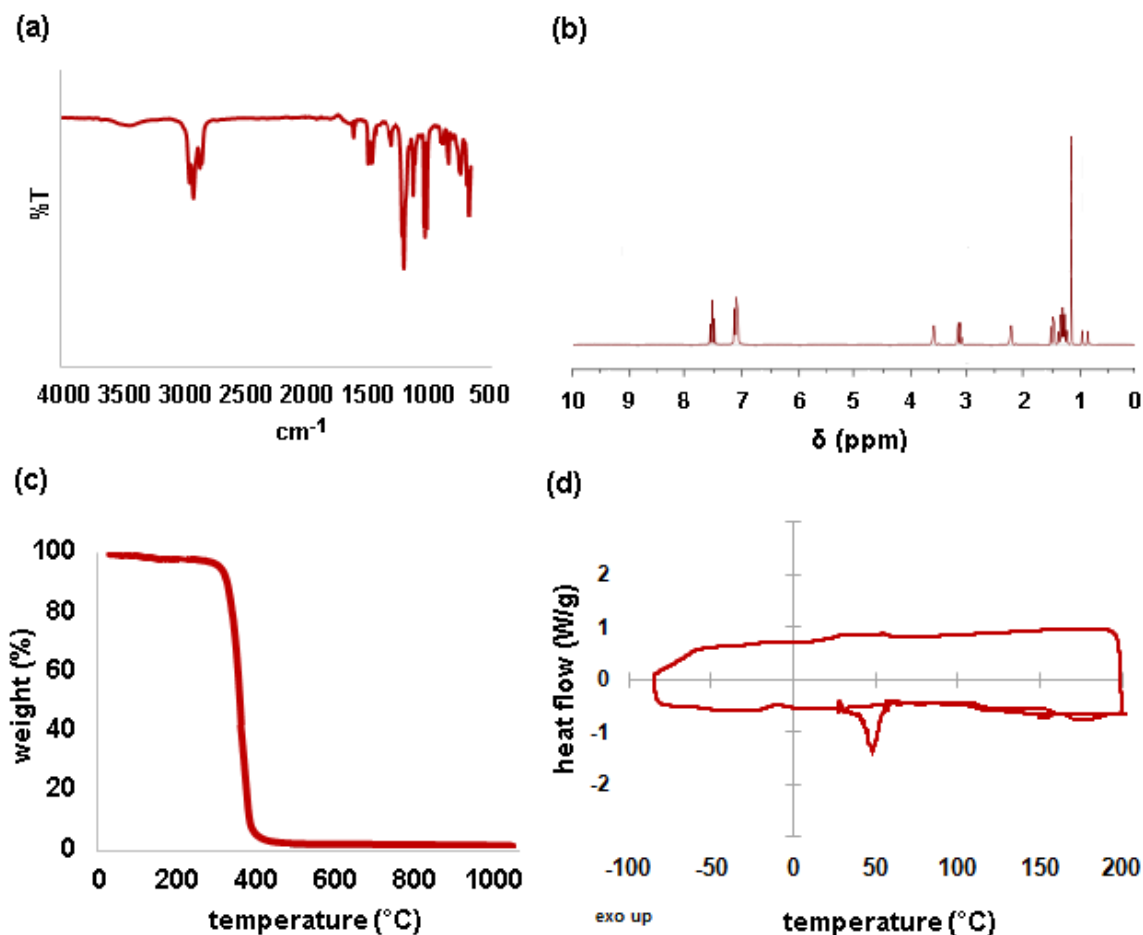


Fig. S8. Characterization of [TBA][C₁₂BSO₃]: (a) FTIR, (b) ¹H-NMR; (c) TGA and (d) DSC.

[TBA][C₁₂BSO₃] - FTIR ν (cm⁻¹): 2960 (C-H of CH₂), 2878 (C-H of CH₃), 1600 (C=C aromatic), 1570 (C=C aromatic), 1492 (C=C aromatic), 1460 (C=C aromatic), 1280 (N-C aliphatic), 1216 (C-O), 1023 (S=O), 832 (aromatic ring). ¹H-NMR (600 MHz, DMSO-d₆) δ (ppm): 7.62-7.51 [m, 2H]; 7.37-7.01 [m, 2H]; 3.61 [t, 2H, J=5.9Hz]; 3.22-3.08 [m, 8H]; 2.2 [t, 2H]; 1.56 [m, 8H]; 1.46-1.32 [m, 18H]; 1.28 [m, 8H, J=6.4 Hz]; 0.91 [t, 12H, J=7.2 Hz]; 0.88 [t, 3H]. Water miscible, 0.67% moisture content. DSC: 48.8 °C (melting point), not detected (crystallization), -49.7 °C (glass transition). TGA: 242-395 °C (weight loss 94.2%, T_{max} = 339 °C). Yield = 92%.

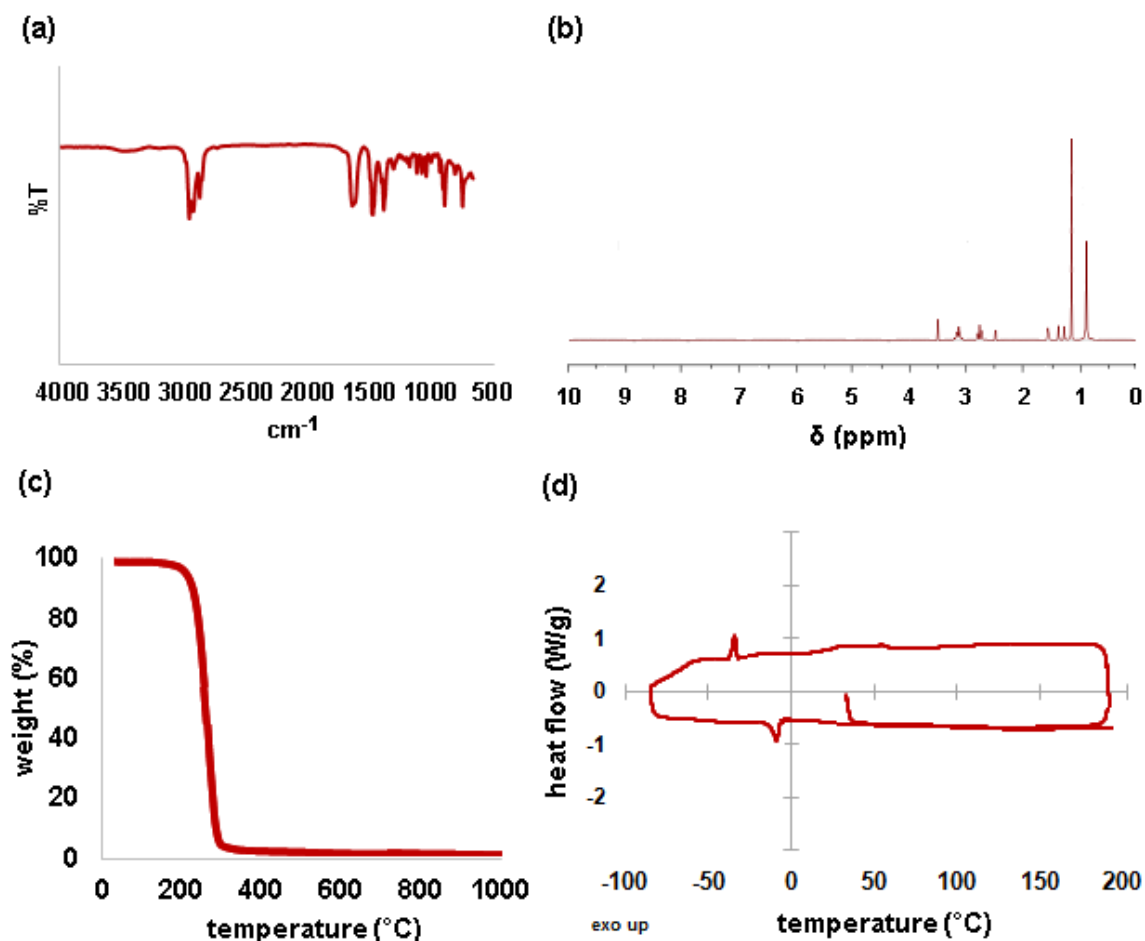


Fig. S9. Characterization of [TBA][C₁₂SAR]: (a) FTIR, (b) ¹H-NMR; (c) TGA and (d) DSC.

[TBA][C₁₂SAR] - FTIR ν (cm⁻¹): 3428 (N-C=O), 2960 (C-H of CH₂), 2875 (C-H of CH₃), 1681 (C=O), 1280-1186 (N-C alifatic). ¹H-NMR (600 MHz, DMSO-d₆) δ (ppm): 3.50 [s, 2H, J=10.1 Hz]; 3.20 – 3.08 [m, 8H]; 2.70 [m, 20H]; 2.48 [s, 3H]; 1.62 [m, 8H]; 1.36 [m, 8H, J=6.5 Hz]; 1.20 [t, 3H]; 0.94 [t, 12H, J=7.1 Hz]. Water miscible, 0.30% moisture content. DSC: -17.1 °C (melting point), -32.0 °C (crystallization), not detected (glass transition). TGA: 181-310 °C (weight loss 96.3%, T_{max} = 224 °C). Yield = 79%.

5. CONCLUSÕES

Neste item estão descritas as principais conclusões obtidas a partir dos resultados apresentados nesta tese. A primeira parte refere-se ao estudo de interação dos líquidos iônicos com água e estes resultados foram publicados no *Journal of Molecular Liquids*. A segunda parte está relacionada ao estudo dos líquidos iônicos como catalisadores na síntese do carbonato de propileno (PC) e estes resultados foram publicados na *Catalysis Letters*. Finalmente a terceira parte se refere ao estudo dos líquidos iônicos como catalisadores na síntese do carbonato de estireno (SC), carbonato de glicidil isopropil éter (GC) e o carbonato de epicloridrina (EC) estes resultados estão submetidos na revista *Reaction Kinetics, Mechanisms and Catalysis*.

→ Interação LIs com água – Artigo 1 (*Journal of Molecular Liquids*).

Ao compararmos os dois cátions utilizados neste estudo ([bmim⁺] e [TBA⁺]) vimos que o [bmim⁺] é um determinante na formação da estrutura gelatinosa. Os dois ânions ([C₁₂SO₄⁻] e [C₁₂ESO₄⁻]) estudados quando ligados ao [bmim⁺] formaram géis com propriedades muito interessantes quando diluídos. Essa propriedade não foi percebida quando estes mesmos ânions foram ligados ao [TBA⁺]. Isso possivelmente é devido ao anel aromático nitrogenado do imidazol. Pelo fato de o nitrogênio ser um elemento eletronegativo, capaz de formar pontes de hidrogênio, é possível que sejam nestes nitrogênios algumas das pontes capazes de estruturar o material em forma gelatinosa formando cristais líquidos altamente organizados.

Quando comparamos os dois ânions ([C₁₂SO₄⁻] e [C₁₂ESO₄⁻]), onde a única diferença entre eles é a ligação éter no meio da cadeia, percebemos uma diferença

muito significativa com a interação com a água. Enquanto que no cátion [bmim⁺] essa ligação (-O-) faz com que os valores de viscosidade aumentem em até 5000x na diluição de 80% quando comparado ao LI puro, devido as interações mais fortes com a água, no cátion [TBA⁺] este éter faz com que o [TBA][C₁₂ESO₄] se torne miscível, visto que o [TBA][C₁₂SO₄] é imiscível em água.

→ LIs como catalisadores para PC – Artigo 2 (*Catalysis Letters*).

Vários líquidos iônicos foram sintetizados ([bmim][C₁₂SO₄], [bmim][C₁₂ESO₄], ([bmim][C₁₂BSO₃], [bmim][C₁₂SAR], [TBA][C₁₂SO₄], [TBA][C₁₂ESO₄], ([TBA][C₁₂BSO₃] e [TBA][C₁₂SAR]) e caracterizados para serem empregados como catalisadores de cicloadição de CO₂ em óxido de propileno e mostraram eficiência catalítica. A melhor condição reacional para a síntese do carbonato de propileno foi de 110 °C, 6 h em 40 bar de pressão inicial. O [TBA][C₁₂SO₄] foi o LI que apresentou melhores atividades catalíticas, atingindo 79,2% de conversão e 87,7% de seletividade, além da alta capacidade de reciclos.

→ LIs como catalisadores para SC, GC e EC – Artigo 3 (*Reaction Kinetics, Mechanisms and Catalysis*).

Em relação ao carbonato de estireno (SC), determinou-se uma condição ideal para a síntese, sendo ela: 80 °C de temperatura, 4 horas e 40 bar de pressão inicial.

O [TBA][C₁₂BSO₃] foi o líquido iônico que apresentou melhores resultados de TON e TOF. Com ele, a conversão chegou a 81,4% e 87,0% de seletividade. Seguido dele, estão [TBA][C₁₂SO₄] e o [TBA][C₁₂ESO₄] que apresentam a mesma atividade catalítica e como destaque também o [bmim][C₁₂BSO₃].

Para a síntese do carbonato de glicidil isopropil éter (GC), foi determinado uma condição ideal, sendo ela: 120 °C de temperatura, 3 horas e 30 bar de pressão inicial.

Finalmente para a síntese do carbonato de epiclorigrina (EC), determinou-se uma condição ideal, sendo ela: 120 °C de temperatura, 2 horas e 30 bar de pressão inicial.

6. PROPOSTA PARA TRABALHOS FUTUROS

- Testar os líquidos iônicos deste trabalho na sorção de CO₂ para aplicação na captura de CO₂ em gases de exaustão;
- Modificar o cátion dos líquidos iônicos partindo de surfactantes catiônicos comerciais.

7. OUTROS TRABALHOS REALIZADOS / APRESENTADOS

- 2015

- AQUINO, A.; Bernard, F.; Borges, J.; Mafra, L.; Vecchia, F.; Oliveira, M.O.; Ligabue, R.; Seferin, M.; Chaban, V.V.; Cabrita, E.; Einloft, S. Rationalizing the role of the anion in CO₂ capture and conversion using imidazolium-based ionic liquid modified mesoporous silica. **RSC Advances**, v. 05, p. 64220-64227, 2015.

- LONGARAY, F.; Vecchia, F.D.; Aquino, A.S.; Borges, J.; Costa, E.M.; Vieira, M.O.; Ligabue, R.; Menezes, S.; Einloft, S. Adição de líquido iônico [bmim][BF₄] em soluções aquosas de aminas: influência sobre o processo de corrosão do aço de baixo carbono em alta pressão e captura de CO₂. **3º Congresso Brasileiro de CO₂**, Rio de Janeiro, 2015.

- AQUINO, A.S.; Vecchia, F.D.; Longaray, F.; Vieira, M.O.; Menezes, S.; Cabrita, E.; Einloft, S. Immobilization of ionic liquids by grafting on mesoporous material MCM-41 for CO₂ adsorption. **3º Congresso Brasileiro de CO₂**, Rio de Janeiro, 2015

- VIEIRA, M.O.; Aquino, A.S.; Longaray, F.; Borges, J.; Ligabue, R.; Einloft, S. Síntese do carbonato de dimetila por conversão química do CO₂ utilizando diferentes líquidos iônicos como catalisadores. **3º Congresso Brasileiro de CO₂**, Rio de Janeiro, 2015.

- VIEIRA, M.O.; Grillo, I.B.; Longaray, F.; Seferin, M.; Einloft, S. Ionic liquids as catalysts for CO₂ transformation in dimethyl carbonate. **Carbon Dioxide Utilisation Faraday Discussion**, Sheffield, UK, 2015.

- GRILLO, I.B.; Vieira, M.O.; Longaray, F.; Einloft, S.; Seferin, M. Multivariate models for ionic liquids catalytic systems in CO₂ cycloaddition to propylene oxide. **Carbon Dioxide Utilisation Faraday Discussion**, Sheffield, UK, 2015.

- VIEIRA, M.O.; EINLOFT, S. Transformação Química de CO₂ em dimetil carbonato: um estudo catalítico de líquidos iônicos. **XV Fórum de Pesquisa Científica e Tecnológica**, Canoas, 2015.

- **2016**

- BERNARD, F.L.; Vecchia, F.; Rojas, M.F.; Ligabue, R.; Vieira, M.O.; Costa, E.M.; Chaban, V.V.; Einloft, S. Anticorrosion Protection by Amine-Ionic Liquid Mixtures: Experiments and Simulations. **Journal of Chemical & Engineering Data**, p. 1803-1810, 2016.

- AURELIANO, M.; Ohlin, C.A.; Vieira, M.O.; Marques, M.P.M.; Casey, W.H.; Carvalho, L.A.E.B. Characterization of decavanadate and decaniobate solutions by Raman spectroscopy. **Dalton Transactions**, v. 45, p. 7391-7399, 2016.

- VIEIRA, M.O.; Aquino, A.S.; Schutz, M.K.; Vecchia, F.D.; Ligabue, R.; Seferin, M.; Einloft, S. Chemical conversion of CO₂: evaluation of different ionic liquids as catalysts in dimethyl carbonate synthesis. **13th International Conference on Greenhouse Gas Control Technologies**, Lousanne, 2016.

- FIGUEIREDO, D.C.; Vieira, M.O. Aspectos didáticos e metodológicos do método João de Deus de ensino de uma escola em Portugal. **XVI Fórum de Pesquisa Científica e Tecnológica**, Canoas, 2016.

- VIEIRA, M.O.; Einloft, S. Influência da modificação no cátion piridínico de líquidos iônicos na síntese do DMC a partir do CO₂ e metanol. **XVI Fórum de Pesquisa Científica e Tecnológica**, 2016, Canoas, 2016.

- **2017**

- VIEIRA, M.O.; Aquino, A.S.; Schütz, M.K.; Vecchia, F.D.; Ligabue, R.; SEFERIN, M.; Einloft, S. Chemical Conversion of CO₂ : Evaluation of Different Ionic Liquids as Catalysts in Dimethyl Carbonate Synthesis. **Energy Procedia**, v. 114, p. 7141-7149, 2017.

- MONTEIRO, W.F.; Vieira, M.O.; Aquino, A.S.; De Souza, M.O.; De Lima, J.; Einloft, S.; Ligabue, R. CO₂ conversion to propylene carbonate catalyzed by ionic liquid containing organosilane groups supported on titanate nanotubes/nanowires. **Applied Catalysis A-General**, v. 544, p. 46-54, 2017.

- MONTEIRO, W.F.; Vieira, M.O.; Toledo, B.O.; Neto, B.S.; De Souza, M.O.; Einloft, S.; Ligabue, R. Atividade catalítica de nanotubos de titanatos com diferentes cátions na conversão química do CO₂. **19º Congresso Brasileiro de Catálise / IX Congresso Mercosul de Catálise**, Ouro Preto, 2017.

- VIEIRA, M.O.; Monteiro, W.F.; Neto, B.S.; Ligabue, R.; Seferin, M.; Einloft, S. Síntese de líquidos iônicos anfífilos e sua utilização como catalisadores na cicloadição de CO₂ em epóxidos. **19º Congresso Brasileiro de Catálise / IX Congresso Mercosul de Catálise**, Ouro Preto, 2017.

- **2018**

- DE SOUZA, A.; Vieira, M.O.; Polesso, B.; Cobalchini, F.; Bernard, F.; Vecchia, F.D.; Einloft, S. Sorção de CO₂ utilizando líquido iônico aditivado com extensores de área superficial. **Química Nova**, v. 41, p. 656-661, 2018.

- VIEIRA, M.O.; Neto, A.M.L.; Figueiredo, D.C. Aspectos didáticos e metodológicos de uma escola em Coimbra (Portugal) que segue o Método João de Deus de Ensino – Um breve relato de experiência. **Olh@res**, v. 6, p. 87-97, 2018.

- VIEIRA, M.O.; Aquino, A.S.; Seferin, M.; Einloft, S. Fixação de CO₂ em dimetil carbonato utilizando líquidos iônicos de cátion imidazólios como catalisadores. **4º Congresso Brasileiro de CO₂**, Rio de Janeiro, 2018.

- VIEIRA, M.O.; Monteiro, W.F.; Scheid, C.M.; Ligabue, R.; Seferin, M.; Einloft, S. Síntese de líquidos iônicos derivados de surfactante e sua utilização como catalisadores na fixação química do CO₂ em ciclocarbonatos orgânicos. **4º Congresso Brasileiro de CO₂**, Rio de Janeiro, 2018.

- MONTEIRO, W.F.; Vieira, M.O.; Scheid, C.M.; Souza, M.O.; Einloft, S.; Ligabue, R. Conversão química do CO₂ utilizando sistemas catalíticos baseado em nanotubos de titanatos. **4º Congresso Brasileiro de CO₂**, Rio de Janeiro, 2018.

- VIEIRA, M.O.; Monteiro, W.F.; Scheid, C.M.; Ligabue, R.; Einloft, S. Síntese de líquido iônico suportado em nanotubos de titanatos e sua utilização como catalisadores na fixação química do CO₂ em carbonato de estireno. **4º Congresso Brasileiro de CO₂**, Rio de Janeiro, 2018.

8. REFERÊNCIAS BIBLIOGRÁFICAS

ANOOUT, M.; Caravanier, M.C.; Dridi, Y.; Jacquemin, J.; Hardacre, C.; Lemordant, D. Liquids Densities Heat Capacities, Refractive Index and Excess Quantities for {Protic Ionic Liquids + Water} Binary Sistem. **Journal Chemistry Thermodynamics**, v. 41, p. 799-808, 2009.

AQUINO, A.S. **Estudos de Solubilidade de CO₂ em Líquidos Iônicos Formados pelo Cátion Dialquilimidazólium e Diferentes Ânions**. Porto Alegre. 2010. Dissertação (Mestrado em Engenharia e Tecnologia de Materiais). Pontifícia Universidade Católica do Rio Grande do Sul, Brasil.

AQUINO, A.S.; Bernard, F.L.; Vieira, M.O.; Borges, J.V.; Rojas, M.F.; Vecchia, F.D.; Ligabue, R.A.; Seferin, M.; Menezes, S.; Einloft, S. A New Approach to CO₂ Capture and Conversion Using Imidazolium Based-Ionic Liquids as Sorbent and Catalyst. **Journal of the Brazilian Chemical Society**, v. 25, n. 12, p. 2251-2257, 2014.

ARAI, M.; Nishiyama, Y.; Ikushima, Y. Optical absorption of fine gold particles in supercritical carbon dioxide for the characterization of solvent properties. **Journal of Supercritical Fluids**, v. 13, p. 149-153, 1998.

ARAKAWA, H.; Aresta, M.; Armor, J.N.; Barteau, M.A.; Beckman, E.J.; Bell, A.T.; Bercaw, J.E.; Creutz, C.; Dinjus, E.; Dixon, D.A.; Domen, K.; Dubois, D.L.; Eckert, J.; Fujita, E.; Gibson, D.H.; Goddard, W.A.; Goodman, D.W.; Keller, J.; Kubas, J.; Kung, H.H.; Lyons, J.E.; Manzer, L.E.; Marks, T.J.; Morokuma, K.; Nicholas, K.M.; Periana, R.; Que, L.; Rostrup-Nielsen, J.; Sachtler, W.M.H.; Schmidt, L.D.; Sen, A.; Somorjai, G.A.; Stair, P.C.; Stults, B.R.; Tumas, W. Catalysis Research of Relevance to

Carbon Management: Progress, Challenges and Opportunities. **Chemical Reviews of American Chemistry Society**, v.101, p. 953-996, 2001.

ARESTA, M.; Dibenedetto, A. The contribution of the utilization option to reducing the CO₂ atmospheric loading: research needed to overcome existing barriers for a full exploitation of the potential of the CO₂ use. **Catalysis Today**, v. 98, p. 455-462, 2004.

ARESTA, M.; Dibenedetto, A.; Angelini, A. The changing paradigm in CO₂ utilization. **Journal of CO₂ Utilization**, v. 3–4, p. 65-73, 2013.

ARSHAD, M. **CO₂ Capture Using Ionic Liquids**. Copenhagen. 2009. 148 p. Tese (Master of Science in Chemical Engineering). Technical University of Denmark, Dinamarca.

BERMÚDEZ, M.D.; Jiménez, A.E.; Sanes, J.; Carrion, F.J. Ionic Liquids as Advanced Lubricant Fluids. **Molecules**, v. 14, p. 2888-2908, 2009.

BLANCHARD, L.A.; Gu, Z.; Brennecke, J.F. High-Pressure Phase Behavior of Ionic Liquid/CO₂ Systems. **Journal of Physical Chemistry B**, v. 105, p. 2437-2444, 2001.

BLANCHARD, L.A.; Hancu, D.; Beckman, E.J.; Brennecke, J.F. Green Processing using Ionic Liquids and CO₂. **Nature**, v. 399, n. 6731, p. 28-29, 1999.

BORG, P.H.; Majer, V.; Gomes, M.F.C. Solubilities of oxygen and carbon dioxide in butyl methyl imidazolium tetrafluoroborate as a function of temperature and at pressures close to atmospheric pressure. **Journal Chemical and Engineering Data**. vol.48, p. 480-485, 2003.

BOURBIGOU, H.O.; Magna, L.; Morvan, D. Ionic Liquids and catalysis: Recent progress from knowledge to applications. **Applied Catalysis A: General**, v. 373, p. 1-56, 2010.

CADENA, C.; Anthony, J. L. Shah, J. K.; Morrow, T. I.; Brennecke, J. F.; Maginn, E. J. Why Is CO₂ So Soluble in Imidazolium-Based Ionic Liquids? **Journal of American Chemistry Society**, v.126, p. 5300-5308, 2004.

CALLEJA, E.T.; Skinner, J.; Tauste, D.G. CO₂ Capture in Ionic Liquids: A Review of Solubilities and Experimental Method. **Journal of Chemistry**, 16 p., 2013.

COKOJA, M.; Bruckmeier, C.; Rieger, B.; Herrmann, W.A.; Kühn, F.E. Transformation of Carbon Dioxide with Homogeneous Transition-Metal Catalysts: A Molecular Solution to a Global Challenge? **Angewandte Chemie**, v. 50, p. 8510-8537, 2011.

CONVENÇÃO INTERNACIONAL SOBRE MUDANÇAS CLIMÁTICAS. Acordo de Paris. 21^o sessão, agenda item 4(b), p. 1–32, 2015.

DAI, W.; YANG, W.; Zhang, Y.; Wang, D.; Luo, X.; Tu, X. Novel isothiuronium ionic liquid as efficient catalysts for the synthesis of cyclic carbonates from CO₂ and epoxides. **Journal of CO₂ Utilization**, v. 17 p. 256–262, 2017.

DOCHERTY, K.M.; Dixon, J.K.; Kulpa, C.F. Biodegradability of imidazolium and pyridinium ionic liquids by an activated sludge microbial community. **Biodegradation**, v. 18, p. 481-493, 2007.

DONG, W.S.; Zhou, X.; Xim, C.; Liu, C.; Liu, Z. Ionic liquid as an efficient promoting medium for synthesis of dimethyl carbonate by oxidative carbonylation of methanol. **Applied Catalysis A: General**, v. 334, p. 100-105, 2008.

DULLIUS, J. **Reações de Oxidação de alcoóis e olefinas promovidas por complexos de metais de transição imobilizados em líquidos iônicos fluorados**. Porto Alegre. 2002. 95 p. Tese (Doutorado em Ciências dos Materiais). Universidade Federal do Rio Grande do Sul, Brasil.

EARLE, M.J.; Seddon, K.R. Ionic Liquids. Green Solvents for the Future. **Pure and Applied Chemistry**, v. 72, p. 1391-1398, 2000.

EPA – United States Environmental Protection Agency, 2016, disponível em: <https://www.epa.gov/ghgemissions/global-greenhouse-gas-emissions-data/>, acesso em 01/09/2017.

ETA, V.; Arvela, P.M.; Salminen, E.; Salmi, T.; Murzin, D.Y.; Mikkola, J.P. The effect of alkoxide ionic liquids on the synthesis of dimethyl carbonate from CO₂ and metanol over ZrO₂ – MgO. **Catalysis Letters**, v. 141, p. 1254-1261, 2011.

FELIX, P.M.F. **Produção de carbonatos utilizando dióxido de carbono**. Lisboa. 2013. Dissertação (Mestrado em Engenharia Química e Bioquímica). Universidade Nova de Lisboa, Portugal.

FREUDENMANN, D.; Wolf, S.; Wolff, M.; Feldmann, C. Ionic Liquids: New Perspectives for Inorganic Synthesis. **Angewandte Chemie International**, v. 50, p. 11050–11060, 2011.

GULDBERG, G.O.; Bruno, J.F. The Impact of Climate Change on the World's Marine Ecosystems. **Science**, v. 328, p. 1523-1528, 2010.

HANSEN, J.; Sato, M.; Kharecha, P.; Beerling, D.; Berner, R.; Delmotte, V.M.; Pagani, M.; Raymo, M.; Royer, D.L.; Zachos, J.C. Target Atmospheric CO₂: Where Should Humanity Aim? **The Open Atmospheric Science Journal**, v. 2, p. 217-231, 2008.

HERZOG, H.; Szulczewki, M.; Macminn, C.; Juanes, R. Lifetime of Carbon Capture and Storage as Climate-change Mitigation Technology. **Proceedings of the National Academy of Sciences of the United States of America**, v. 109, p. 5185-5189, 2012.

HUDDLESTON, J.G.; Visser, A.E.; Reichert, M.; Willauer, H.D.; Broker, G.A.; Rogers, R.D. Characterization and comparison of hydrophilic and hydrophobic room temperature ionic liquids incorporating the imidazolium cation. **Green Chemistry**, v. 3, p. 156-164, 2001.

IEA – International Energy Agency. Special Report. CO₂ Emissions form Fuel Combustion, Paris, 2015.

IONIC LIQUID DATABASE: Property Data of Pure Ionic Liquids, 2006. Disponível em: <<http://ilthermo.boulder.nist.gov/>>. Acesso em: 13/10/2016. Ionic Liquids Database (ILThermo). National Institute of Standards and Technology (NIST).

IPCC – Intergovernmental Panel on Climate Change, 2011.

IPCC – Intergovernmental Panel on Climate Change, 2014.

JU, H.Y.; Manju, M.D.; Kim, K.H.; Park, S.W.; Park, D.W. (A) Chemical fixation of carbon dioxide to dimethyl carbonate from propylene carbonate and methanol using ionic liquid catalysts. **Korean Journal of Chemical Engineering**, v. 24, p. 917-919, 2007.

JU, H.Y.; Manju, M.D.; Kim, K.H.; Park, S.W.; Park, D.W.; Choe, Y.; Park, S.W. (B) Performance of ionic liquid as catalysts in the synthesis of dimethyl carbonate from ethylene carbonate and methanol. **Reaction Kinetics and Catalysis Letters**, v. 90, p. 3-9, 2007.

JU, H.Y.; Manju, M.D.; Kim, K.H.; Park, S.W.; Park, D. W. Catalytic performance of quaternary ammonium salts in the reaction of butyl glycidyl ether and carbon dioxide. **Journal of Industrial and Engineering Chemistry**, v.14, p. 157–160, 2008.

KOEL, M. **Ionic Liquids in Chemical Analysis**. CRC Press., 448 p., 2009.

LEITNER, W. Green Solvents – Progress in science and applications. **Green Chemistry**, v. 11, p. 603, 2009.

LI, L.; Zhao, N.; Wei, W.; Sun, Y. A review of research progress on CO₂ capture, storage, and utilization in Chinese Academy of Sciences. **Fuel**, v. 108, p. 112-130, 2011.

MAEDA, C.; Miyazaki, Y.; Ema, T. Recent progress in catalytic conversions of carbon dioxide. **Catalysis Science & Technology**, v. 4, p. 1482-1497, 2014.

MIGLIORINI, M.V. **Líquidos Iônicos para a Preparação de Híbridos de Sílica e Suas Aplicações na Formação de Compósitos Poliméricos**. Porto Alegre. 2009. 90 p. Dissertação (Mestrado em Química). Universidade Federal do Rio Grande do Sul, Brasil.

MOFARAH, M.; Khojasteh, Y.; Khaledi, H.; Farahnak, A. Design of CO₂ absorption plant for recovery of CO₂ from flue gases of gas turbine. **Energy**, v. 33, 1311–1319, 2008.

MONTOYA, C.A.; Paninho, A.B.; Felix, P.M.; Zakrzewska, M.E.; Vital, J., Vlsak, V.N.; Nunes, A.V.M. Styrene carbonate synthesis from CO₂ using tetrabutylammonium bromide as a non-supported heterogeneous catalyst phase. **The Journal of Supercritical Fluids**, v. 100, p. 155-159, 2015

MULDOON, M.J.; Aki, S.N.V.K.; Anderson, J.L.; Dixon, J.K.; Brennecke, J.F. Improving Carbon Dioxide Solubility in Ionic Liquids. **Journal Physical Chemistry B**, v. 111, p. 9001-9009, 2007.

NOAA – National Organic & Atmospheric Administration. Trend in Atmospheric Carbon Dioxide – Mauna Loa. 2017, disponível em: http://www.esrl.noaa.gov/gmd/ccgg/trends/mlo.html#mlo_full, acesso em 29/10/2018.

NORTH, M.; Pasquale, R.; Young, C. Synthesis of cyclic carbonates from epoxides and CO₂. **Green Chemistry**, v. 12, p. 1514-1539, 2010.

OTTO, A.; Grube, T.; Schiebahna, S.; Stolten, D. Closing the loop: captured CO₂ as a feedstock in the chemical industry. **Energy & Environmental Science**, v. 8, p. 3283-3297, 2015.

PANINHO, A.B.; Ventura, A.L.R.; Branco, L.C.; Pombeiro, A.J.L.; Silva, M.FC.G.; Ponte, M.N.; Mahmudov, K.T.; Nunes, A.V.M. CO₂ + ionic liquid biphasic system for reaction/product separation in the synthesis of cyclic carbonates. **Journal of Supercritical Fluids**, v. 132, p. 71-75, 2018.

PLECHKOVA, N.V.; Seddon, K.R. Applications of ionic liquids in the chemical industry. **Chemical Society Reviews**, v. 37, p. 123-150, 2008.

POLIAKOFF, M.; Fitzpatrick, J.M.; Farren, T.R.; Anastas, P.T. Green Chemistry: Science and Politics of Change. **Green Chemistry**, v. 297, p. 807-810, 2002.

POLIAKOFF, M.; Leitner, W.; Streng, E.S. The Twelve Principles of CO₂ CHEMISTRY. **Faraday Discussions**, v. 183, p. 9-17, 2015.

RAHMAN, M.H.; Sijaj, M.; Larachi, F. Ionic liquids for CO₂ capture—Development and progress. **Chemical Engineering and Processing**, v. 49, p. 313–322, 2010.

RAFIEE, A.; Khalilpour, K.R.; Milani, D.; Panahi, M. Trends in CO₂ conversion and utilization: A review from process systems perspective. **Environmental Chemical Engineering**, v. 6, p. 5771-5794, 2018.

ROGELJ, J.; Meinshausen, M.; Knutti, R. Global warming under old and new scenarios using IPCC climate sensitivity range estimates. **Nature Climate Change**, v. 2, p. 248-253, 2012.

SAKAKURA, T.; Choi, J.; Yasuda, H. Transformation of Carbon Dioxide. **Chemical Reviews of American Chemistry Society**.v.107, p. 2365-2387, 2007.

SAKAKURA, T.; Kohno, K. The synthesis of organic carbonates from carbon dioxide. **Chemical Communications**, p. 1312-1330, 2009.

SEDDON, K.R. Ionic Liquids for Clean Technology. **Journal of Chemical Technology and Biotechnology**, v. 68, n. 4, p. 351-356, 1997.

SILVERSTEIN, R.M.; Bassler, G.C.; Morrill, T.C. Identificação Espectrométrica de Compostos Orgânicos. Tradução Ricardo Bicca de Alencastro. Rio de Janeiro: Editora Guanabara Koogan S.A., 1979. 387 p.

SOCRATES, G.; Infrared Characteristic Group Frequencies: Tables and Charts. Chichester: John Wiley and Sons Ltd., 1994. 249 p.

SUAREZ, P.A.Z. ; Einloft, S.M.O.; Dullius, J.E.L.; Souza, R.F.; Dupont, J. Synthesis and physical-chemical properties of ionic liquids based on 1- n-butyl-3-methylimidazolium cation. **Journal de Chimie Physique et de Physico-Chimiebiologique**, v. 95, n. 7, p. 1626-1639, 1998.

SUN, J.; Fujita, S.; Bhanage, B.M.; Arai, M. One-pot synthesis of styrene carbonate from styrene in tetrabutylammonium bromide. **Catalysis Today**, v. 93, 383–388, 2004.

SUN, J.; Cheng, W.; Fan, W.; Wang, Y.; Meng, Z.; Zhang, S. Reusable and efficient polymer-supported task-specific ionic liquid catalyst for cycloaddition of epoxide with CO₂. **Catalysis Today**, v. 148, p. 361-367, 2009.

TARIK, M.; Forte, P.A.; Gomes, M.F.; Lopes, J.N.; Rebelo, L.P. Densities and Refractive indices of Imidazolium and Phosphonium Based Ionic Liquids: Effect of Temperature, Alkyl Chain Length and anion. **Journal Chemistry Thermodynamics**, v. 41, p. 790-798, 2009.

TINOCO, R.R.; Boallou, C. Comparison of absorption rates and absorption capacity of ammonia solvents with MEA and MDEA aqueous blends for CO₂ capture. **Journal of Cleaner Production**, v. 18, n. 9, p. 875-880, 2010.

TKATCHENKO, D.B.; Chambrey, S.; Keiski, R.; Ligabue, R.; Plasseraud, L.; Richard, P.; Turunen, H. Direct synthesis of dimethyl carbonate with supercritical carbon dioxide: Characterization of a key organotin oxide intermediate. **Catalysis Today**, v. 115, p. 80-87, 2006.

VIEIRA, M.O. **Síntese e utilização de líquidos iônicos como catalisadores na transformação química de CO₂ em carbonato de dimetila**. Porto Alegre. 2015. 96 p. Dissertação (Mestrado em Engenharia e Tecnologia de Materiais). Pontifícia Universidade Católica do Rio Grande do Sul, Brasil.

VIEIRA, M.O.; Aquino, A.S.; Schütz, M.K.; Vecchia, F.D.; Ligabue, R.; Seferin, M.; Einloft, S. Chemical conversion of CO₂: evaluation of different ionic liquids as catalysts in dimethyl carbonate synthesis. **Energy Procedia**, v. 114, p. 7141-7149, 2017.

WAPPEL, D.; Gronal, G.; Kalb, R.; Draxler, J. Ionic liquids for Post-Combustion CO₂ Absorption. **International Journal of Greenhouse Gas Control**, v. 4, p. 486-494, 2010.

WANG, J.; Zhao, D.; Zhou, E.; Dong, Z. Desulfurization of gasoline by extraction with N-alkyl-pyridinium-based ionic liquids. **Journal of Fuel Chemistry and Technology**, v. 35, n. 3, p. 293- 296, 2007.

WASSERSCHIED, P.; Welton, T.; Ionic Liquids in Synthesis. Weinheim: Wiley-VCH Verlags GmbH & Co, 368 p., 2008.

WELTON, T. Ionic liquids in catalysis. **Coordination Chemistry Reviews**, v. 248, p. 2459-2477, 2004.

WILKES, J.S.; Levisky, J.A.; Wilson, R.A.; Hussey, C.L. Dialkylimidazolium chloroaluminate melts: A new class of room-temperature ionic liquids for electrochemistry, spectroscopy, and synthesis. **Inorganic Chemistry**, v. 21, n. 3, p. 1263- 1264, 1982.

YANG, Z.Z.; He, L.N.; Miao, C.X.; Chanfreau, S. Lewis basic ionic liquids-catalyzed conversion of carbon dioxide to cyclic carbonates. **Advanced Synthesis & Catalysis**, v. 352, p. 2233-2240, 2010.

ZHANG, H.; Kong, X.; Cao, C.; Pang, G.; Shi, Y. An efficient ternary catalyst $ZnBr_2/K_2CO_3/[Bmim]Br$ for chemical fixation of CO_2 into cyclic carbonates at ambient conditions. **Journal of CO_2 Utilization**, v. 14, p. 76–82, 2016.

ZHU, M.; Srinivas, D.; Bhogeswararao, S.; Ratnasamy, P.; Carreon, M.A. Catalytic activity of ZIF-8 in the synthesis of styrene carbonate from CO_2 and styrene oxide. **Catalysis Communications**, v. 32, p. 36-40, 2013.



Pontifícia Universidade Católica do Rio Grande do Sul
Pró-Reitoria de Graduação
Av. Ipiranga, 6681 - Prédio 1 - 3º. andar
Porto Alegre - RS - Brasil
Fone: (51) 3320-3500 - Fax: (51) 3339-1564
E-mail: prograd@pucrs.br
Site: www.pucrs.br